



University of
Stavanger

Faculty of Science and Technology
MASTER'S THESIS

Study program/Specialization Master i Konstruksjoner og Materialer	Spring semester, 2022 Open / Restricted access
Writer: Syed Abrar Ahmad -261967	...Syed Abrar Ahmad ... (Writer's signature)
Faculty supervisor: Sudath C. Siriwardane External supervisor(s)	
Thesis title: <i>Behavior of steel beams subjected to LTB at elevated temperature/Fire</i>	
Credits (ECTS): 30	
Key Words: LTB FEM Temperature Elevation	Pages: + enclosure: Stavanger, 15/06/2022 Date/year

Frontpage for master thesis
Faculty of Science and Technology



Universitetet i Stavanger

Master Thesis

Study Program: *Bygg – Konstruksjoner og Materialer*

Author: Syed Abrar Ahmad -261967

Course Leader: *Sudath C. Siriwardane*

Supervisor: *Sudath C. Siriwardane*

Title: *Behavior of steel beams subjected to LTB at elevated temperature/Fire
Institutt for maskin, bygg og materialteknologi Universitetet i Stavanger
15/06/2021*

Abstract

When the steel beam is subjected to fire, there are great chances for the steel beam to decrease its stiffness due to which the flexural and lateral torsional buckling capacity (LTB) properties of respective steel beam affected. At an elevated temperature, there exist a non-linear stress-strain behavior of steel beam at an elevated temperature. The steel beam is subjected to fire under different elevated temperatures in Finite Element Modeling tools and ANSYS to investigate the behavior and changing properties during the elevated temperature. The FEM is considered validated instead of experimentation for fire in laboratory because to get such high temperature just for prototype or modeling is not achievable, thus, to study the behavior of steel using modeling techniques. The specific modeling tools create an experimental model to study by carrying the set of parametric studies. The steel beam is analyzed by changing the thermal properties, mechanical and physical properties at an elevated temperature.

The main theme of this research congested only with lateral torsional buckling moment capacity of I-beam and non-dimensional slenderness ratio. Buckling plays an important in the stability of structures.

To investigate this, there are five cases while analyzing the I-Beam throughout the cross-section and at various locations when subjected to fire or elevated temperature.

- 1) **Case 01:** No fire or elevated temperature: In this case, the steel beam is analyzed without having elevated temperature.
- 2) **Case 02:** Whole cross-section of the beam is subjected to fire or elevated temperature of same nature. The reduction in physical properties are applied throughout the beam.
- 3) **Case 03:** The elevated temperature in the beam is subjected to whole bottom flange and half of web in uniform way.

4) **Case 04:** In this case, the elevated temperature is subjected to top and bottom flange and web at $L/3$.

5) **Case 05:** In this case, the elevated temperature is subjected to $1/3$ of mid-span length of the I-beam at the bottom flange and the lower half of the web.

The purpose and objective of this study to analyze how the steel beam behave in case of subjected to fire, in different scenarios discussed above, on lateral torsional buckling capacity ($M_{b,Rd}$). When different test is applied through FEM, then it came to know that the steel specimen is getting failed under LTB irrespective of fire and end support condition. There exist two kinds of buckling while studying; one is linear buckling analysis and nonlinear buckling analysis. It is common observation that, with the increase in temperature, the length of the steel beam also increases due to the phenomenon of expansion or contraction properties of steel in an increasing or decreasing way of external temperature. By increase in the length of the steel beam, the lateral buckling capacity and flexural strength decrease that may result in the collapse of structure, thus this study is carried out to analyze this behavior to improve and suggest the modifications while designing the structures based on fire loading. After doing the analysis, the results are explained in a detailed way.

At an elevated temperature, there is reduction in strength of steel and stiffness of material with which beam is made, i.e., stainless steel. As stainless steel is alloy of different material, so it provides better retention as compared to carbon steel.

Stainless steel beams are capable of bearing more temperature because they have high value of coefficient of thermal expansion as compared to carbon steel.

Acknowledgment

This thesis was written by Syed Abrar Ahmad during spring 2022 with the collaboration of faculty of University of Stavanger. The thesis was part in the completion of Masters in “Mechanical and Structural engineering and material science”.

In this regard, I would like to offer my gratitude to instructors who guided my throughout my term to successfully complete my thesis. I would like to honor and express my acknowledgement to the professor “Sudath C. Siriwardane”. Moreover, during my journey to complete this thesis successfully I would like to pay my gratitude to co supervisor “Sanat Wables” for his guidance and timely help.

Table of Contents

Abstract.....	3
Acknowledgment	5
<i>Table of Contents</i>	6
<i>List of tables</i>	8
<i>List of figures</i>	9
<i>List of Symbols and Abbreviations</i>	11
1-Introduction	12
1.1-Background.....	12
1.2-Problem Statement/Research Gap	15
1.3-Objectives	16
1.4-Outline/Framework of thesis	17
2-Lateral Torsional Buckling (LTB).....	18
2.1- Review of LTB	18
2.2- Design Codes for LTB.....	22
2.2.1-Stepwise Method conservatively used.....	28
2.3-Capacity of LTB beam at elevated temperature	33
3- Analytical Approach.....	35
3.1- Need for Analysis	35
3.2- Analysis Criteria	36
3.2.1-For Load-Bearing Resistance	36
3.2.2-Time.....	36
3.2.3-Temperature.....	36
3.3- Static Linear Analysis.....	37
3.4- Critical Elastic Moment, Slenderness Ratio and LTB Moment Capacity	37
3.5- Step by step procedure for design calculation of all cases	39
4-Finite Element Modeling	40
4.1-ANSYS Simulations	40
4.1.1-Methods of Performing LTB on ANSYS	41
4.2-Finite Element Simulation	42
4.2.1-Flow chart used for Static Analysis in ANSYS.....	42
4.2.2-Mechanical Properties	43
4.2.3-Geometry	44

4.2.4-Meshing	44
4.2.5-Load	45
4.2.6-Boundary conditions.....	45
4.3- Cases; at different elevated temperature.....	46
4.3.1-For case of temperature 500°C	47
4.3.2-For case Of 800°C	49
4.3.3-Temperature 1000°C.....	51
4.3.4-Temperature 1200°C.....	53
4.3.5-Temperature 1500°C.....	55
4.3.6-Temperature 1500°C.....	57
4.4- Results and Analysis.....	60
5-Discussion.....	86
5.1- Analysis	86
5.1.1- Static Linear Analysis.....	101
5.1.2- Linear Buckling Analysis	102
5.1.3- Non-Linear Buckling Analysis	103
5.1.4- Non-Linear Buckling Analysis	104
5.1.5- LTB Moment Resistance	105
6- Conclusion	106
7- References	108
Appendix.....	111
Appendix A.....	111
Appendix B	115
Appendix C.....	118
Appendix D.....	122

List of tables

Table 1- values for LTB curves for specific cross-sections Eurocodes (Table 6.4)	28
Table 2- imperfection factor values for LTB. (Euro Codes Design Table 6.3)	28
Table 3- A_m/V values of any cross-section with c time for temperature	29
Table 4- reduction factors at elevated temperature for stainless steel	30
Table 5- Determination of A_m/V for temperature	31
Table 5- the responses of steel structure members under high thermal actions.....	34
Table 6- Assumptions for boundary value condition for FEM Model	46
Table 7- the application of moments and the resulting deflection.....	60
Table 8- No temperature conditions $L=1m$	62
Table 9- no temperature elevation but change in impact factor by keeping same length.....	64
Table 10- No temperature with $L=2$ meters (Different Imperfection Scale Factor Values).....	66
Table 11- No temperature, $L=2m$ with Different Imperfection Scale Factor Values.....	68
Table 12- the values for App. Moment vs Lat. Deflection for $L=1.5$ m, for 5 cases.....	69
Table 13- the values for App. Moment vs Lat. Deflection for $L=2$ m, for 5 cases.....	70
Table 14- the values for App. Moment vs Lat. Deflection for $L=2.3m$, for 5 cases.....	71
Table 15- the values for App. Moment vs Lat. Deflection for $L=2.5m$, for 5 cases.....	73
Table 16- the values for App. Moment vs Lat. Deflection for $L=3m$, for 5 cases.....	74
Table 17- the values for App. Moment vs Lat. Deflection for $L=3.4m$, for 5 cases.....	75
Table 18- the values for App. Moment vs Lat. Deflection for $L=4m$, for 5 cases.....	77
Table 19- the values for App. Moment vs Lat. Deflection for $L=5m$, for 5 cases.....	78
Table 20- the values for App. Moment vs Lat. Deflection for $L=7m$, for 5 cases.....	79
Table 21- the values for App. Moment vs Lat. Deflection for $L=10m$, for 5 cases.....	80
Table 22- no change in temperature of the I-Beam	81
Table 23- At temperature of $500^{\circ}C$ of the I-Beam	82
Table 24- At temperature of $800^{\circ}C$ of the I-Beam	83
Table 25- the properties of I-Beam selected for FEM in ANSYS workbench.	86
Table 26- For calculation of M_{cr} from Eigenvalue	87
Table 27- the conditions for boundary values of FEM.	88
Table 28- Table to determine the imperfection length.....	90
Table 29- the cross-sectional properties of I-beam, an input in ANSYS workbench.....	91
Table 30- This table illustrates the conditions for boundary values of FEM.....	94
Table 31- the calculation of elastic critical moment M_{cr}	97
Table 32- The curves order obtained from the fig.	104

List of figures

Fig. 2.1.1- LTB in I-Beam (a) Elevation, (b) longitudinal axis plan and (c) Cross-Section ...	19
Fig. 2.1.2- Lat. Buckling of Cantilever beam hanging with couple of weights.....	19
Fig. 2.1.3- Lat. Torsional Buckling of I-Beam viewing in 3D	20
Fig. 2.1.4- Graph Representing the elastic/inelastic critical moment of I-beam.....	21
Fig. 2.1.5- Time dependent stress-strain behavior of Steel beam at high temperature.....	21
Fig. 2.2.1- ratio of width to thickness for compression parts.	22
Fig. 2.2.2- ratio of width to thickness for compression parts.	23
Fig. 2.2.1- Buckling Curves.....	28
Fig. 2.2.2- temperature VS reduction factor	29
Fig. 2.3.1- Failure of beam due to buckling.....	33
Fig. 2.3.2- the variation of strength of steel by increasing temperature	34
Fig. 3.1.1- steel beam acting under the fire when upward load is applied.....	35
Fig. 3.1.2- Steel beam at high temperature	35
Fig. 3.3.1- Cross-section of Steel I-beam for static analysis.	37
Fig. 4.1.1- Computational Model used in ANSYS	41
Fig. 4.2.1.1- Flow chart used for Static Analysis in ANSYS	42
Fig. 4.2.2.1- Mechanical Properties in ANSYS Workbench 2020	43
Fig. 4.2.3.1- Geometry.....	44
Fig. 4.2.4- Meshing for finding elemental density.....	44
Fig. 4.2.5.1- Load applied in ANSYS Workbench.....	45
Fig. 4.2.6.1- Boundary Condition	45
Fig. 4.3.1.1- Loading Temperature 500°C in ANSYS workbench	47
Fig. 4.3.1.2- Deformation resulting from Loading	47
Fig. 4.3.1.3- Eigenvalue Deformation	48
Fig. 4.3.1.4- Graph plotted between applied moment and deformation at 500°C	48
Fig. 4.3.2.1- Loading Temperature 800°C in ANSYS workbench	49
Fig. 4.3.2.2- Deformation resulting from Loading	49
Fig. 4.3.2.3- Eigenvalue Deformation	50
Fig. 4.3.2.4- Graph plotted between applied moment and deformation at 800°C	50
Fig. 4.3.3.1- Loading Temperature 1000°C in ANSYS workbench	51
Fig. 4.3.3.2- Deformation resulting from Loading	51
Fig. 4.3.3.3- Eigenvalue Deformation	52
Fig. 4.3.3.4- Graph plotted between applied moment and deformation at 1000°C	52
Fig. 4.3.4.1- Loading Temperature 1200°C in ANSYS workbench	53
Fig. 4.3.4.2- Deformation resulting from Loading	53
Fig. 4.3.4.3- Eigenvalue Deformation	54
Fig. 4.3.4.4- Graph plotted between applied moment and deformation at 1200°C	54
Fig. 4.3.5.1- Loading Temperature 1500°C in ANSYS workbench	55
Fig. 4.3.5.2- Eigenvalue Deformation	55
Fig. 4.3.5.3- Deformation resulting from Loading	56
Fig. 4.3.5.4- Graph plotted between applied moment and deformation at 1500°C	56
Fig. 4.3.6.1- Loading Temperature 2000°C in ANSYS workbench	57
Fig. 4.3.6.2- Deformation resulting from Loading	57
Fig. 4.3.6.3- Eigenvalue Deformation	58

Fig. 4.3.6.4- Graph plotted between applied moment and deformation at 1500°C	58
Fig. 4.3.6.5- max. Applied stress effect on the beam to make deflection in it	59
Fig. 4.3.6.5- the stress-strain behavior of FEM Model	59
Fig. 4.4.1- resulting deflection due to App. moment	61
Fig. 4.4.2- No temperature conditions L=1m	63
Fig. 4.4.3- no temperature elevation but change in impact factor by keeping same length	65
Fig. 4.4.4- No temperature L=2meters (Different Imperfection Scale Factor Values).....	67
Fig. 4.4.5- No temperature, L=2m with Different Imperfection Scale Factor Values.....	68
Fig. 4.4.6- App. Moment vs Lat. Deflection for L=1.5 m, for 5 cases	69
Fig. 4.4.6- App. Moment vs Lat. Deflection for L=2 m, for 5 cases	70
Fig. 4.4.7- App. Moment vs Lat. Deflection for L=2.3m, for 5 cases	72
Fig. 4.4.8- App. Moment vs Lat. Deflection for L=2.5m, for 5 cases	73
Fig. 4.4.9- App. Moment vs Lat. Deflection for L=3m, for 5 cases	74
Fig. 4.4.10- App. Moment vs Lat. Deflection for L=3.4m, for 5 cases	76
Fig. 4.4.11- App. Moment vs Lat. Deflection for L=4m, for 5 cases	77
Fig. 4.4.12- App. Moment vs Lat. Deflection for L=5m, for 5 cases	78
Fig. 4.4.13- App. Moment vs Lat. Deflection for L=7m, for 5 cases	79
Fig. 4.4.14- App. Moment vs Lateral Deflection for L=10m, for 5 cases	80
Fig. 4.4.15- no change in temperature of the I-Beam (Reduction factor vs Non-dimensional)	81
Fig. 4.4.16- Reduction factor vs non-dimensional – 500°C Temperature elevation.....	82
Fig. 4.4.17- Reduction factor vs non-dimensional – 800°C Temperature elevation.....	83
Fig. 4.4.18- Reduction factor vs non-dimensional – 1200°C Temperature elevation.....	84
Fig. 4.4.19- Reduction factor vs non-dimensional – 1500°C Temperature elevation.....	84
Fig. 4.4.20- Reduction factor vs non-dimensional – 2000°C Temperature elevation.....	85
Fig. 5.1.1- Assumptions of 1 st Boundary Condition	88
Fig. 5.1.2- Assumptions of 2 nd Boundary Condition	88
Fig. 5.1.3- Load Multiplier obtained from Egenbuckling vs Meshing Size/Density.....	93
Fig. 5.1.4- Assumptions of 1 st Boundary Condition	94
Fig. 5.1.5- Assumptions of 2 nd Boundary Condition	94
Fig. 5.1.6- App. Moment- Displacement Curve	96
Fig. 5.1.7- Tangent method to find MbRd 2 and MbRd 3	96
Fig. 5.1.7- the increase in non-dimensional slenderness ratio, decreases the MbRd.....	100
Fig. 5.1.8- A simply supported Beam with App. moments on both ends.....	101
Fig. 5.1.9- Graph between FEM calculated MbRd and determined from the code.....	103
Fig. 5.1.10- App. Moment vs Deflection for 5 cases.....	104
Fig. 5.1.11- non-dimensional slenderness ratio with LTB moment capacity.....	105

List of Symbols and Abbreviations

Symbols/Abbreviation	Description
LTB	Lateral Torsional Buckling
UDL	Uniformly distributed load
FEM	Finite Element Modeling
FEA	Finite Element Analysis
f_y	Yield Stress
T_f	Thickness of flange
T_w	Thickness of web
I_t	Torsional Constant
I_w	Wrapping Constant
I_{yy}	Moment of Inertia along y-axis
I_{zz}	Moment of Inertia along z-axis
B	Width of beam
H	Height of beam
ν	Poisson's Ratio
A	Cross-sectional Area
A_{eff}	Effective cross-sectional area
θ_{crit}	Critical Temperature
M_y	Maximum moment applied to the beam.
$W_{pl,y}$	Plastic Sectional Modulus
$k_{y,\theta,com}$	Reduction factor at maximum temperature
M_{brd}	Lateral torsional Buckling moment capacity
M_{cr}	Elastic Critical Moment
I_{eff}	Effective second moment of area
λ_{LT}	Non-dimensional slenderness
A_m	Area of Perimeter/Surface Area exposed to fire
$f_{p,\theta}$	Tensile limit at an elevated temperature
MAXARC	Maximum Multiplier for Arc-length
MINARC	Maximum Multiplier for Arc-length

Chapter 1

1-Introduction

1.1-Background

If not properly dealt with, fire has the potential to cause significant hazard to people life. It has the potential to result in the loss of human assets and lives. Steel structure construction are commonly implemented for large span industrial buildings and community halls. Therefore, the study of steel behavior under fire is important so that to consider this action when designing the steel structure.

Under the action of fire, steel shows poor nature and behavior because of the reason that the steel has high value of thermal conductivity which cause the reduction in thickness of steel structure. The response of steel structure due to fire or elevated temperature depends on the properties of steel induced, i.e., stiffness, thermal conductivity, strength, thickness, tensile property of steel, thermal gradient and thermal expansion. From different studies, it came to know that the mechanical properties of the steel like, strength and stiffness are reduced. At elevated temperature or action of fire, the yield strength and elastic modulus are reduced, the reason behind the reduction in these properties is due to forces induced due to thermal action and lateral buckling capacity of steel beam. Due to the action of elevated temperature, the stress strain curve of the steel beam also changes and show different behavior as compared to normal room temperature. Because of these thermal forces induced in the steel structure, deformations and safety of steel structure is not properly in understanding while designing and not given in the structural codes.

When the steel beam is under fire, then there exists a twisting and wrapping, which always does not cause the lowering of strength of steel. In the cases, when steel is dealt at very temperature and then cooled rapidly, the mechanical and physical properties are totally

disturbed and there is no such consideration for the re-use of this rapidly cooled steel anyways and in any case for the existing structure.

The part, where steel beam is connected with slab or column has less chances to be exposed to fire as compared to other part of beam because at connection, there exists additional bolts, plates etc., thus, connections often have more material. So, the temperature and effectiveness of connection is less as compared to other part of steel beam. Thus, the connection part is less critical as compared to other part.

The strength of steel beam remains unaffected at the temperature below 600°C and there exists almost half of residual strength at the temperature of 1100°C. The steel loses all of its capacity at the temperature of 2700°C, thus for the design consideration, we should have to keep in mind that the steel loses all of its strength at 2200°C for additional factor of safety. It is observed that the steel beam failed at the temperature between 650°C-1100°C. As the upper part of structure is standing on beam, i.e., slab is supported by beam, so the structure collapses at elevated temperature.

Beam is the main part of global structure, which is in connection with slab from top and at its bottom, connected with column. Thus, during the fire condition, the beam deforms, loses strength, or may fail, resulting in the deformation/failure of other structural members which may affect the stability of whole structure. There are two types of thermal restraints, one is axial restraint which causes the lateral deformations in steel beam and other is rotational restraint, which is responsible for creating rotations at the ends or connections and creates bending moment in the beam.

As discussed above, action of fire or elevated temperature has an ability to reduce the thickness of the steel beam and with decrease in thickness affects other cross-sectional properties like area, moment of inertia (along x-axis and y-axis), torsional and twisting constant. As beam is

a flexural member with open cross-section, which has the capacity of Lateral Torsional Buckling (LTB) under the action of fire or elevated temperatures. After all, the stiffness, strength, mechanical properties are reduced to that specific path of beam which is under elevated temperature.

1.2-Problem Statement/Research Gap

In the previous literature, there were a few numbers of research studies presented related to the action of fire and decrease in (LTB) of the open cross-sectional areas such as beam, columns etc. There are several studies exist in which many experimental studies were performed to understand the LTB capacity of the steel beam when it comes in contact with very high temperature or fire. Thus, there is no analytical approach and formula or design code or method to determine the (M_{cr}) residual elastic critical moment and the ($M_{b,rd}$) lateral torsional buckling moment which then be applied to the damaged parts due to fire. There is another thing for lacking this literature is, in normal practices, it is not possible to attain such temperature for prototype testing, to make a kiln to study the properties of affected part. Therefore, the prototype of beam is tested using some software tools like ANSYS, SAP2000 and other Simulation and FEM tools and techniques. FEM is a technique for simulating non-linear structural behavior and non-linear behavior of lateral torsional buckling of steel structure is often challenging in nature because of the reason that interaction effect of local buckling and with both geometrical and non-linearity of material behavior and numerical complexities at the support/end connections. The main question is that how the accuracy of software related results is i.e. from FEM and other modeling tools in case of structural beam, the features available in FEM and ANSYS interface is an example of it.

1.3-Objectives

In order to overcome the gaps available in studies and literature (as explained in problem statement section), the thesis is going to provide the following objectives,

- 1) The main objective is to provide framework for I-Beam that is affected under an elevated temperature and framework contain the formulas for degradation which are depending on time
 - effective 2nd moment of area (I_{eff}),
 - effective lateral torsional constant (IT) and
 - Effective warping constant.

These parameters are required in order to obtain degradation of elastic critical bending moment (M_{cr}) and buckling moment capacity ($M_{b,rd}$).

- 2) The second objective of this study is fill the gap by simulating the non-linear lateral torsional buckling behavior of the patch affected due an elevated temperature.
- 3) Investigating and examining the effect of steel beam at different elevated temperatures to find the reduction model for buckling reduction factor (χ) against non-dimensional slenderness ratio ($\bar{\lambda}$).

The study is parametric in nature and is held at different temperatures and changing the length of steel beam and changing the cross-sectional properties of the beam as well. The change in the length of beam is under the imperfection scale factor of $L/1000$. This change in length of the beam sets the initial imperfections by varying the length of beam and in addition, this support the boundary conditions and types of loading mechanism and results are changed in each parametric study.

1.4-Outline/Framework of thesis

- The first chapter that is discussed above is about the introductory part related to fire, effect of fire on steel beam, problem statement and objectives etc.
- In second chapter, the main focus is Lateral Torsional Buckling Capacity of steel beam in depth. The second chapter discussed about design codes for LTB and the capacity of LTB beam under the action of fire.
- In third chapter, literature review is taken into consideration for better understanding of project and how previously different studies are performed.
- In chapter four, the simulation conducted using FEM modeling tools and ANSYS are presented and discussed in depth.
- The chapter five consists of discussion of results obtained from Modeling techniques and ANSYS and comparison of these obtained results.
- The chapter 6 presents the concluding remarks, summery of whole study and recommendations for the studies being conducted in future.

Chapter 2

2-Lateral Torsional Buckling (LTB)

2.1- Review of LTB

The phenomenon of buckling in an unstrained beam is noticed, in the case when a steel beam is subjected to load by fire that results in twisting and displacement which occurs in lateral direction is termed as Lateral Torsional Buckling in beam. If the beam is not provided some sufficient lateral support or lateral stiffness, as a result, the steel beam which is applied by load in its stiffer plane may have a tendency to buckle out of plane. In the case, when LTB phenomenon occurs, the steel beam is subjected to combined effect of fire loading and impact, then it became difficult to identify due to intricacy of two-load interaction effects. It is observed that due to action of fire loading, the elastic buckling occurs and due to impact, the plastic buckling in the steel beam occurs.

The steel beam is considered to be idealized when there is no out-of-plane deformation unless the applied moment due to external loading may reach the elastic buckling moment. At that point when applied moment approaches, then steel beam buckles out-of-plane resulting deflection of steel beam laterally and twisting occurs.

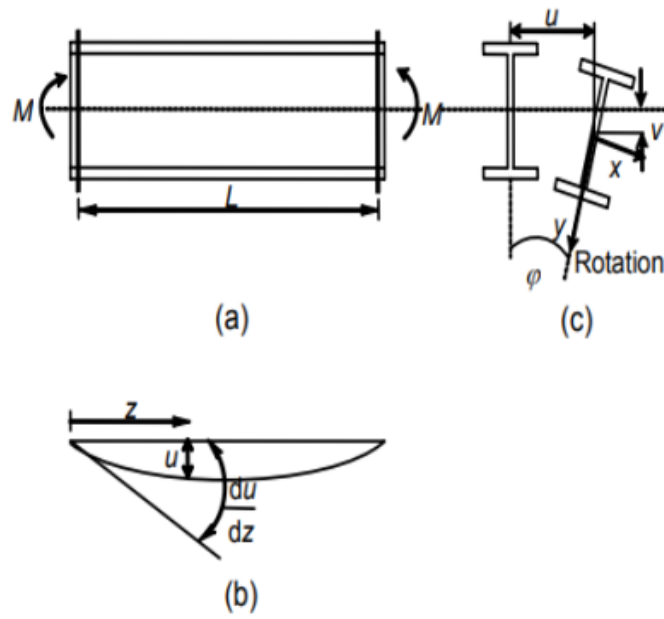


Fig. 2.1.1- LTB in I-Beam (a) Elevation, (b) longitudinal axis plan and (c) Cross-Section



Fig. 2.1.2- Lat. Buckling of Cantilever beam hanging with couple of weights

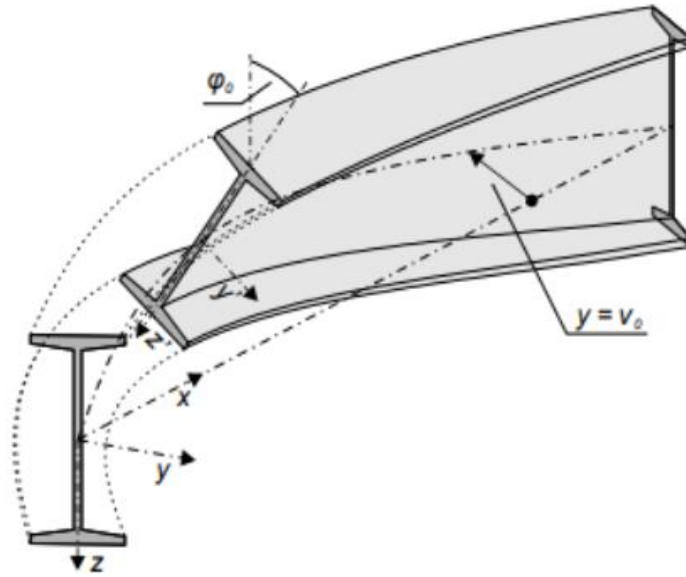


Fig. 2.1.3- Lat. Torsional Buckling of I-Beam viewing in 3D

The phenomenon of occurrence of Lateral Torsional in beam at any given load depends on the classes made for I-beam. These classes explained as;

Class 4

- Very Stocky Beams sections
- Inelastic Moment $>$ in-plane plastic Moment (M_p)
- In this case, the lateral torsional buckling has no effects or little effect the moment resistance of beams.
- This class exits when the process of necking starts in I-beam.

Class 3

- Semi-Compacted beams sections
- In this class, the inelastic moments occurs after the yielding moment and before the in-plane moment.
- This class exits when the process of strain-hardening starts in I-beam.

Class 2

- Slender beam sections
- Elastic Moment occurs in the beam before yielding.

All these cases are presented in the form of graph.

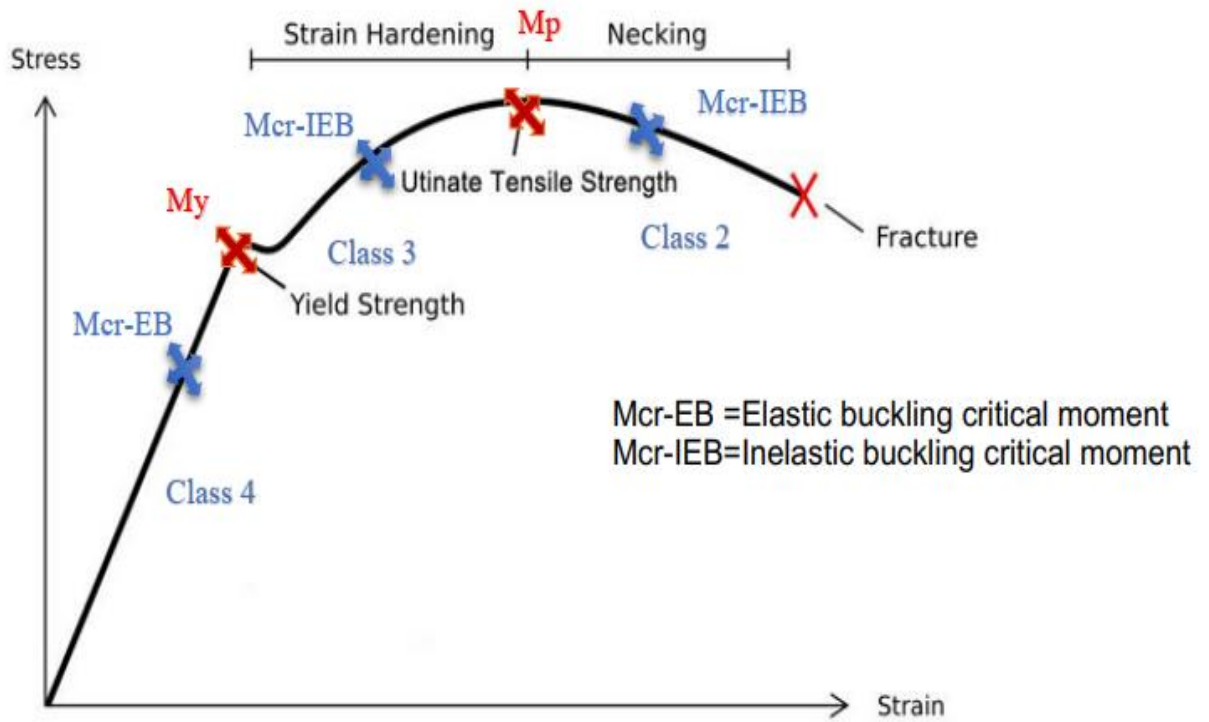


Fig. 2.1-4- Graph Representing the elastic/inelastic critical moment of I-beam

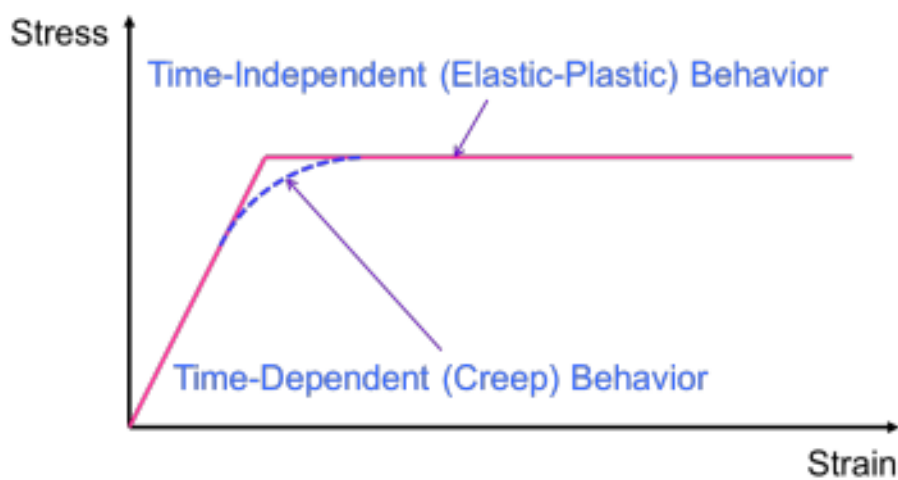


Fig. 2.1.5- Time dependent stress-strain behavior of Steel beam at high temperature.

2.2- Design Codes for LTB

The determination of LTB includes the followings, such as Critical Elastic Moment (M_{cr}), Non-dimensional slenderness λ_{LT} and buckling resistance moment $M_{b, Rd}$. To determine these parameters, first we need to find out the moment of inertia about z-axis (I_{zz}), about y-axis (I_{yy}), torsional constant (I_t) and warping constant (I_w).

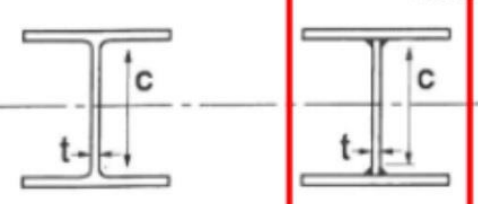
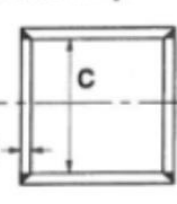
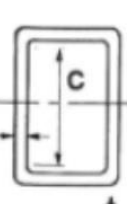
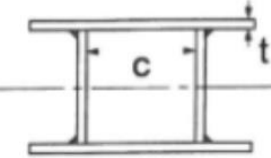
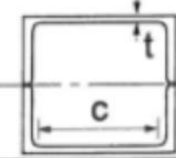
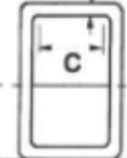
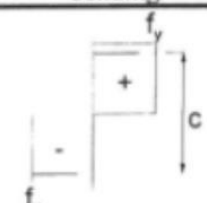
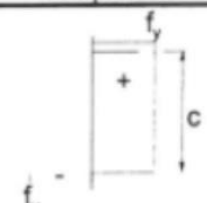
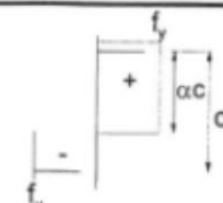
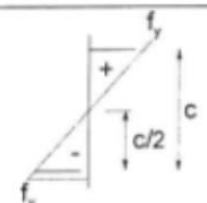
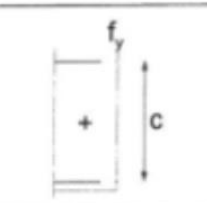
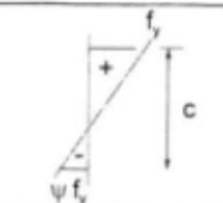
Class Classification

Table 5.2 (sheet 2 of 3): Maximum width-to-thickness ratios for compression parts

		Outstand flanges				
		Rolled sections		Welded sections		
Class	Part subject to compression	Part subject to bending and compression				
		Tip in compression		Tip in tension		
	Stress distribution in parts (compression positive)					
1	$c/t \leq 9\epsilon$	$c/t \leq \frac{9\epsilon}{\alpha}$	$c/t \leq \frac{9\epsilon}{\alpha\sqrt{\alpha}}$			
2	$c/t \leq 10\epsilon$	$c/t \leq \frac{10\epsilon}{\alpha}$	$c/t \leq \frac{10\epsilon}{\alpha\sqrt{\alpha}}$			
	Stress distribution in parts (compression positive)					
3	$c/t \leq 14\epsilon$	$c/t \leq 21\epsilon\sqrt{k_\sigma}$ For k_σ see EN 1993-1-5				
$\epsilon = \sqrt{235/f_y}$	f_y	235	275	355	420	460
	ϵ	1,00	0,92	0,81	0,75	0,716

Fig. 2.2.1- ratio of width to thickness for compression parts.

Table 5.2 (sheet 1 of 3): Maximum width-to-thickness ratios for compression parts

Internal compression parts						
						Axis of bending
						Axis of bending
Class	Part subject to bending	Part subject to compression	Part subject to bending and compression			
Stress distribution in parts (compression positive)						
1	$c/t \leq 72\epsilon$	$c/t \leq 33\epsilon$	when $\alpha > 0,5$: $c/t \leq \frac{396\epsilon}{13\alpha - 1}$ when $\alpha \leq 0,5$: $c/t \leq \frac{36\epsilon}{\alpha}$			
2	$c/t \leq 83\epsilon$	$c/t \leq 38\epsilon$	when $\alpha > 0,5$: $c/t \leq \frac{456\epsilon}{13\alpha - 1}$ when $\alpha \leq 0,5$: $c/t \leq \frac{41,5\epsilon}{\alpha}$			
Stress distribution in parts (compression positive)						
3	$c/t \leq 124\epsilon$	$c/t \leq 42\epsilon$	when $\psi > -1$: $c/t \leq \frac{42\epsilon}{0,67 + 0,33\psi}$ when $\psi \leq -1^{*)}$: $c/t \leq 62\epsilon(1 - \psi)\sqrt{(-\psi)}$			
$\epsilon = \sqrt{235/f_y}$	f_y	235	275	355	420	460
	ϵ	1,00	0,92	0,81	0,75	0,71

*) $\psi \leq -1$ applies where either the compression stress $\sigma \leq f_y$, or the tensile strain $\epsilon_t > f_y/E$

Fig. 2.2.2- ratio of width to thickness for compression parts.

Class Classification Calculation

Flange compression

$$\frac{cf}{tf\epsilon} = \frac{(90 - 7.5 - 2 * 8.5)}{2} < 9$$
$$= 3.57 < 9 \text{ flange in class 1}$$

Class 1 < 9

Class 2 < 10

Class 3 < 14

Class 4 > 14

Web compression

$$\frac{cw}{tw\epsilon} = \frac{h - 2tf}{tw\epsilon} < 33$$
$$\frac{cw}{tw\epsilon} = \frac{177 - 4 - 28.5}{7.5 * 0.81} < 33$$
$$= 26.4 < 33 \text{ web is class 1}$$

Class 1 < 33

Class 2 < 38

Class 3 < 42

Class 4 > 42

Classification when there is an effect of fire on I-beam

Compression in Flange

$$\frac{cfc}{tfc\epsilon} = \frac{(bc - twc)}{2} < 9$$

Bending in web

$$\frac{cwc}{twc\epsilon} = \frac{hc - 2tfc}{twc\epsilon} < 72$$

$$\epsilon = \sqrt{\frac{235}{fy}}$$

Here;

cw = Web Depth

cf= is the with of the flange

cwc= depth of web effected by fire

cfc= is the with of the flange effected by fire

ϵ =coefficient depending on fy.

Moment of Inertia (MOI)

MOI about Z-axis

MOI for Rectangular cross-section about z-z-axis is determined by;

$$I_{zz} = \frac{tf * B^3}{12}$$

MOI of I-beam having two flanges and one web is given by;

$$I_{zz} = 2 * \left(\frac{tf * B^3}{12} \right) + \frac{Bw * tw^3}{12}$$

MOI about Y-axis

MOI for Rectangular cross-section about y-y-axis is determined by;

$$I_{yy} = \frac{B * tf^3}{12}$$

MOI of I-beam having two flanges and one web is given by;

$$I_{yy} = 2 * \left(\frac{B * tf^3}{12} \right) + 2 * \left(B * tf * \left(\frac{H}{2} - \frac{tf}{2} \right)^2 \right) + \frac{tw * Bw^3}{12}$$

Torsional Rigidity (It)

Torsional rigidity of I-beam having two flanges and one web is determined by;

$$I_t = 2 * \left(\frac{B * tf^3}{3} \right) + \left(\frac{Bw * tw^3}{3} \right)$$

Torsional Wrapping

Torsional wrapping of I-beam having two flanges and one web is determined by;

$$I_w = \frac{B^3 * (H - tf)^2 * tf}{24}$$

M_{cr}

M_{cr} is the critical elastic moment that is determined by;

$$M_{cr} = \sqrt{\left(\frac{\pi^2 EI_{zz}}{L^2}\right) * \left(GIt + \left(\frac{\pi^2 EI_w}{L^2}\right)\right)}$$

Non-Dimensional Slenderness Ratio

The formula to determine non-dimensional slenderness ratio is;

$$\lambda_{LT} = \sqrt{\frac{(W_y * f_y)}{M_{cr}}}$$

$W_y = W_{ply}$ For Class 1 or 2 Cross Section

$W_y = W_{el, y}$ For Class 3 Cross Section

$W_y = W_{el, y}$ For Class 4 Cross Section

Plastic Section Modulus

$$W_{ply} = \left(B * tf * \frac{H - tf}{2}\right) * 2 + \left(\left(\frac{H}{2} - tf\right) * tw * \frac{\frac{H}{2} - tf}{2}\right) * 2$$

2.2.1-Stepwise Method conservatively used

Table 1- values for LTB curves for specific cross-sections Eurocodes (Table 6.4)

Cross-section	Limits	Buckling Curve
Rolled I-sections	$h/b \leq 2$	a
	$h/b > 2$	b
Welded I-sections	$h/b \leq 2$	c
	$h/b > 2$	d
Other cross-sections	-	d

Step 1

Choose the cross-section to study.

Step 2

From the selected cross-section, set the limits by using height, width and depth parameters of cross-section. This will help to get the buckling curve.

Table 2- imperfection factor values for LTB. (Euro Codes Design Table 6.3)

Buckling curve	a	b	c	d
Imperfection factor - α_{LT}	0.21	0.34	0.49	0.76

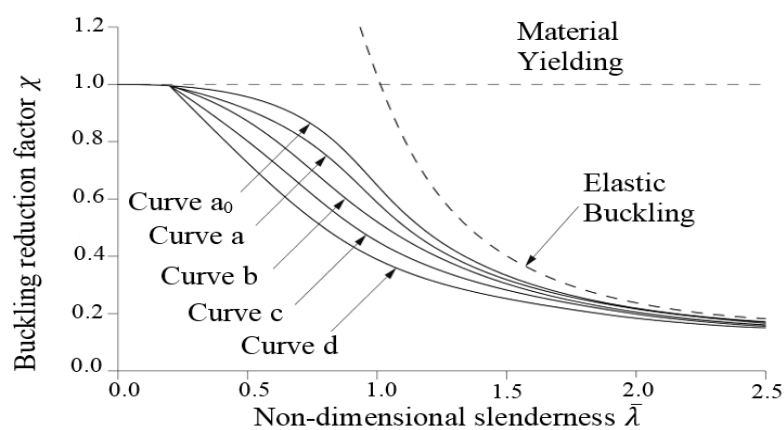


Fig. 2.2.1- Buckling Curves

Table 3- A_m/V values of any cross-section with c time for temperature

Tabell 13.7 Ståltemperatur i uisolert komponent under ISO brann [13.6]

A_m/V (m ⁻¹)	400	200	100	60	40	25
Tid (min)	Ståltemperatur °C					
0	20	20	20	20	20	20
5	430	291	177	121	90	65
10	640	552	392	276	204	142
11	661	587	432	308	228	159
12	678	616	469	340	253	177
13	693	642	503	371	278	194
14	705	663	535	402	303	212
15	716	682	565	432	328	230
16	725	698	591	460	353	249
18	736	721	638	513	401	286
20	754	734	676	561	447	323
22	780	744	706	604	491	360
24	799	767	726	641	532	396
26	813	792	735	674	570	431
28	826	813	746	701	604	466
30	837	828	767	721	636	498

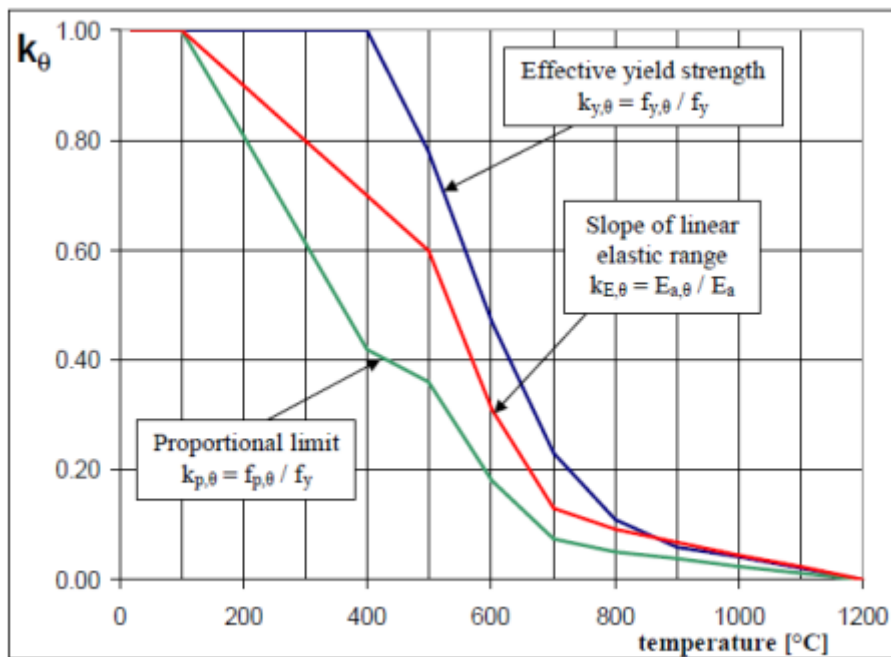


Fig. 2.2.2- temperature VS reduction factor

Table 4- reduction factors at elevated temperature for stainless steel

Steel Temperature θ_a [°C]	$k_{E,\theta} = \frac{E_{a,\theta}}{E_a}$	$k_{p,\theta} = \frac{f_{ap,\theta}}{f_{ay}}$	$k_{y,\theta} = \frac{f_{ay,\theta}}{f_{ay}}$	$k_{u,\theta} = \frac{f_{au,\theta}}{f_{ay}}$
20	1,00	1,00	1,00	1,25
100	1,00	1,00	1,00	1,25
200	0,90	0,807	1,00	1,25
300	0,80	0,613	1,00	1,25
400	0,70	0,420	1,00	
500	0,60	0,360	0,78	
600	0,31	0,180	0,47	
700	0,13	0,075	0,23	
800	0,09	0,050	0,11	
900	0,0675	0,0375	0,06	
1000	0,0450	0,0250	0,04	
1100	0,0225	0,0125	0,02	
1200	0	0	0	

Reduction Factor

The reduction factor used in case of LTB is determined in accordance with the formula given in Eurocodes 3.

$$X_{LT,fi} = \frac{1}{\phi_{LT,\theta,com} + \sqrt{[\phi_{LT,\theta,com}]^2 - [\lambda_{LT,\theta,com}]^2}} \dots\dots\dots (I)$$

And,

$$\phi_{LT,\theta,com} = \frac{1}{2} \left[1 + \alpha \lambda_{LT,\theta,com} + (\lambda_{LT,\theta,com})^2 \right] \dots\dots\dots (II)$$

$$\alpha = 0.65 \sqrt{235/f_y} \dots\dots\dots (III)$$

Here, α is the imperfection factor

Non-Dimensional Slenderness Ratio

$$\lambda_{LT,\theta,com} = \lambda_{LT} \left[\frac{k_{y,\theta,com}}{k_{E,\theta,com}} \right]^{0,5} \dots\dots\dots (IV)$$

Lat. Torsional Buckling Moment

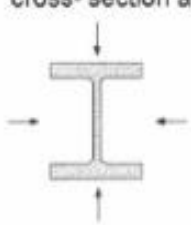
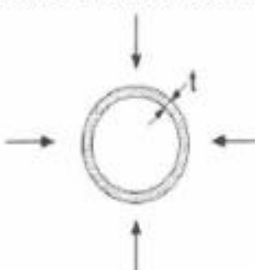
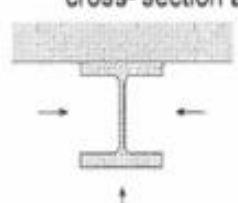

$$M_{fi,t,Rd} = \frac{X_{LT,fi} W_{pl,y} k_{y,\theta,com} f_y}{\gamma_{M,fi}} \dots\dots\dots (V)$$

$W_{pl,y}$ = Plastic Section Modulus

$k_{y,\theta,com}$ = Reduction factor at maximum temperature

$\gamma_{M,fi}$ = Partial Safety factor for fire

Table 5- Determination of A_m/V for temperature

<p>Open section exposed to fire on all sides:</p> $\frac{A_m}{V} = \frac{\text{perimeter}}{\text{cross-section area}}$ 	<p>Tube exposed to fire on all sides: $A_m/V = 1/t$</p> 
<p>Open section exposed to fire on three sides:</p> $\frac{A_m}{V} = \frac{\text{surface exposed to fire}}{\text{cross-section area}}$ 	<p>Hollow section (or welded box section of uniform thickness) exposed to fire on all sides:</p> <p>If $t \ll b$: $A_m/V \approx 1/t$</p> 
<p>I-section flange exposed to fire on three sides:</p> $A_m/V = (b + 2t_f)/(bt_f)$ <p>If $t \ll b$: $A_m/V \approx 1/t_f$</p>	<p>Welded box section exposed to fire on all sides:</p> $\frac{A_m}{V} = \frac{2(b + h)}{\text{cross-section area}}$

Design Steps

- I.** Select the cross section and determine its geometrical properties like MOI, slenderness ratio, gross area, volume etc.
- II.** Choose the case of fire, at which point/region, cross-section is exposed to fire. Take the ratio of perimeter and volume.
- III.** Use table 03, we have value of time and A_m/V , so look upon the corresponding temperature from the table 03. In this way, value of temperature is determined.
- IV.** There is a fig 2.2.2 in which graph is in between reduction factor and temperature. $K_{p,e}$ is known from the graph and find tensile limit at an elevated temperature $f_{p,e}$.
- V.** Find the value of reduction factor and non-dimensional slenderness ratio by using eq. (I) to (IV).
- VI.** Reduced buckling moment M_{brd} is calculated using the formula (V).

2.3-Capacity of LTB beam at elevated temperature

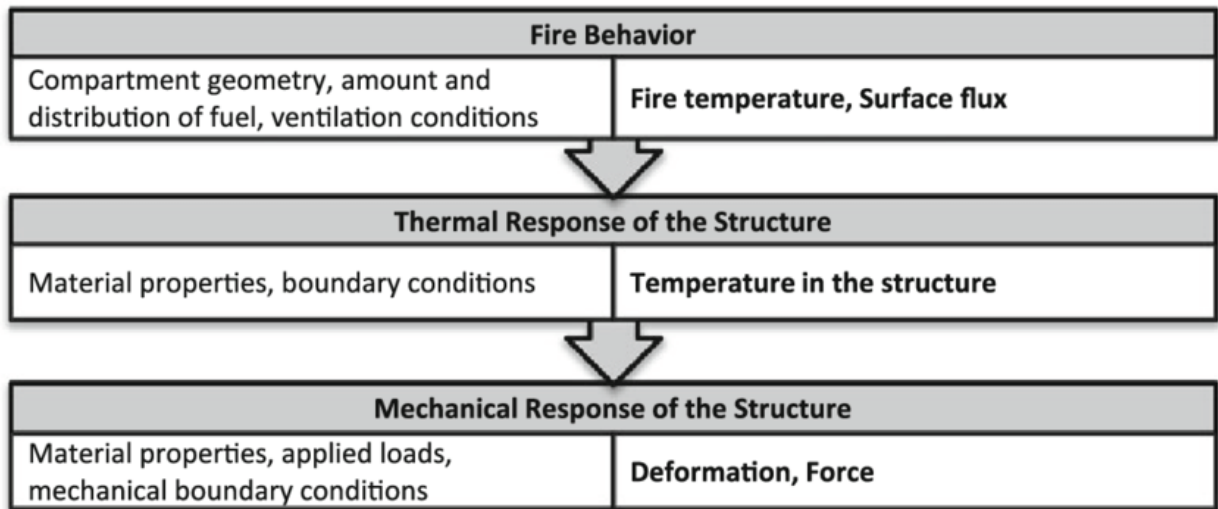
In the steel girder, there are two portions, one is web and others are flanges. When load is applied on the beam either in the form of point load, distributed load or loading caused by fire, a situation may arise at the temperature when shear stress applied on the cross-section increases the strength of cross-section, there at first beam may start buckle as shown in the fig. below.



Fig. 2.3.1- Failure of beam due to buckling

Increase the temperature of the any structural steel member can disturbs its physical and mechanical properties. The material properties that are disturbed are ultimate strength, elastic modulus, yield strength and coefficient of thermal expansion. There is an excessive plastic deformation produced in the beam due to an elevated temperature due to which twisting or bending produced in steel beams.

Table 5- the responses of steel structure members under high thermal actions



Steel show very complex behavior when exposed to fire or elevated temperature. This complexity in structure depends on the restraints at the end of any structural member.

When the temperature of steel is continuous to increase, a stage has come when it starts losing its strength. When temperature exceeds above 350°C then there is start of losing the strength factor. When it reaches to 550°C, at this time, the steel almost lost its 40% strength. The complete failure occurs when temperature reaches above 1150°C, and structure will collapse.

The whole phenomenon is elaborated in the graph shown below.

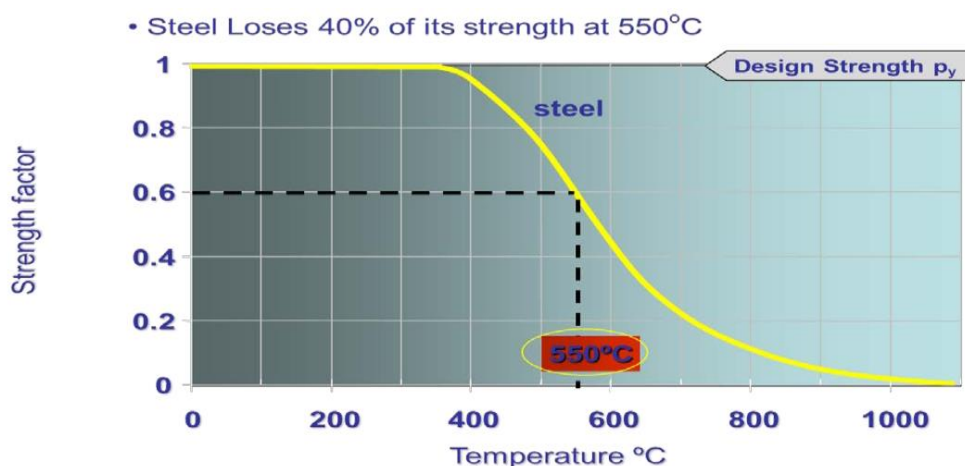


Fig. 2.3.2- the variation of strength of steel by increasing temperature

Chapter 3

3- Analytical Approach

3.1- Need for Analysis

Steel when exposed to local fire, withstand the fire load at some level and the members of steel structure start buckling due to extra fire loading applied on it. Figure 3.1-01 illustrates that the load is applied in the form of uniformly distributed load (UDL) and beneath the beam, there is a local fire. Due to this local fire, the steel beam start buckling and damaging of one member of any structure, can destabilize it and chances of collapse of structure in this way. And we know that most of the steel structures are proposed for industrial buildings and in industries, there are more chances of spreading of fire, thus we need to design the steel structure against fire. The main goal of fire design is protecting the structure and society from economic and livelihood damage that could be awful.

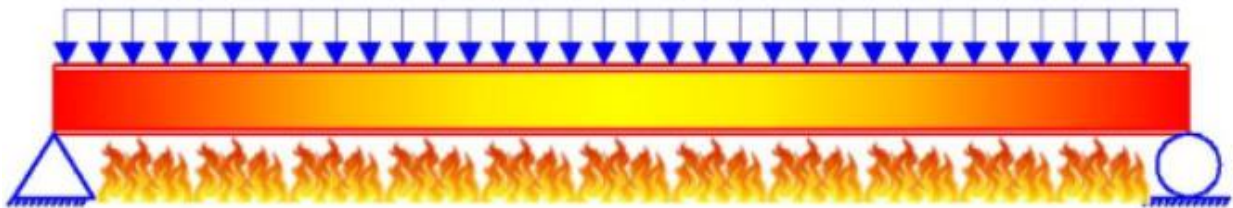


Fig. 3.1.1- steel beam acting under the fire when upward load is applied

If the thickness of beam is high, then buckling can be avoided but structure may be heavy and more expensive. In this case, the steel beam also damages as shown in figure 3.1-02 because of the phenomenon of rusting.

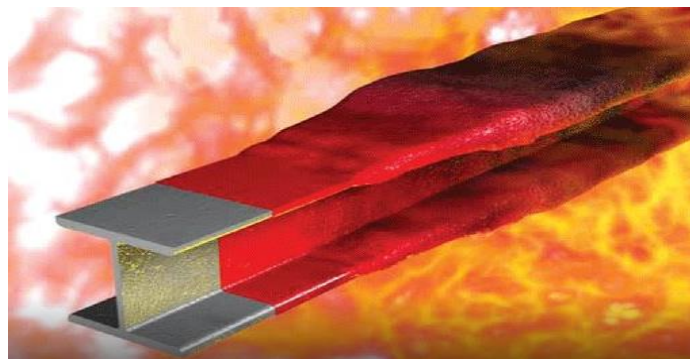


Fig. 3.1.2- Steel beam at high temperature

3.2- Analysis Criteria

During the design of steel beam, following three criteria are required to design so that fire can be resisted by beam or structural members, when it spreads.

- 1) First parameter is **R** which is the function of load bearing resistance
- 2) Thermal Insulation **I**
- 3) **E** which is the function of Integrity Spreading.

The above-mentioned criteria are used independently or in a coupled manner.

At the uniform distribution of temperature/fire on structural beam, a temperature comes when beam start to fail and this temperature is called critical temperature. This temperature is denoted by Θ_{crit} .

For example, in the case when there is required mechanical resistance due to fire, then structural beams are designed and erected in such a way by maintaining the load-bearing function **R** of the beam. The following equations written below explains the satisfaction of load-bearing function of any structure.

3.2.1-For Load-Bearing Resistance

$$E_{f_i,d,t} \leq R_{f_i,d,t}$$

3.2.2-Time

$$t_{f_i,d} \leq t_{f_i,req.}$$

This relation is mostly used for advanced computational studies.

3.2.3-Temperature

$$\Theta_{Cr,d} \leq \Theta_d$$

Where;

$E_{f_i,d,t}$ = Design Effect of fire at any given time

$R_{f_i,d,t}$ = Design Resistance offered by steel beam at any time during fire

$\Theta_{Cr,d}$ = Critical Temperature

Θ_d = Design Temperature

$t_{f_i,d}$ = Designed Time

$t_{f_i,req.}$ = Time required for approach of critical temperature

3.3- Static Linear Analysis

Static linear analysis is carried out when there is maximum stress applied on the beam and resulting maximum displacement is observed because of application of stress. In most cases, maximum flexural stress is determined to analyze the static behavior of beam.

The maximum flexural/bending stress is determined by following equation.

$$\sigma_{max} = \frac{My}{I_{yy}}$$

Where,

My is the maximum moment applied to the beam.

I_{yy} is moment of Inertia along y-axis.

Y is the centroidal distance from neutral axis to top of beam.

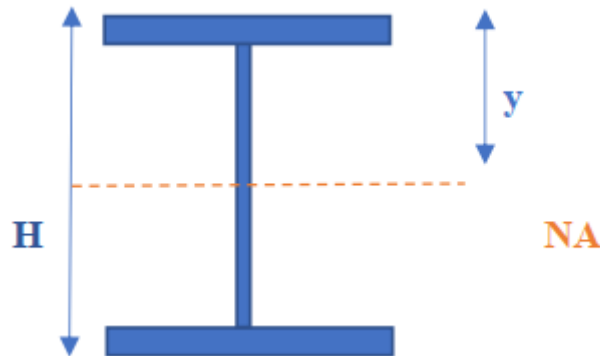


Fig. 3.3.1- Cross-section of Steel I-beam for static analysis.

3.4- Critical Elastic Moment, Slenderness Ratio and LTB Moment Capacity

M_{cr} is the critical elastic moment, that is determined by;

$$M_{cr} = \sqrt{\left(\frac{\pi^2 EI_{zz}}{L^2}\right) * \left(GIt + \left(\frac{\pi^2 EI_w}{L^2}\right)\right)}$$

The formula to determine non-dimensional slenderness ratio is;

$$\lambda_{LT} = \sqrt{\frac{(W_y * f_y)}{M_{cr}}}$$

$W_y = W_{ply}$ For Class 1 or 2 Cross Section

$W_y = W_{el, y}$ For Class 3 Cross Section

$W_y = W_{el, y}$ For Class 4 Cross Section

Plastic sectional modulus of beam is given by,

$$W_{ply} = \left(B * tf * \frac{H - tf}{2} \right) * 2 + \left(\left(\frac{H}{2} - tf \right) * tw * \frac{H}{2} \right) * 2$$

The reduction factor used in case of LTB is determined in accordance with the formula given in Euro Codes 3.

$$X_{LT,fi} = \frac{1}{\phi_{LT,\theta,com} + \sqrt{[\phi_{LT,\theta,com}]^2 - [\lambda_{LT,\theta,com}]^2}}$$

And,

$$\phi_{LT,\theta,com} = \frac{1}{2} \left[1 + \alpha \lambda_{LT,\theta,com} + (\lambda_{LT,\theta,com})^2 \right]$$

$$\alpha = 0.65 \sqrt{235/f_y}$$

Non-Dimensional Slenderness Ratio

$$\lambda_{LT,\theta,com} = \lambda_{LT} \left[\frac{k_{y,\theta,com}}{k_{E,\theta,com}} \right]^{0,5}$$

Lateral Torsional Buckling Moment

$$M_{fi,t,Rd} = \frac{X_{LT,fi} W_{pl,y} k_{y,\theta,com} f_y}{\gamma_{M,fi}}$$

$W_{pl,y}$ = Plastic Section Modulus

$k_{y,\theta,com}$ = Reduction factor at maximum temperature

$\gamma_{M,fi}$ = Partial Safety factor for fire

3.5- Step by step procedure for design calculation of all cases

- VII.** Select the cross section and determine its geometrical properties like MOI, slenderness ratio, gross area, volume etc.
- VIII.** Choose the case of fire, at which point/region, cross-section is exposed to fire. Take the ratio of perimeter and volume.
- IX.** Use table 03, we have value of time and Am/V , so look upon the corresponding temperature from the table 03. In this way, value of temperature is determined.
- X.** There is a fig 2.2.2 in which graph is in between reduction factor and temperature. $K_{p,\theta}$ is known from the graph and find tensile limit at an elevated temperature $f_{p,\theta}$.
- XI.** Find the value of reduction factor and non-dimensional slenderness ratio by using eq. (I) to (IV).
- XII.** Reduced buckling moment M_{brd} is calculated using the formula (V).

All these equations I, II, III, IV, V and VI are written in chapter 2.

Chapter 4

4-Finite Element Modeling

4.1-ANSYS Simulations

In order to understand the buckling stainless-steel beam response with fire and to evaluate the impact of important parameters, a study using numerical modeling was conducted. The massive deflection response of axially restrained steel I-beams at extreme temperatures was investigated using numerical modelling. The finite element (FE) tool ANSYS was used to model the behavior of structures of steel in fire and I-beams of stainless steel which are simply supported, which has been effectively used in prior similar research. Comparisons with the results of fire tests on constrained carbon (steel) beams were done to prove the validity of the proposed FE models.

The analysis of steel I-beam limit states using nonlinear FEM is a difficult issue that necessitates the processing of huge volumes of data. Stability problems with defects, such as geometrical and material imperfections, can be studied using nonlinear geometrical and material solutions. As the FEM progresses, Additional data should be added as software input.

The anisothermal fire tests required the creation of a consecutively coupled thermal-stress analysis as part of the modelling method. To estimate the structural reaction in the action of load and temperature, the nonlinear thermal analysis was first performed to compute the temperature increase in the beams, after that another analysis was performed based on geometry and materially.

In the heat transfer model, the furnace “temperature-time curve” was used for exposed surfaces of the beam specimens, and variation of temperature was modeled using the three methods of heat transfer (convection, radiation, conduction).solely, the bottom &web flanges of the beam specimens were unvieled to fire to imitate the experimental conditions where the top flange

was shielded, and temperature growth in the top flange was reproduced only through conduction.

The thermal analysis model's temperature-time curves were then used to the stress analysis model to analyze the restrained steel beams structural reaction when temperatures rose.

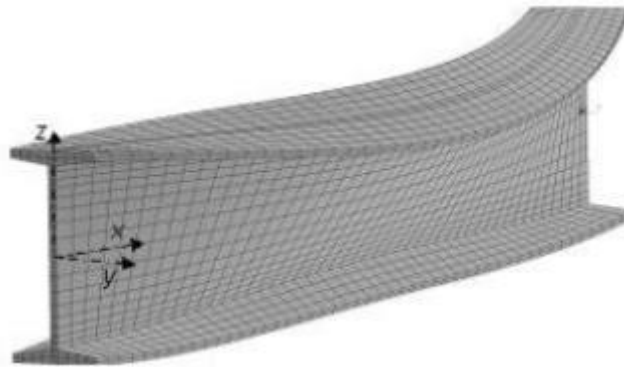


Fig. 4.1.1- Computational Model used in ANSYS

4.1.1-Methods of Performing LTB on ANSYS

There are three different ways for the determination and checking the LTB behavior of I-beam.

1. First, perform the static linear analysis and buckling analysis to form the buckling mode in LTB and we can get the LTB model to perform the buckling analysis on it by elevating the temperature for different ranges.
2. The second way is to get the LTB behavior, by the application of lateral load and evenly distributed load on the bottom flange and top of the beam to get the LTB behavior.
3. Perm the non-linear analysis by making a computational model with an initial boundary values and conditions.

4.2-Finite Element Simulation

ANSYS workbench 2020 is an FEM modeling software that is widely used for simulation. We use this software to get models and important results for LTB behavior.

1. Engineering data
2. Geometry
3. Model
4. Setup
5. Solution
6. Results

4.2.1-Flow chart used for Static Analysis in ANSYS

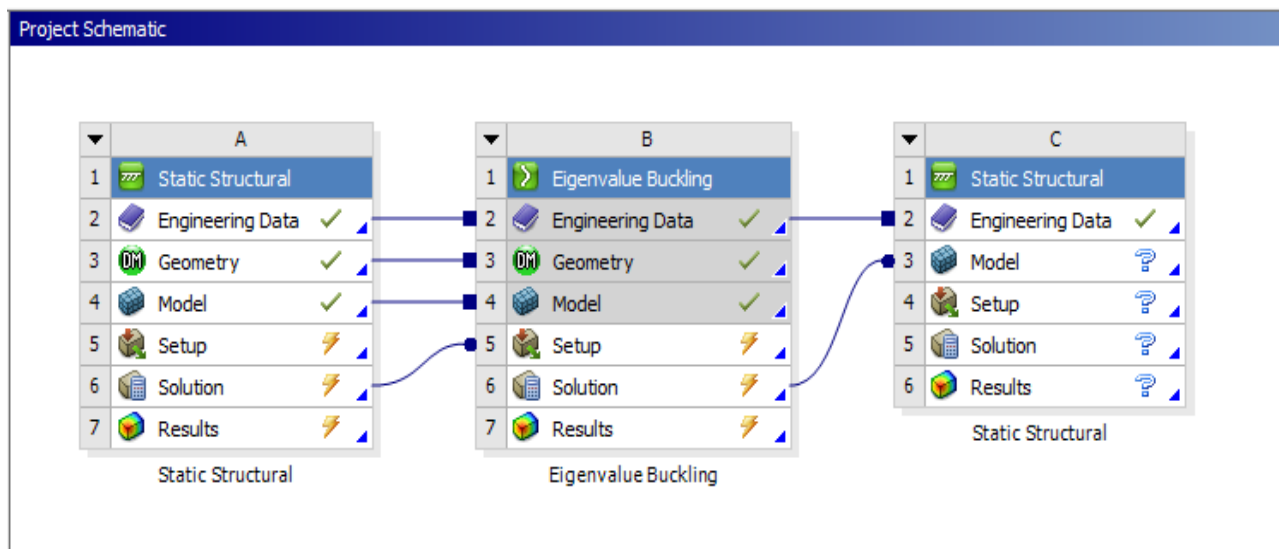


Fig. 4.2.1.1- Flow chart used for Static Analysis in ANSYS

4.2.2-Mechanical Properties

The screenshot displays the ANSYS Workbench 2020 interface. The main window is titled "nocorr - Workbench" and shows the "Engineering Data Sources" tab. The left sidebar contains a "Toolbox" with various material property categories, including "Physical Properties", "Linear Elastic", "Hyperelastic Experimental Data", "Hyperelastic", "Chaboche Test Data", "Plasticity", "Creep", "Life", "Strength", "Gasket", "Viscoelastic Test Data", "Viscoelastic", "Shape Memory Alloy", "Geomechanical", "Damage", "Cohesive Zone", "Fracture Criteria", "Crack Growth Laws", and "Custom Material Models".

The central area shows the "Engineering Data Sources" table with the following data:

	A	B	C	D
1	Data Source		Location	Description
3	Granta Design Sample Materials			More than 100 sample datasheets for standard engineering materials, including polymers, metals, ceramics and woods. Courtesy of Granta Design.

Below this is the "Outline of Granta Design Sample Materials" table:

	A	B	C	D	E
1	Contents of Granta Design Sample Materials	Add	source		Description
36	High strength low alloy steel (HSLA)				High strength low alloy steel, cold rolled Sample materials data from Granta Design. Additional data and information available through

The bottom section shows the "Properties of Outline Row 36: High strength low alloy steel (HSLA)" table:

	A	B	C
1	Property	Value	Unit
2	Density	7850	kg m ⁻³
3	Isotropic Secant Coefficient of Thermal Expansion		
4	Coefficient of Thermal Expansion	1.2E-05	C ⁻¹
5	Isotropic Elasticity		
6	Derive from	Young...	
7	Young's Modulus	2.1E+11	Pa
8	Poisson's Ratio	0.3	

On the right side, there are two panels: "Table of Properties Row 5: Isotropic Elastic" and "Chart: No data". The "Table of Properties Row 5: Isotropic Elastic" panel shows the following data:

	A	B
1	Young's Modulus (Pa)	Poisson's Ratio
2	2.1E+11	0.3

The status bar at the bottom indicates "Ready" and shows "Job Monitor...", "Show Progress", and "Show 0 Messages".

Fig. 4.2.2.1- Mechanical Properties in ANSYS Workbench 2020

4.2.3-Geometry

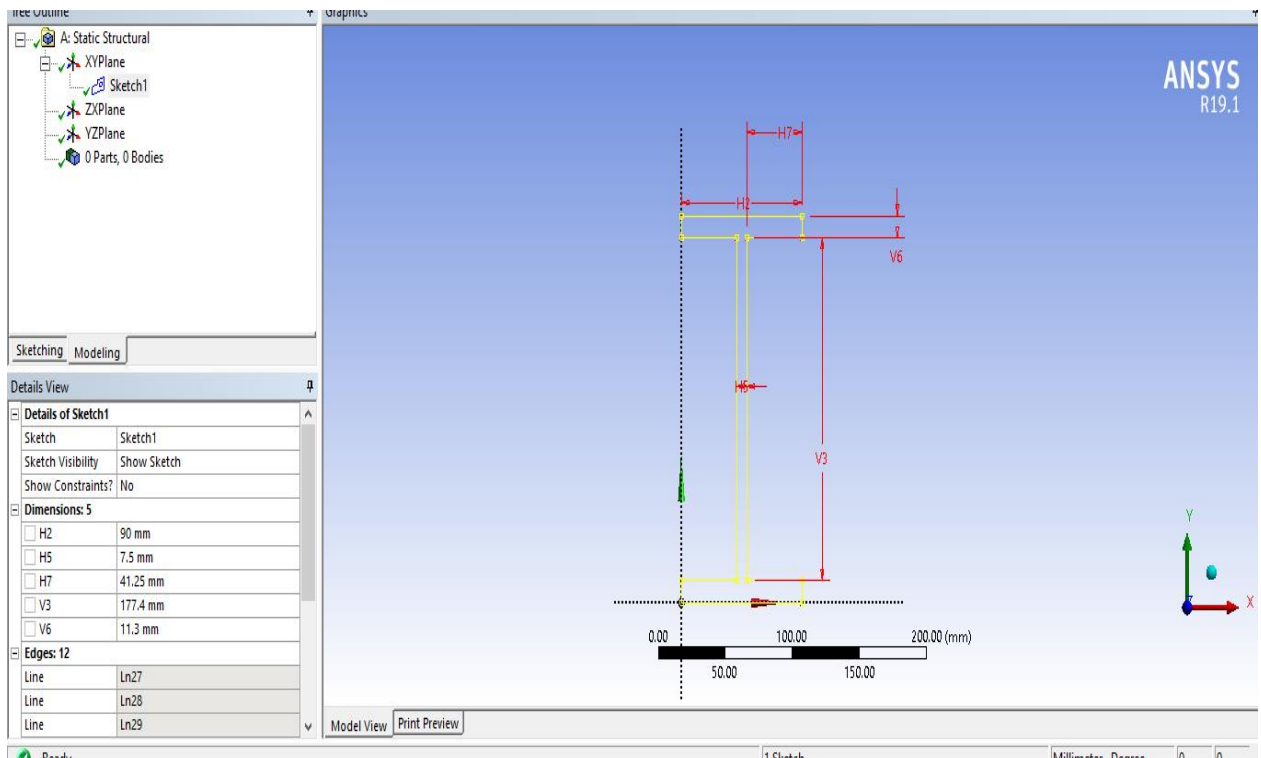


Fig. 4.2.3.1- Geometry

4.2.4-Meshing

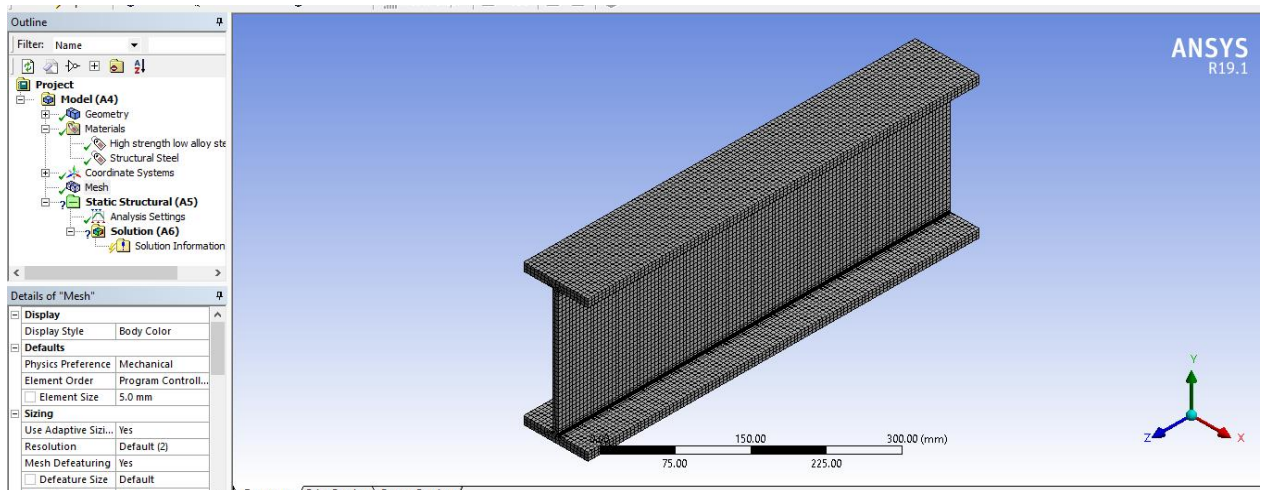


Fig. 4.2.4- Meshing for finding elemental density

4.2.5-Load

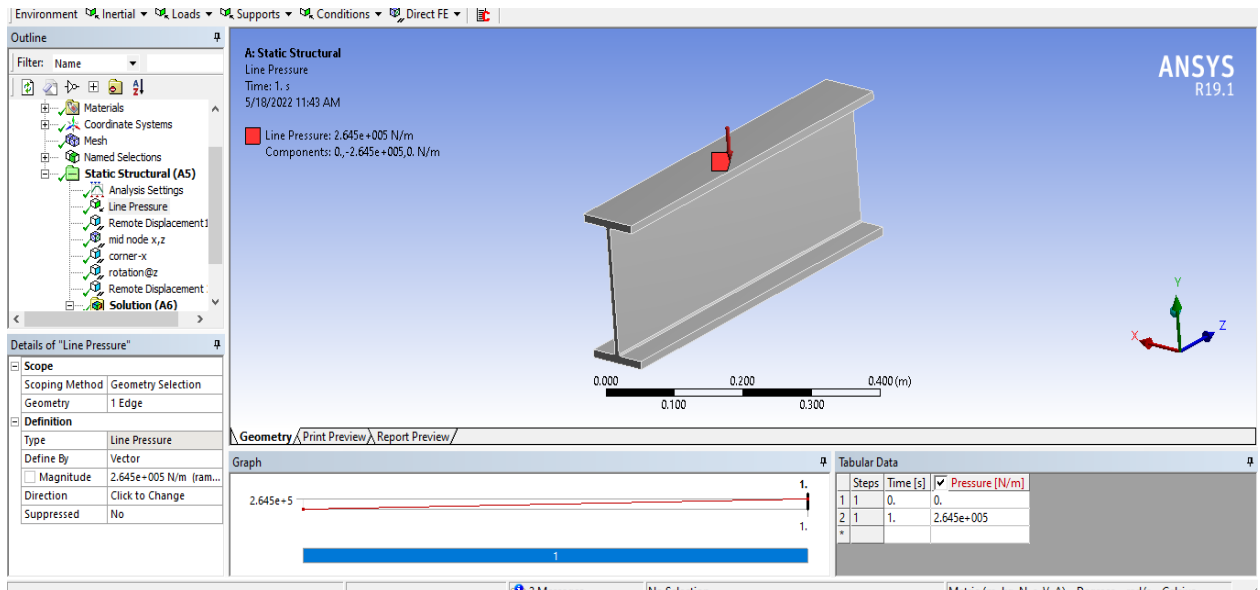


Fig. 4.2.5.1- Load applied in ANSYS Workbench

4.2.6-Boundary conditions

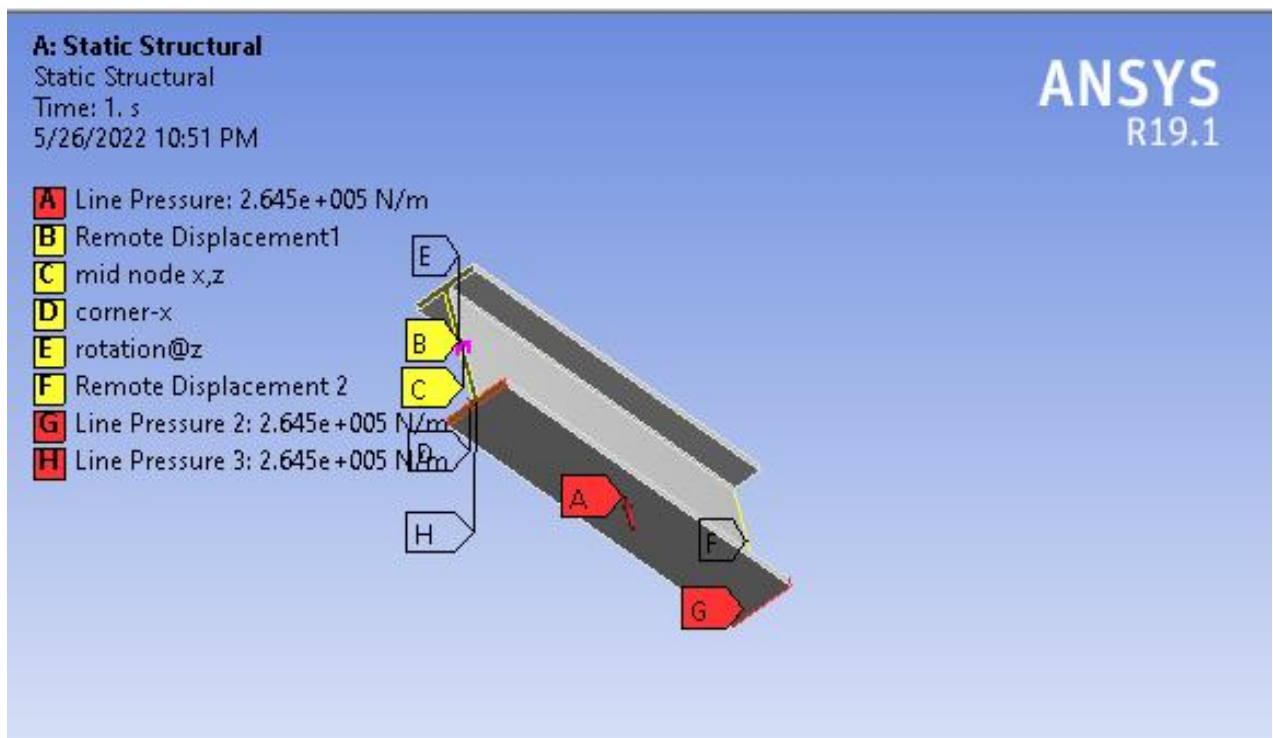


Fig. 4.2.6.1- Boundary Condition

Table 6- Assumptions for boundary value condition for FEM Model

	U_x	U_y	U_z	UR_x	UR_y	UR_z
Corner_X	0	0	-	-	-	-
Rotation_@Z	-	0	-	-	-	-
Mid_Node_X, Z	0	-	0	-	-	-
Remote Displacement 1	-	0	-	-	-	-
Remote Displacement 2	-	0	-	-	-	-

In this table,

Displacement along the direction of x-axis is U_x

Displacement along the direction of y-axis is U_y

Displacement along the direction of z-axis is U_z

Rotation along the direction of x-axis is UR_x

Rotation along the direction of y-axis is UR_y

Rotation along the direction of z-axis is UR_z

4.3- Cases; at different elevated temperature

There are five steps for modeling in ANSYS. These are;

1. Temperature Loading
2. Deformation Check
3. Eigenvalue Deformation
4. Plotting of Graph

4.3.1-For case of temperature 500°C

Loading Temperature 500°C

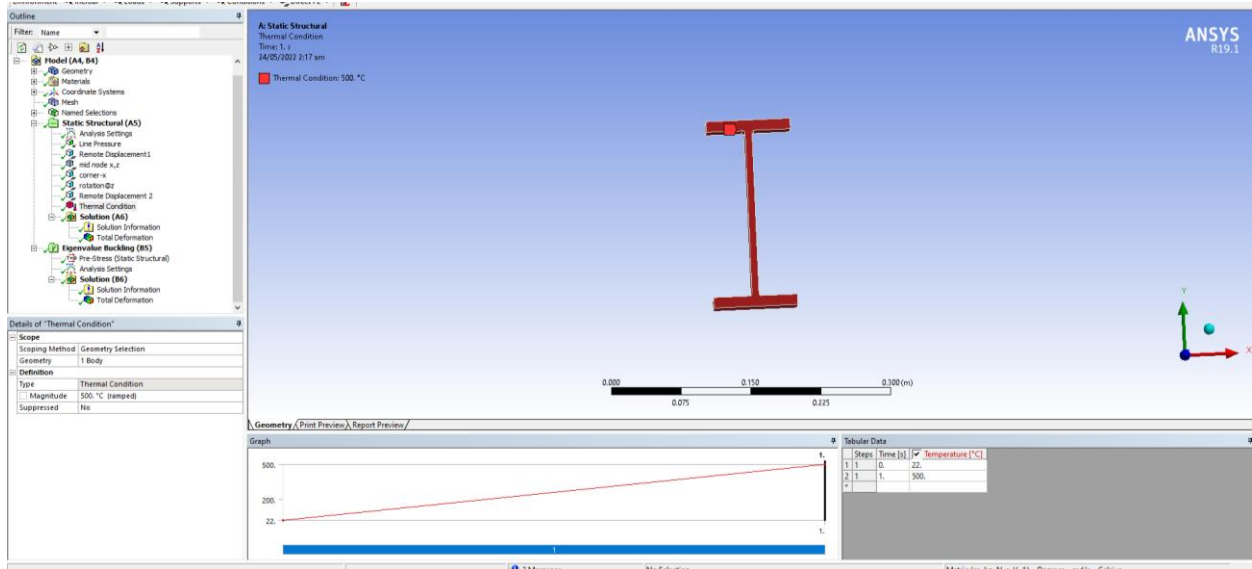


Fig. 4.3.1.1- Loading Temperature 500°C in ANSYS workbench

Deformation

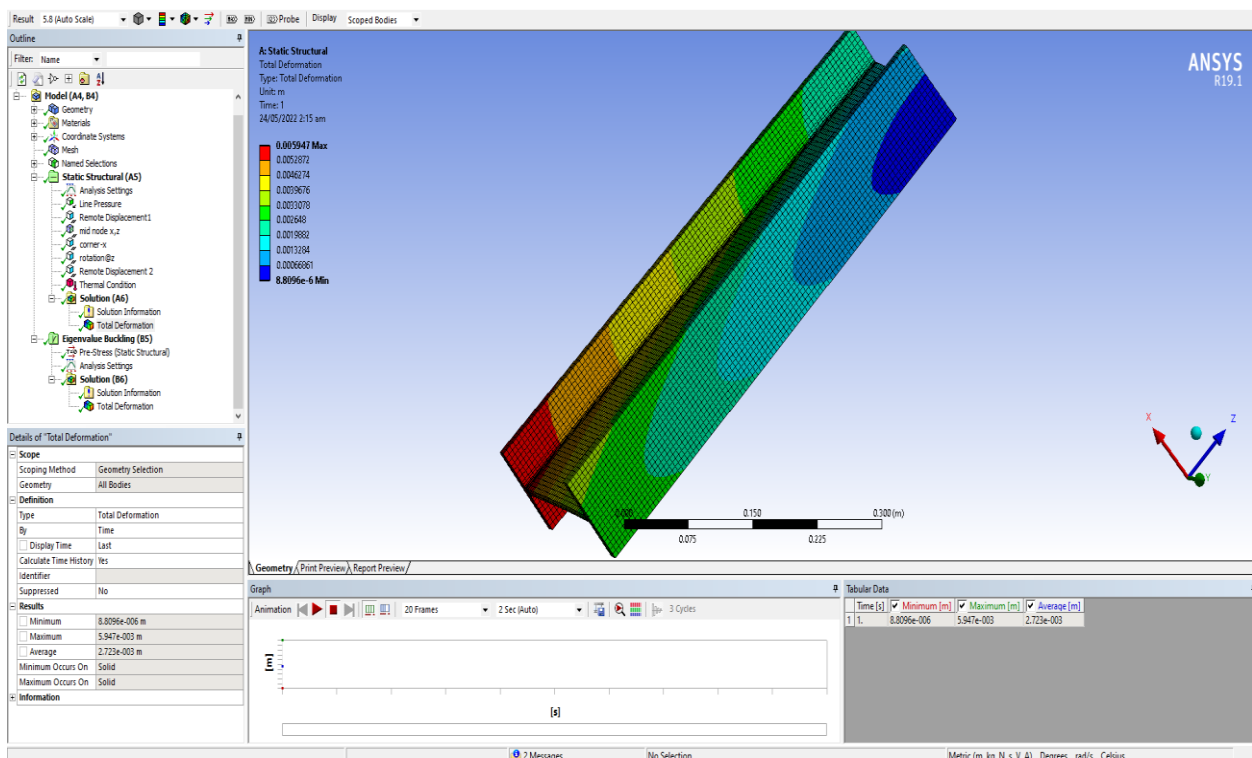


Fig. 4.3.1.2- Deformation resulting from Loading

Eigenvalue deformation

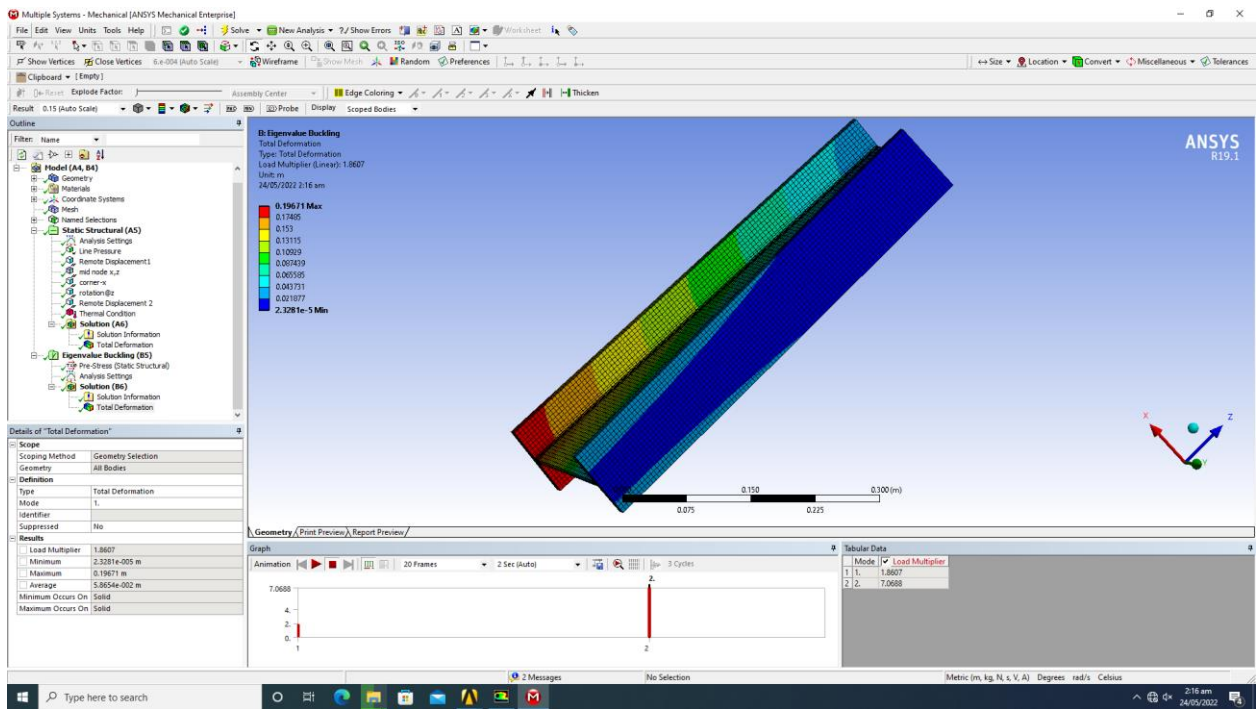


Fig. 4.3.1.3- Eigenvalue Deformation

Graph

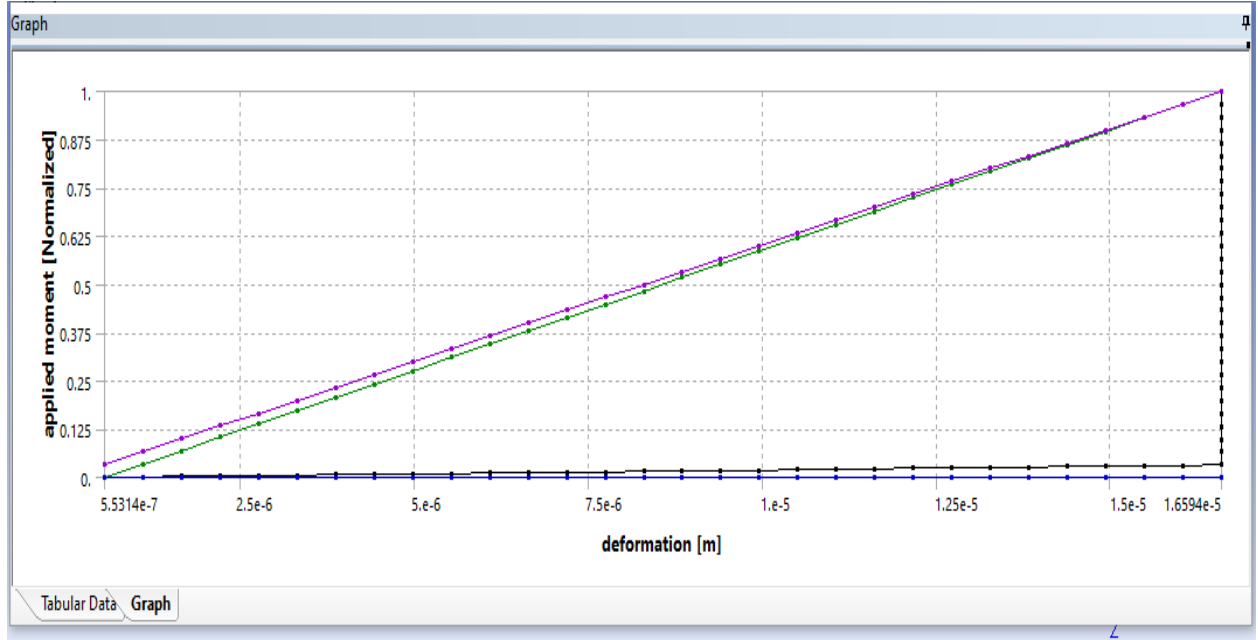


Fig. 4.3.1.4- Graph plotted between applied moment and deformation at 500°C

4.3.2-For case Of 800°C

Temperature load of 800°C

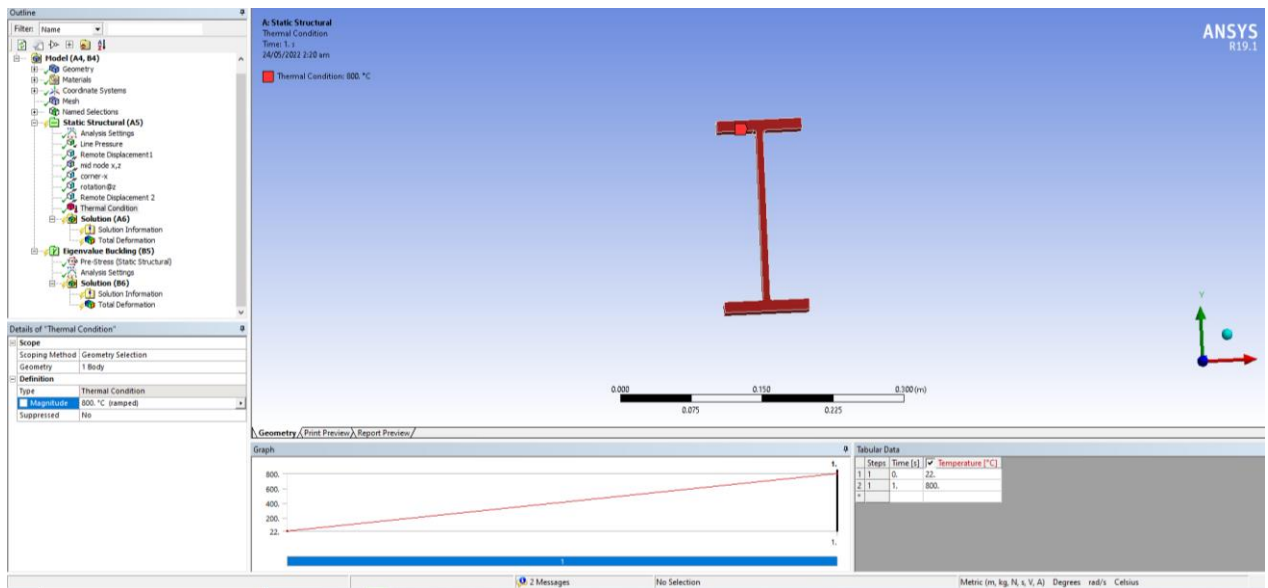


Fig. 4.3.2.1- Loading Temperature 800°C in ANSYS workbench

Deformation

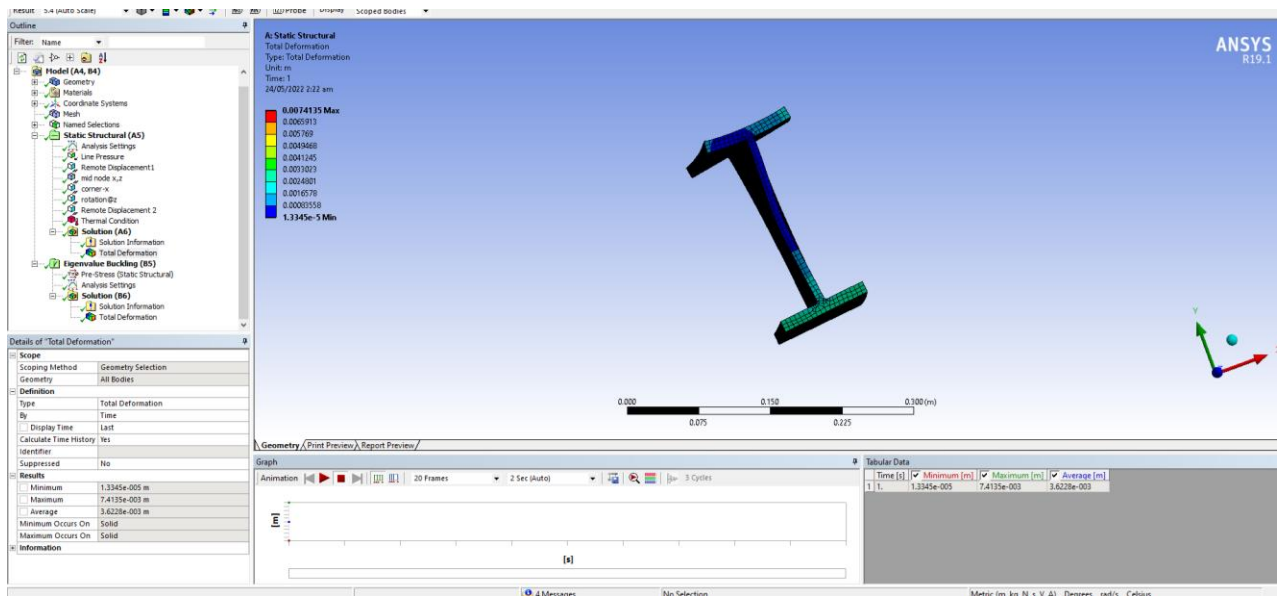


Fig. 4.3.2.2- Deformation resulting from Loading

Eigenvalue buckling

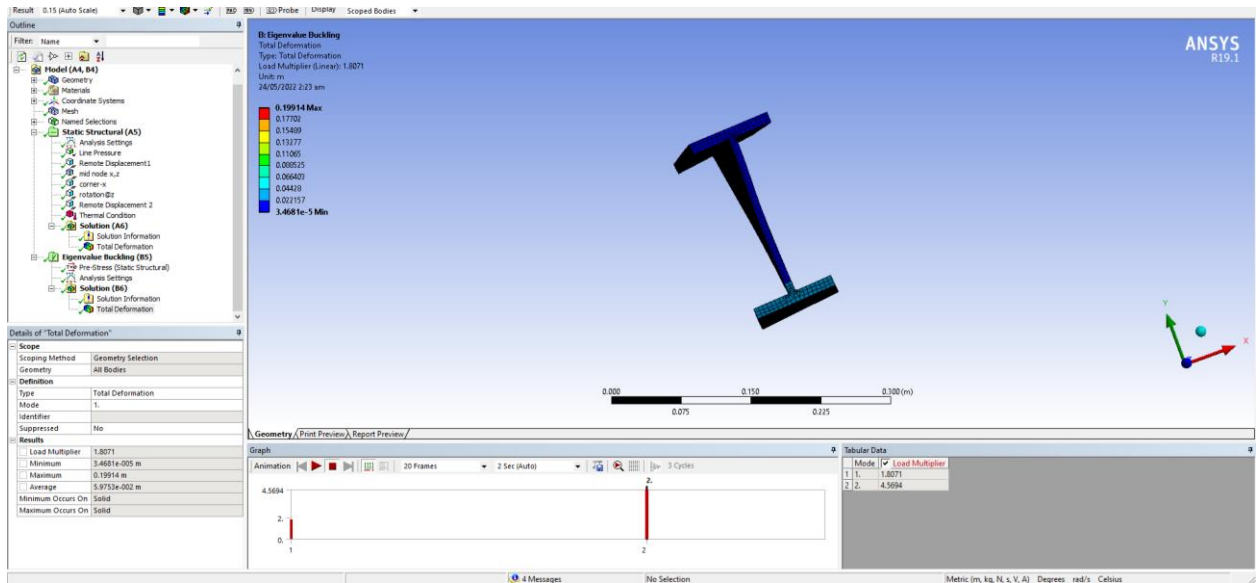


Fig. 4.3.2.3- Eigenvalue Deformation

Graph

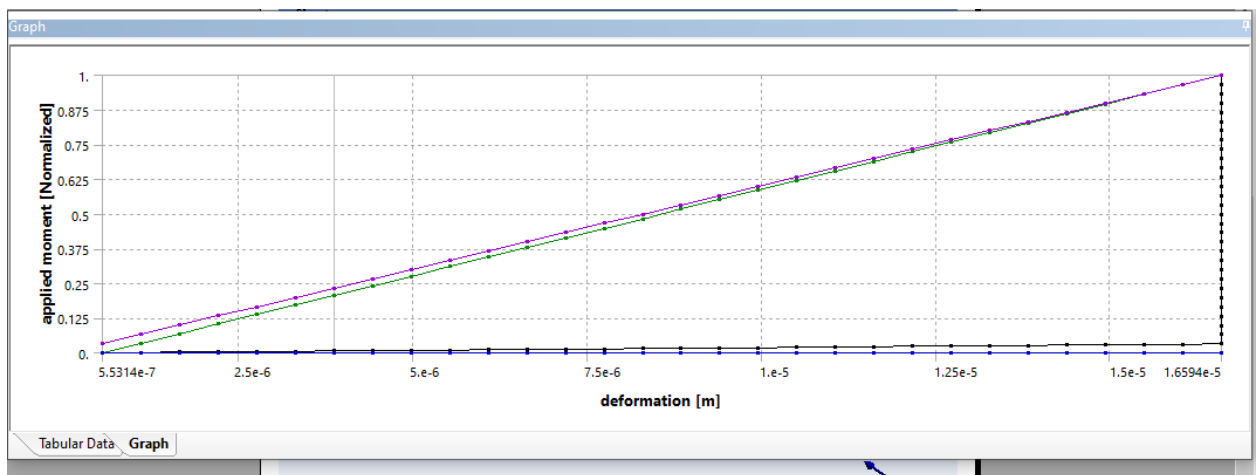


Fig. 4.3.2.4- Graph plotted between applied moment and deformation at 800°C

4.3.3-Temperature 1000°C

Temperature loading

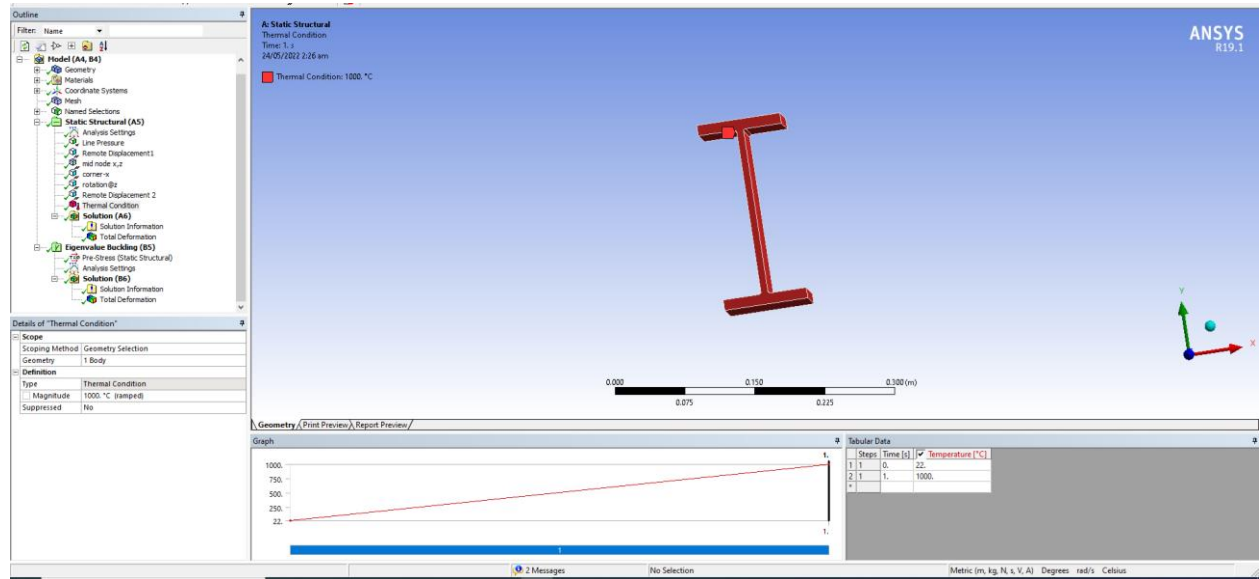


Fig. 4.3.3.1- Loading Temperature 1000°C in ANSYS workbench

Deformation

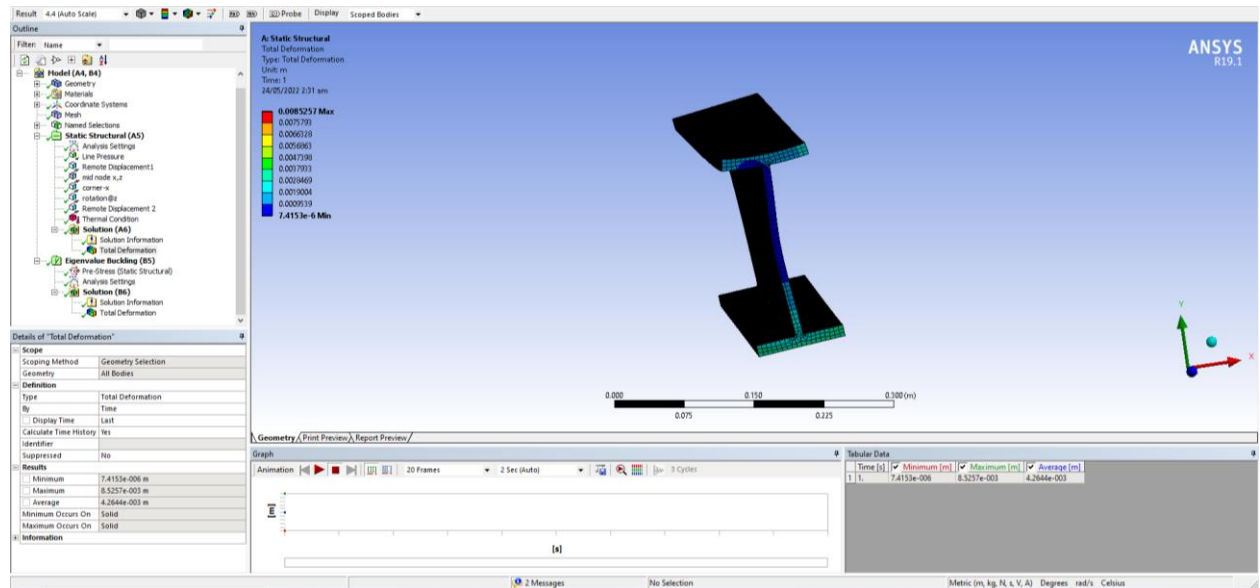


Fig. 4.3.3.2- Deformation resulting from Loading

Eigenvalue buckling

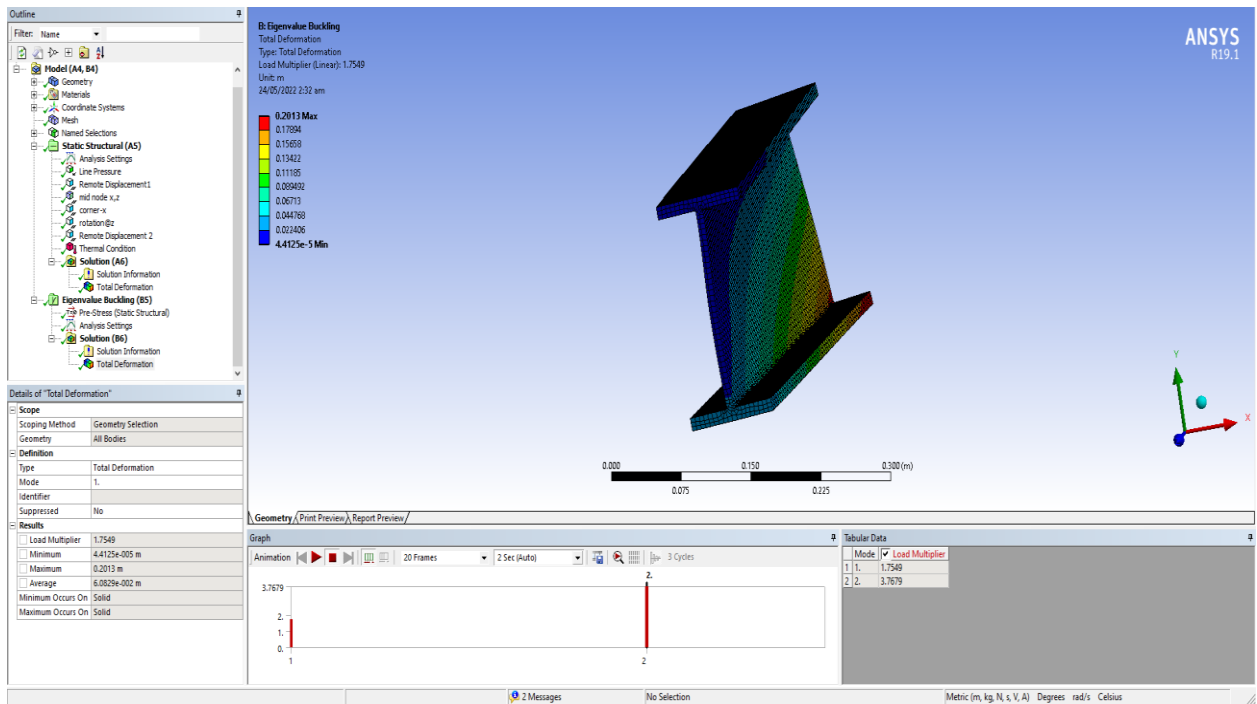


Fig. 4.3.3.3- Eigenvalue Deformation

Graph

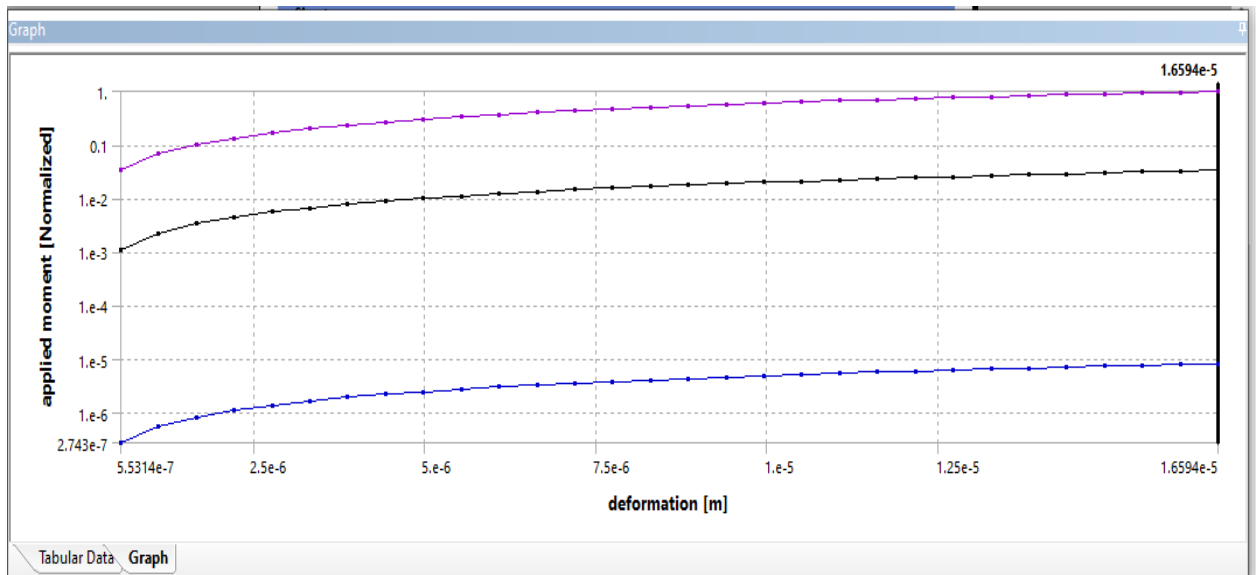


Fig. 4.3.3.4- Graph plotted between applied moment and deformation at 1000°C

4.3.4-Temperature 1200°C

Temperature Loading

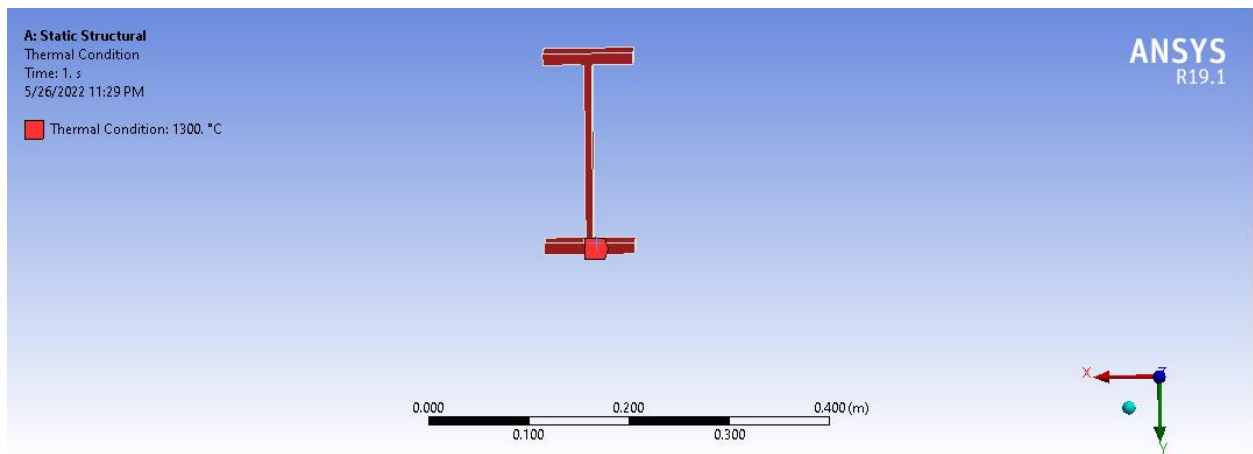


Fig. 4.3.4.1- Loading Temperature 1200°C in ANSYS workbench

Deformation

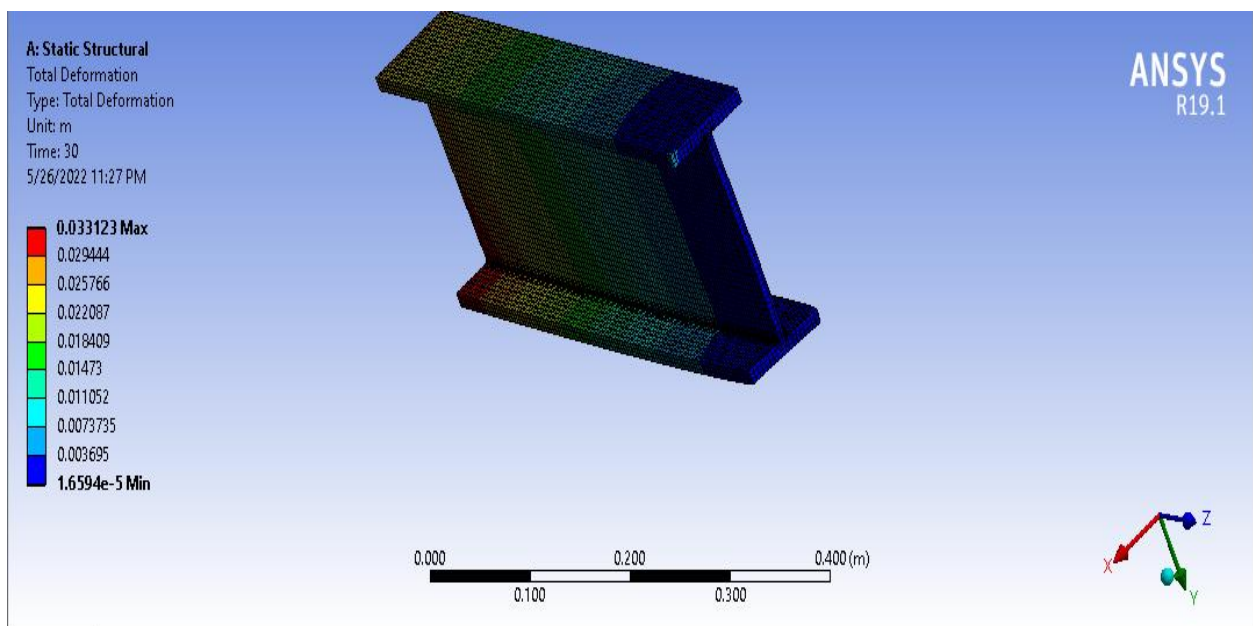


Fig. 4.3.4.2- Deformation resulting from Loading

Eigenvalue

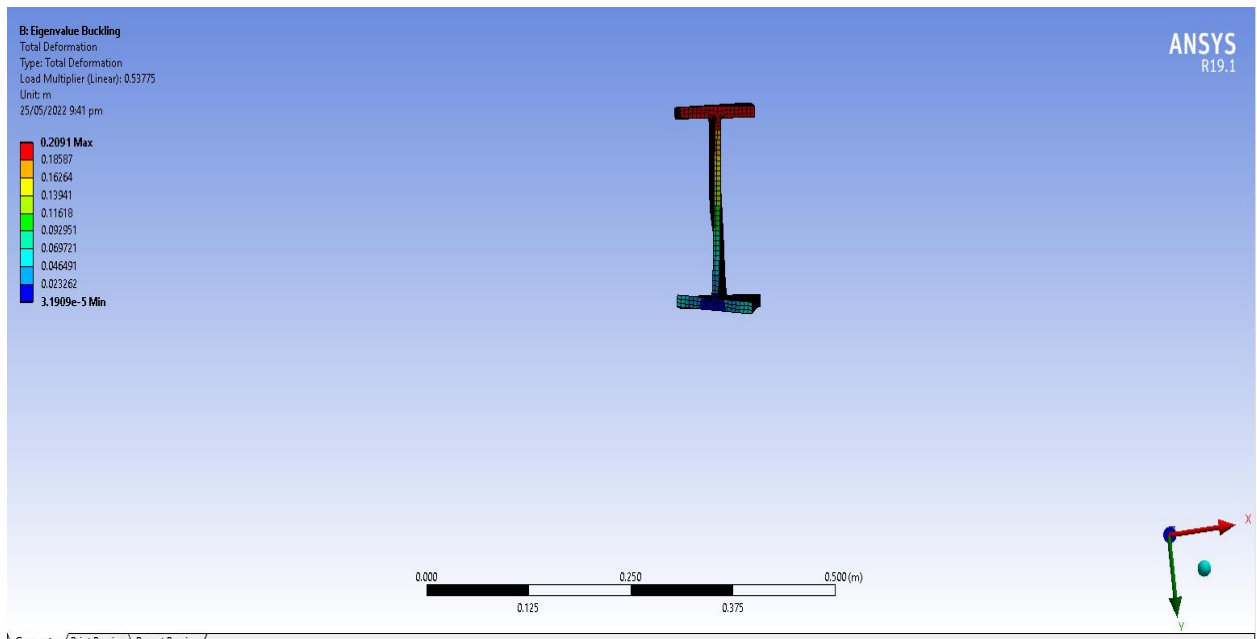


Fig. 4.3.4.3- Eigenvalue Deformation

Graph

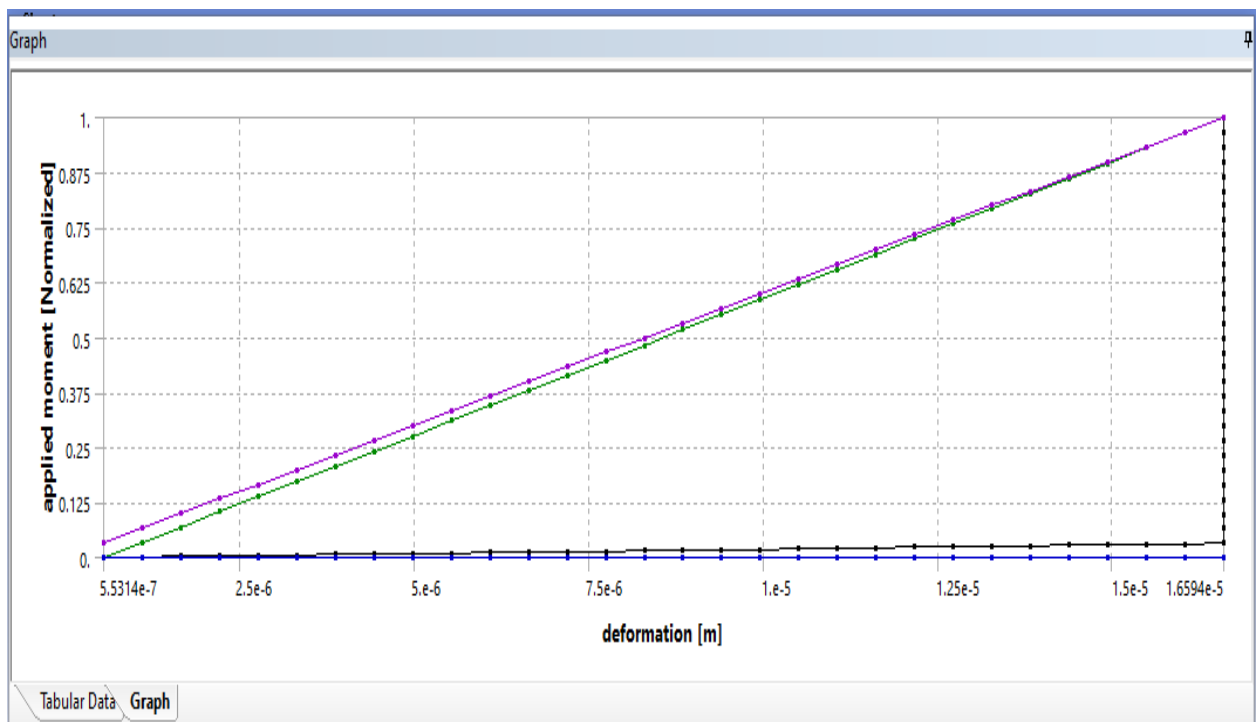


Fig. 4.3.4.4- Graph plotted between applied moment and deformation at 1200°C

4.3.5-Temperature 1500°C

Temperature Loading

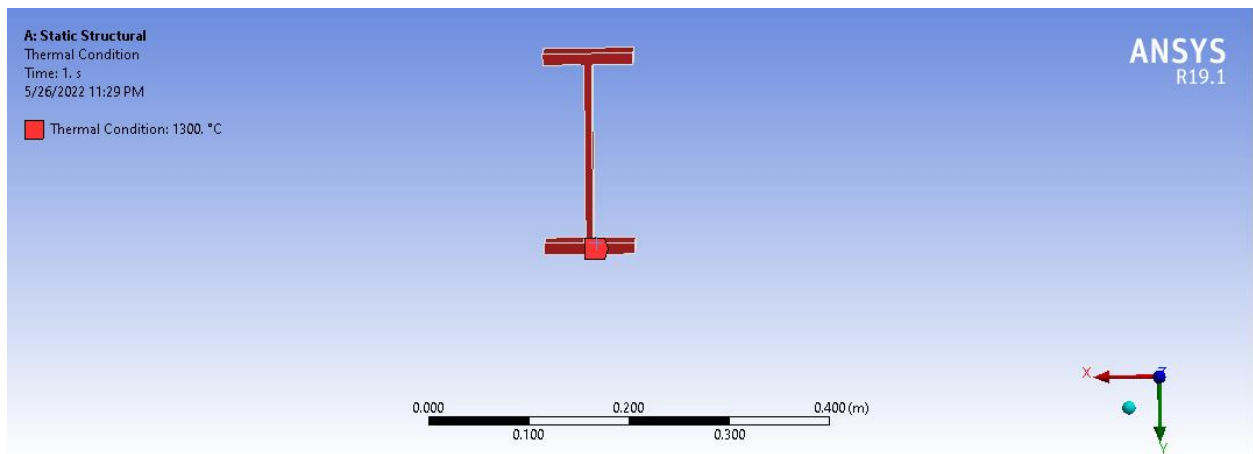


Fig. 4.3.5.1- Loading Temperature 1500°C in ANSYS workbench

Eigenvalue

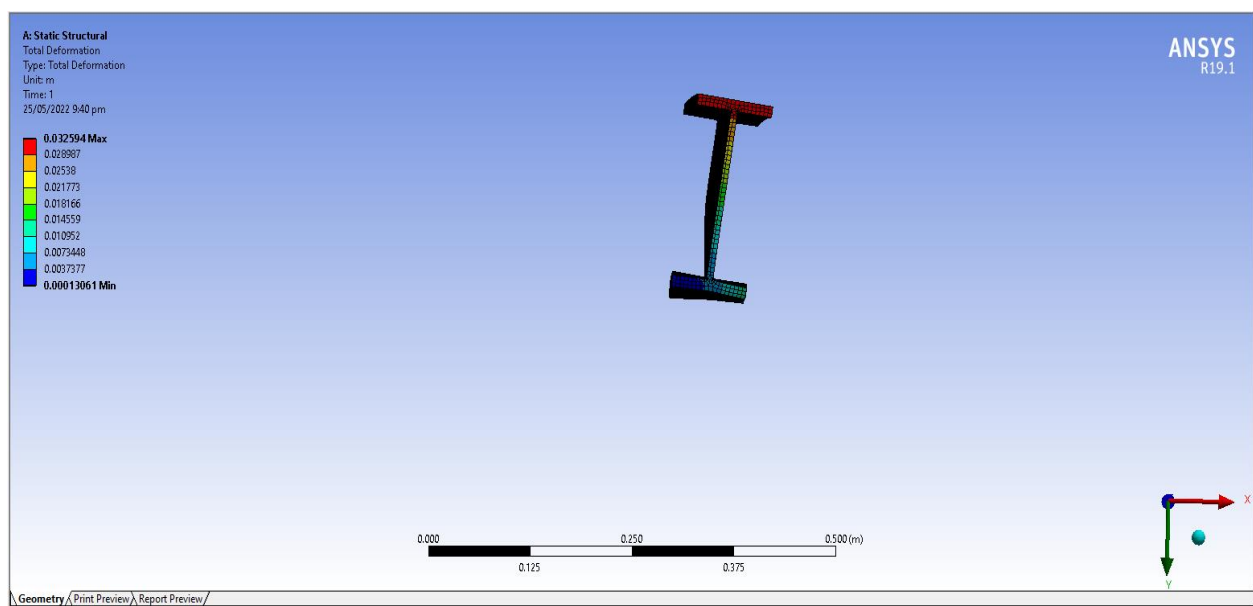


Fig. 4.3.5.2- Eigenvalue Deformation

Deformation

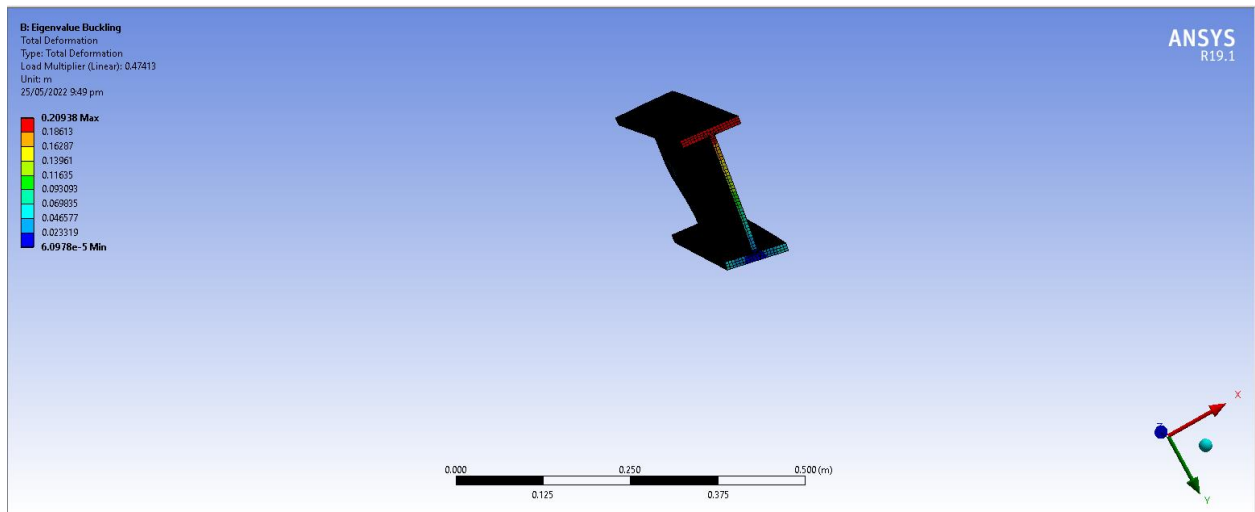


Fig. 4.3.5.3- Deformation resulting from Loading

Graph

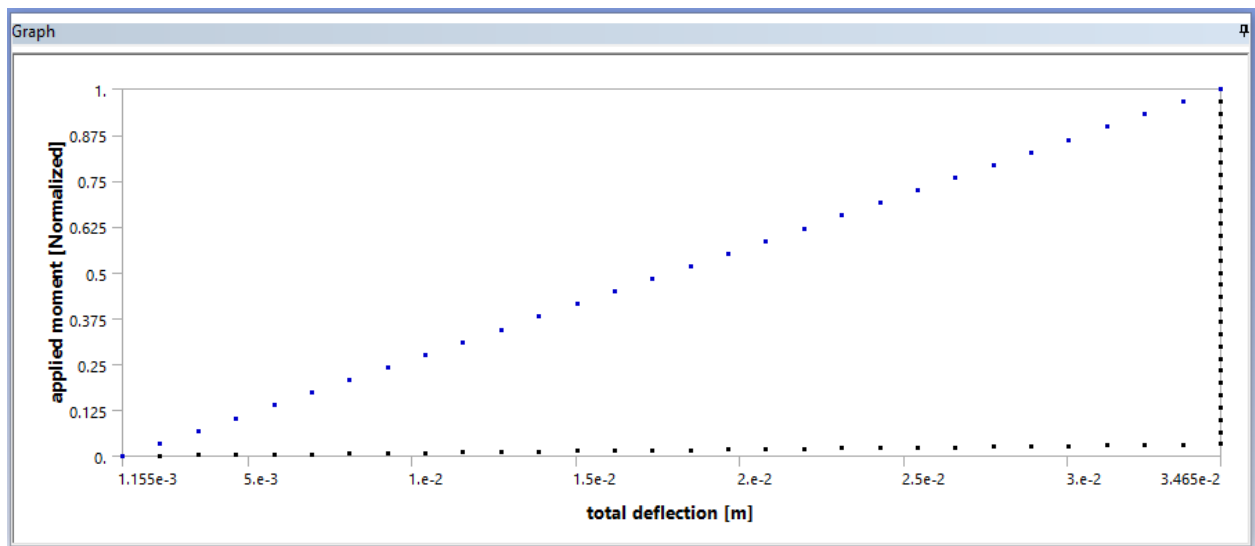


Fig. 4.3.5.4- Graph plotted between applied moment and deformation at 1500°C

4.3.6-Temperature 1500°C

Thermal load

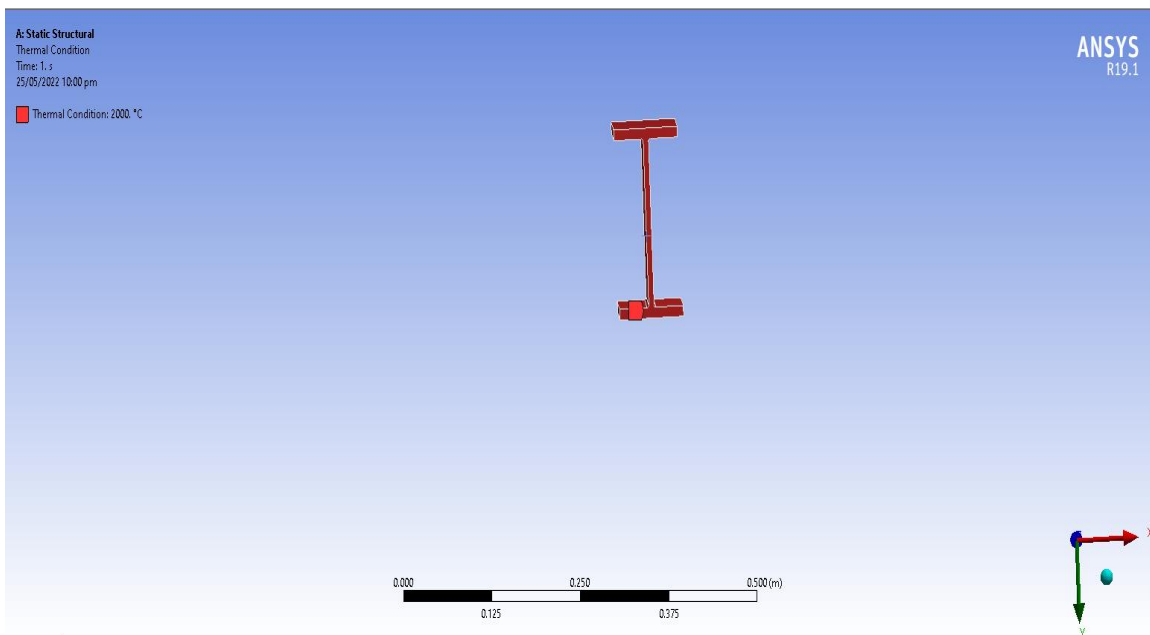


Fig. 4.3.6.1- Loading Temperature 2000°C in ANSYS workbench

Deformation

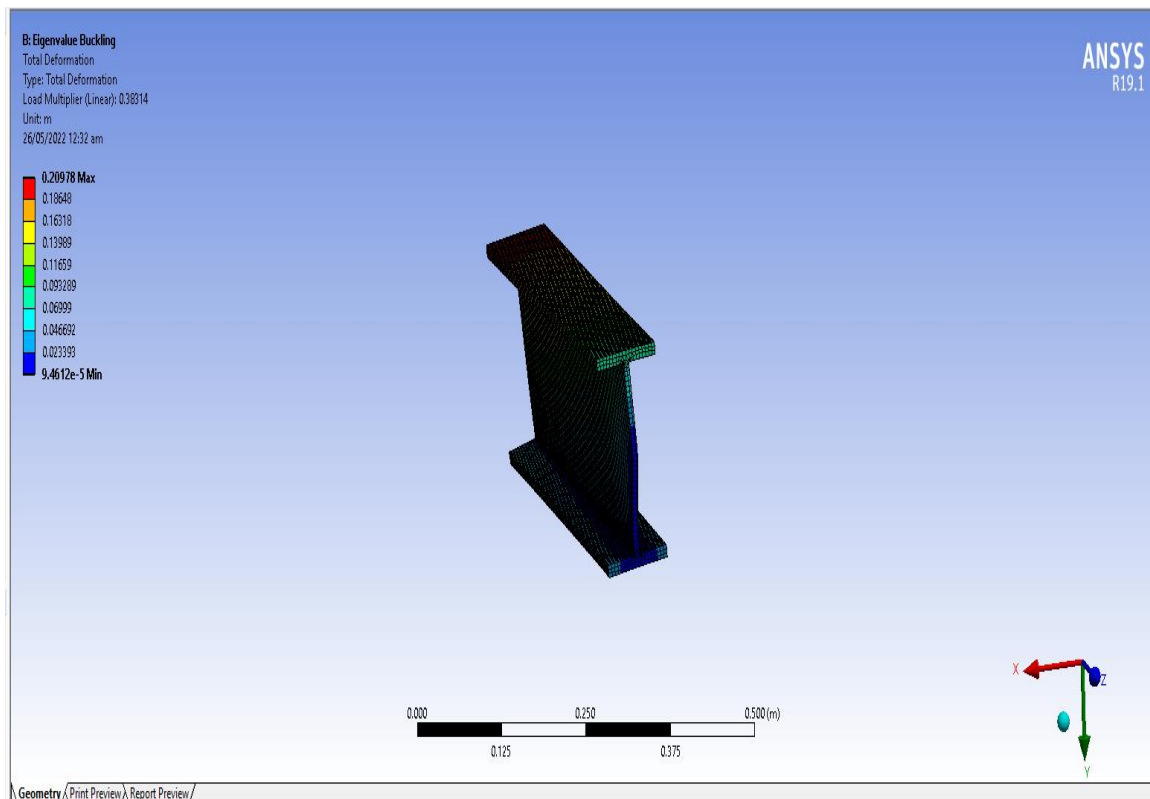


Fig. 4.3.6.2- Deformation resulting from Loading

Eigenvalue

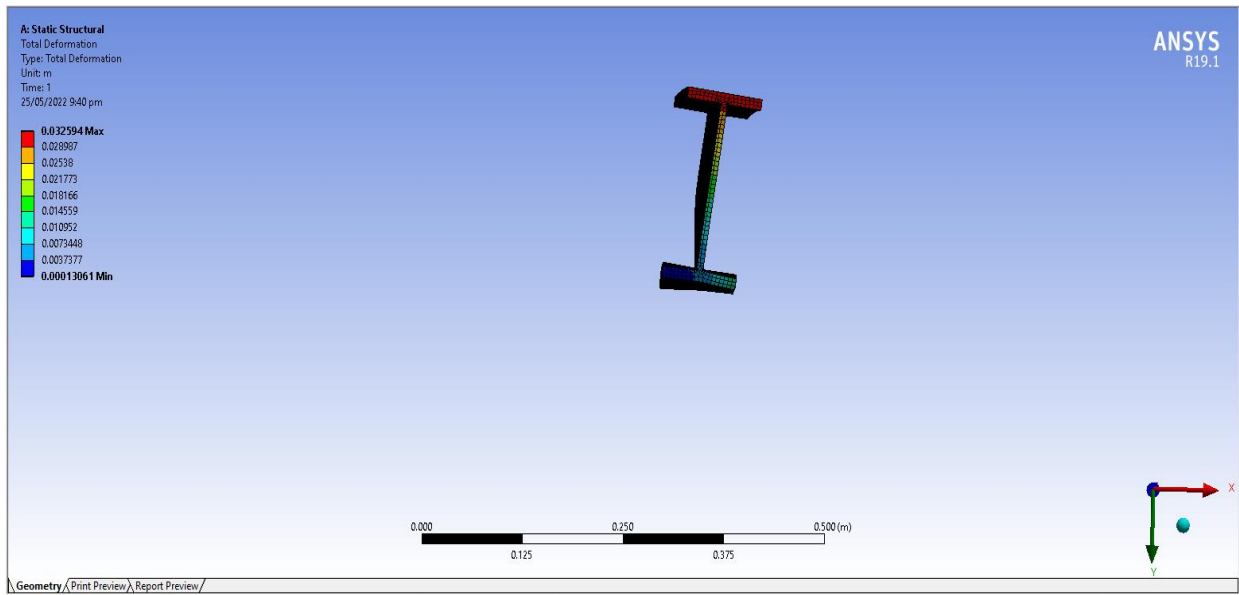


Fig. 4.3.6.3- Eigenvalue Deformation

Graph

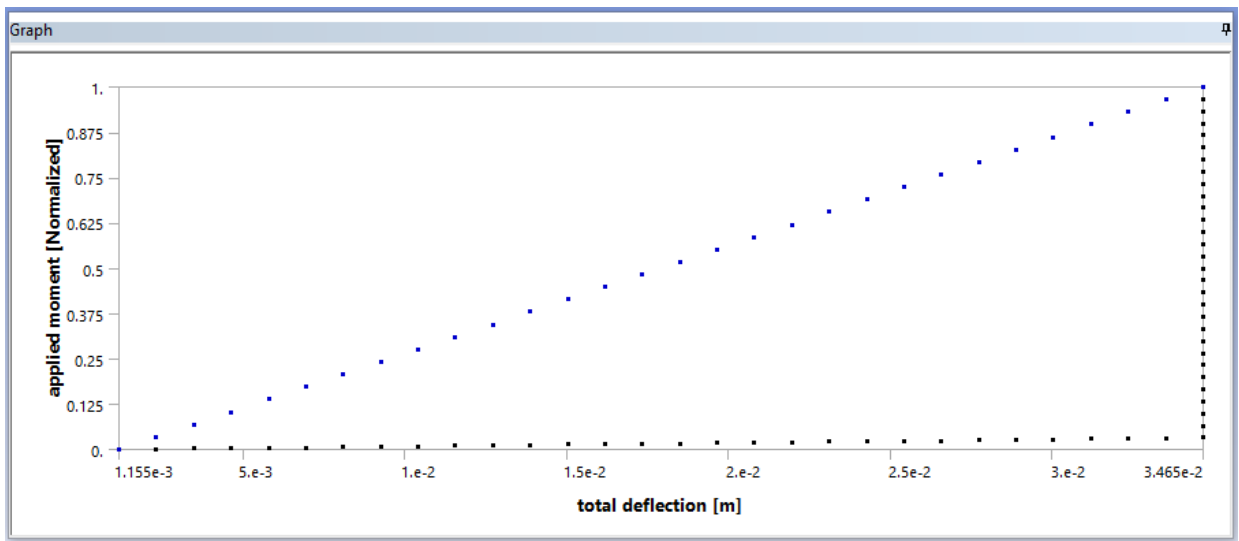


Fig. 4.3.6.4- Graph plotted between applied moment and deformation at 1500°C

Deformation vs load graph

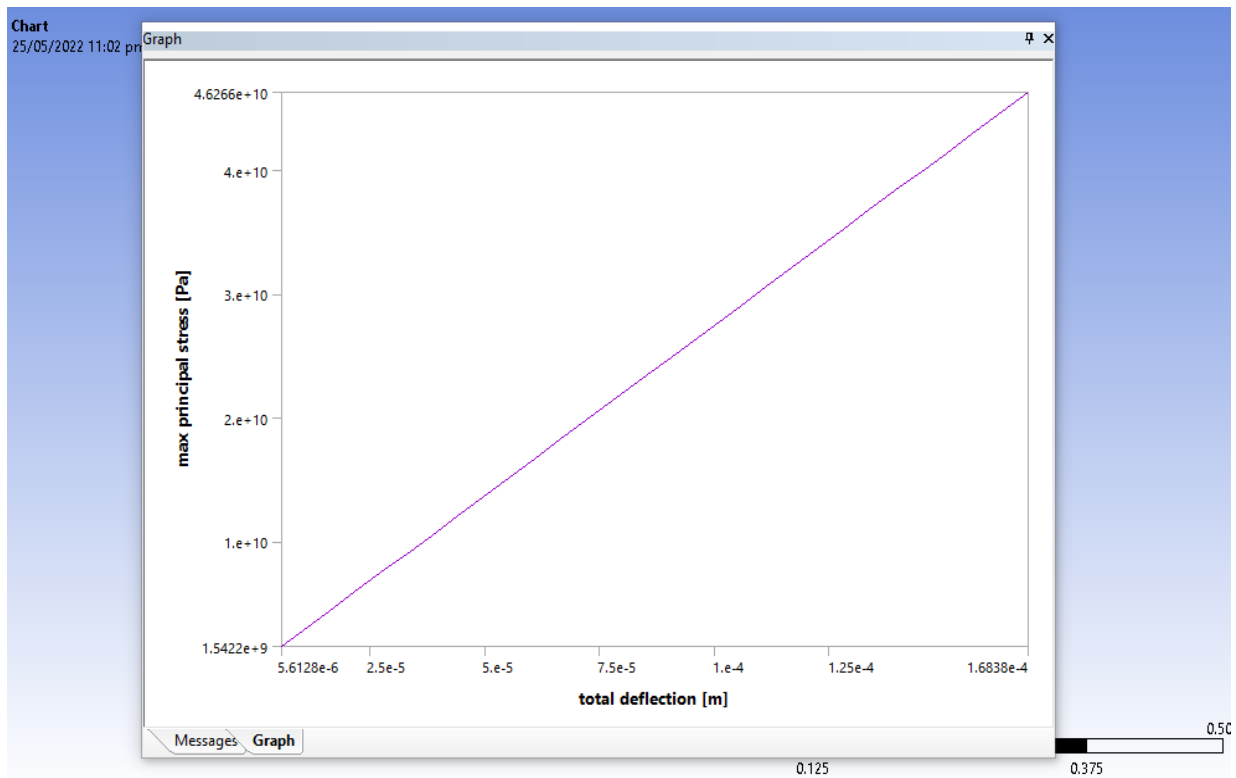


Fig. 4.3.6.5- max. Applied stress effect on the beam to make deflection in it

Stress vs strain

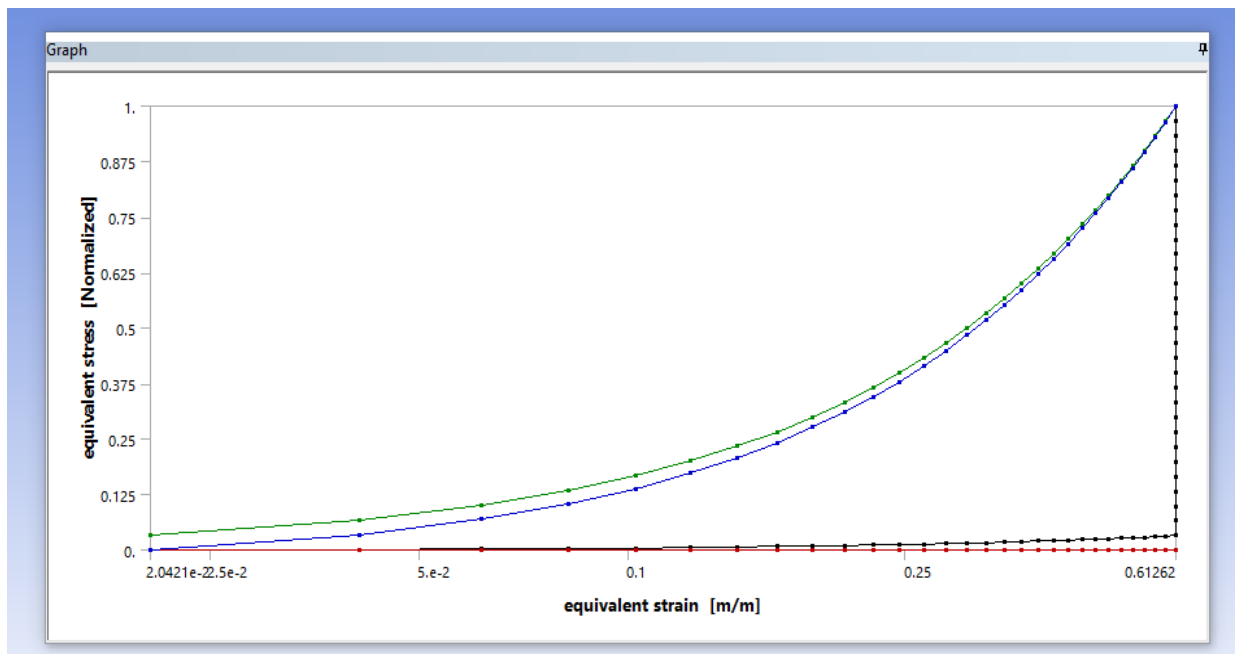


Fig. 4.3.6.5- the stress-strain behavior of FEM Model

4.4- Results and Analysis

Table 7- the application of moments and the resulting deflection

Lat. Deflection	Applied Moment	Lat. Deflection	Applied Moment
0	0.268152962	9.642790935	47.8232776
-0.003444705	3.256277266	10.24790701	46.63798499
0.067745502	6.100981339	10.67504554	46.16387518
0.067745502	9.65685917	11.24456447	45.21563748
0.174530132	12.9756821	11.81408341	44.03034487
0.245720339	16.53155993	12.34800792	43.08210716
0.35250497	19.37625496	12.77514916	42.3709334
0.566074231	21.98390413	13.23788211	41.65975965
0.637264438	24.8286082	13.80740376	40.47446704
0.708454644	28.38448603	14.37692269	39.52622933
0.815239275	31.94036386	14.87525278	38.34093672
0.922023906	35.7332966	15.37358015	37.15564411
0.993214113	38.57800067	15.87191024	36.44447035
1.135594526	42.1338785	16.37024033	35.02212284
1.242379156	45.92681124	16.79737885	34.31094908
1.384758212	49.24563416	17.22452009	33.36271138
1.527138625	52.09033371		
1.740707886	55.40915664		
2.061063137	58.25385619		
2.417012811	60.86150084		
2.844152692	63.46914548		
3.271292574	63.70620491		
3.734026879	62.5209123		
4.16116676	60.62444141		
4.695091272	58.72797504		
5.086635371	57.30562301		
5.584965459	55.64621154		
6.083294189	53.9868046		
6.652813125	53.03857142		
7.115548788	52.09033371		
7.542687312	51.14210053		
8.076611824	49.95680792		
8.646133476	49.48269359		
9.144460848	48.53445588		

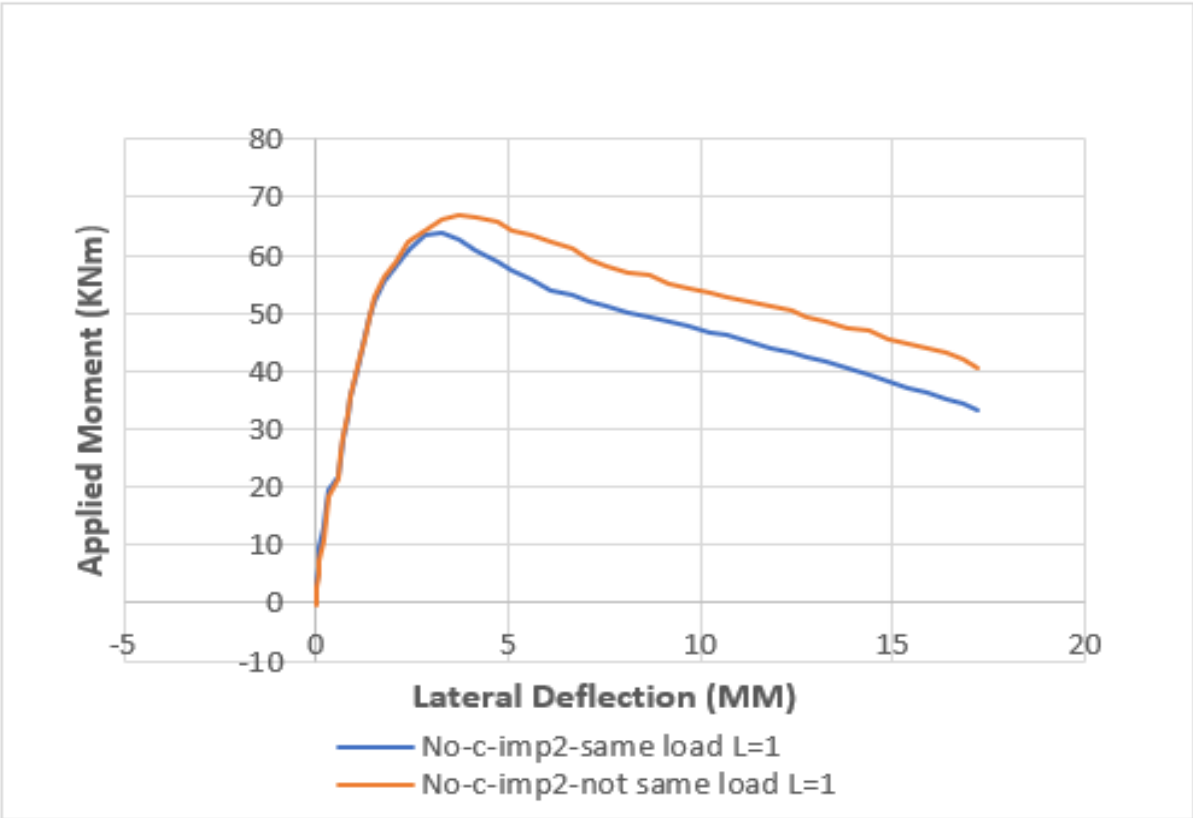


Fig. 4.4.1- resulting deflection due to App. moment

Table 8- No temperature conditions $L=1m$

imp 1.5(GK)- No-C- same load	Applied Moment	imp 1,5(GK)- No-C not same load	Applied Moment
0.012779514	1.61797272	0	1.41573
0.076677086	8.08988398	-0.025559029	8.49438
0.102236544	12.1348294	0	12.3371
0.115016058	15.7752816	0.025559029	15.9775
0.140575087	19.8202202	0.038338543	19.8202
0.166134115	23.4606724	0.051118057	23.6629
0.191693144	27.5056177	0.089457029	27.7079
0.230032116	31.1460632	0.115016058	31.7528
0.268370659	35.1910085	0.153354601	35.3933
0.293929688	38.8314608	0.17891363	39.6404
2.249201388	58.2471911	2.223642359	61.8876
2.46645356	56.629215	2.415335503	60.0674
4.33226866	46.7190981	4.306709631	50.3596
4.549520833	45.5056186	4.498402775	49.5506
4.779552949	44.8988788	4.741213977	48.7416
5.009585065	43.4831459	4.984025178	46.9213
5.239616323	42.067413	5.201278209	46.3146
5.482428382	40.8539334	5.431310325	45.1011
5.712460498	39.8426937	5.674121526	43.8876
5.9552717	38.4269676	5.904153642	42.8764
6.185303816	37.4157278	6.159744787	41.4607
6.389776045	36.2022483	6.389776045	40.2472
6.632588105	34.988762	6.619808161	39.236
6.88817925	33.3707824	6.837061192	37.8202
7.118210508	32.3595495	7.092651479	36.6067
7.335463538	31.5505631	7.297124566	35.191
7.565495654	30.5393234	7.527156682	34.382
7.833865885	29.3258439	7.757188799	33.1685

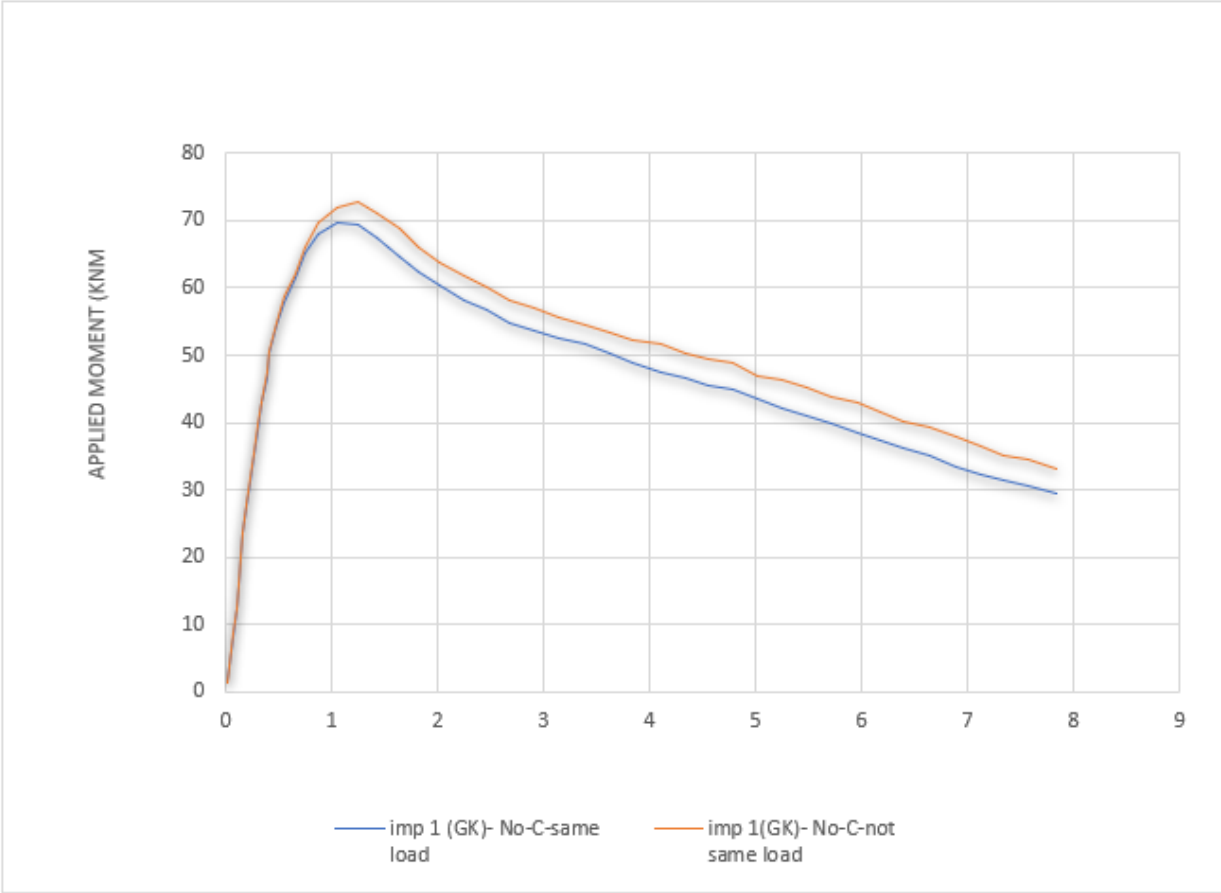


Fig. 4.4.2- No temperature conditions $L=1m$

Table 9- no temperature elevation but change in impact factor by keeping same length.

Applied Moment	No-c-imp2 L=1.5	Applied Moment	No-c imp1.9 L=1.5	Applied Moment	No-c imp1.8 L=1.5	Applied Moment	No-c imp1.5 L=1.5
- 0.032520228	1.11111523	- 0.065040455	0.66666466	- 0.032520228	0.22222155	- 0.065040455	0.44444
0	6.88889057	0	6.00000435	- 0.065040455	6.22222591	- 0.032520228	5.11111
0.097560683	10.888886	0.065040455	10.6666645	0.065040455	10.888886	0	8.88889
0.097560683	14.4444458	0.065040455	14.2222242	0.13008091	14.4444458	0	12.6667
0.227642685	17.7777766	0.16260223	17.3333335	0.13008091	17.555555	0.065040455	17.1111
0.227642685	20.4444427	0.195122457	21.3333364	0.195122457	20.6666642	0.13008091	21.3333
0.357723595	24.0000025	0.29268314	24.4444456	0.195122457	24.222224	0.260162912	24
0.455284278	26.6666686	0.325203367	26.6666686	0.260162912	27.5555548	0.260162912	27.1111
0.520325825	29.5555563	0.455284278	30.2222209	0.357723595	30.8888931	0.325203367	30.8889
0.617886507	33.3333376	0.552846052	33.7777807	0.455284278	33.5555592	0.42276405	34
1.00813033	46.2222251	1.073170785	46.8888897	0.87804942	45.777782	0.813007873	46.4444
1.170731468	49.3333343	1.170731468	51.5555573	1.040650557	49.5555559	0.813007873	50
1.365853925	51.7777789	1.365853925	55.5555565	1.170731468	52.4444473	0.943089875	52.6667
1.495934835	55.1111134	1.593496609	58.000001	1.30081347	55.5555565	1.105691013	56.2222
1.756097747	57.5555579	1.85365843	60.6666672	1.528455063	58.888891	1.235773015	59.1111
2.113821342	60.4444456	2.178861797	63.1111117	1.72357752	61.111114	1.43089438	62
2.373984255	62.2222218	2.471544937	65.5555563	1.951220204	63.7777801	1.626016837	65.5556
2.699187622	64.2222232	2.959349443	66.8888893	2.243902253	66.6666678	1.85365843	68.2222
3.024389898	64.8888916	3.28455281	66.0000031	2.536585392	67.7777793	2.113821342	70.6667
3.44715504	63.7777801	3.70731686	64.6666663	3.056911217	67.7777793	2.471544937	72
3.86991909	62.0000002	4.130082002	63.1111117	3.479675267	66.4444462	3.089431445	71.3333
6.796748305	53.555555	7.056910125	54.2222234	6.373984255	56.2222249	5.85365843	60
7.186991036	52.8888904	7.479674175	53.1111119	6.86178876	55.5555565	6.43902471	58.2222
7.544714631	52.0000004	7.86991909	52.6666688	7.382114584	54.0000019	6.99186967	56.2222
7.902438226	51.1111142	8.195121365	51.7777789	7.83739777	53.3333335	7.479674175	55.3333
8.227642685	50.8888926	8.487804505	51.3333358	8.29268314	52.4444473	7.967480864	54.6667
8.455285369	50.2222205	8.87804942	50.4444421	8.682928054	51.5555573	8.325204459	54
8.8455281	49.5555559	9.26829215	49.7777774	9.170732559	50.8888926	8.910568555	52.8889
9.203251695	48.8888912	9.626015745	49.5555559	9.658537065	49.999999	9.365853925	51.5556
9.495934835	48.4444481	10.01626066	49.1111127	10.08130111	49.3333343	9.788617975	50.8889
9.788617975	47.777776	10.37398425	47.9999975	10.60162694	48.6666696	10.3089438	49.7778
10.08130111	47.1111113	10.73170785	47.777776	11.05691013	47.777776	10.89431008	49.3333
10.37398425	47.1111113	11.18699322	46.4444466	11.41463372	46.8888897	11.57723595	48

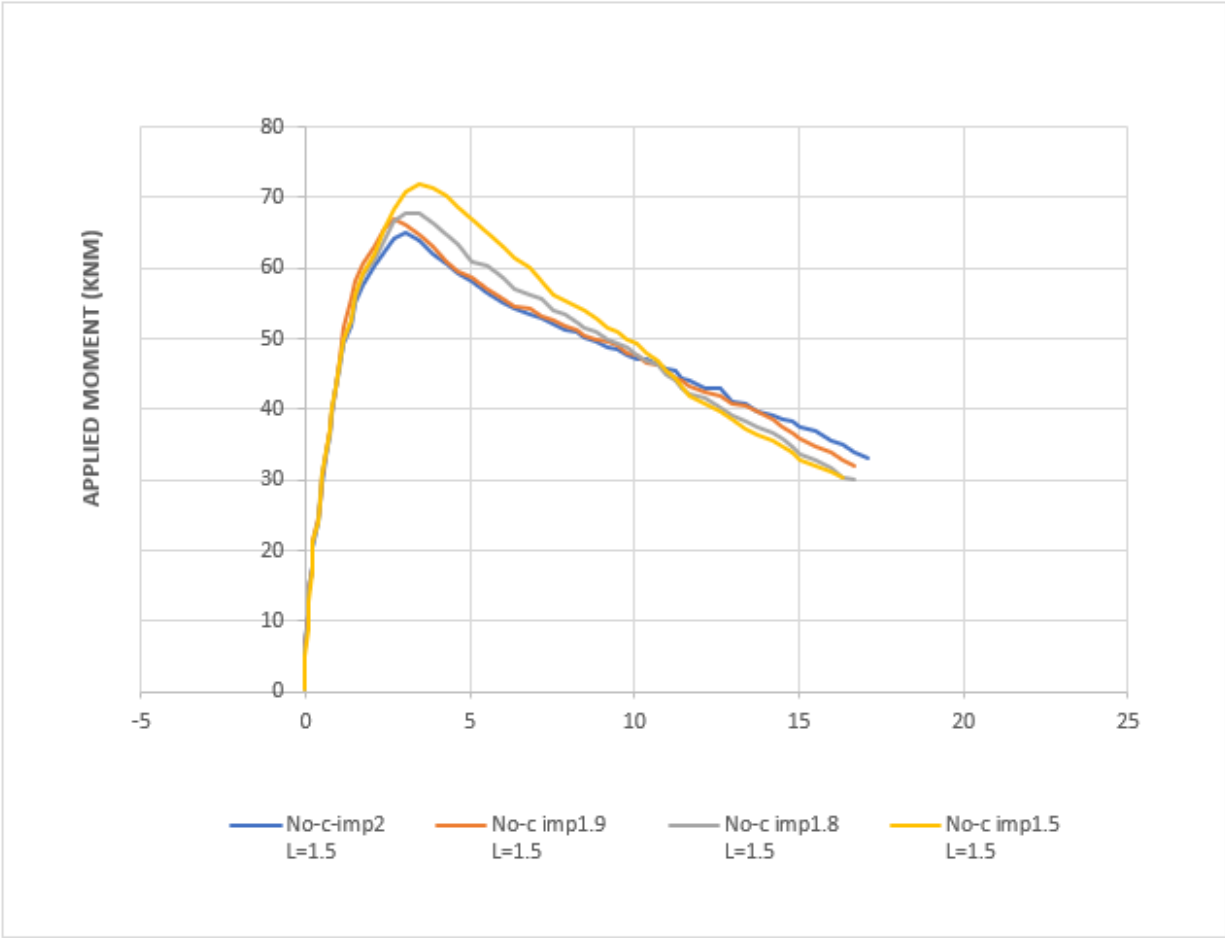


Fig. 4.4.3- no temperature elevation but change in impact factor by keeping same length

Table 10- No temperature with L=2meters (Different Imperfection Scale Factor Values)

App. Moment	No-c-imp4.0 L=2	App. Moment	No-c-imp3.9 L=2	App. Moment	No-c-imp3.7 L=2	App. Moment	No-c-imp3.5 L=2	App. Moment	No-c-imp3.3 L=2
0.02941 3	0.153851	0	-0.1538	0.0294 1	0	0.02941	0	0.02941	0.153850 851
0.08823 6	1.692308	0.02941	3.69231	0.0882 4	2.1538 5	0.05882	3.0769 2	0.11765	3.384615 421
0.23529 4	4.615386	0.08824	5.07692	0.1764 7	4.6153 9	0.17647	5.3846 2	0.17647	5.230768 818
0.38235 4	7.076927	0.23529	6.46154	0.2352 9	6	0.26471	7.0769 3	0.23529	7.230773 065
0.5	9.538464	0.38235	8.30769	0.3529 4	8.3076 9	0.32353	9.3846 2	0.35294	9.692309 206
0.61764 7	11.53846	0.5	10.6154	0.4705 9	10.615 4	0.47059	11.692 3	0.47059	11.84615 397
0.79411 8	14	0.61765	12.6154	0.5882 4	12.615 4	0.61765	14.307 7	0.58824	14.00000 391
0.94117 7	15.84616	0.67647	14.6154	0.7352 9	14.615 4	0.70588	16.307 7	0.67647	16.46154 005
1.02941 3	18	0.82353	16.6154	0.8529 4	16.769 2	0.82353	18.461 5	0.82353	18.46153 913
1.82353	28.92308	1.47059	25.8462	1.4117 7	25.692 3	1.58824	29.846 2	1.5	29.38461 899
2.02941 2	30.92308	1.55882	27.5385	1.5588 2	27.692 3	1.70588	31.384 6	1.64706	31.38461 807
2.20588 2	32.76923	1.67647	29.2308	1.7352 9	29.692 3	1.97059	33.230 8	1.88235	33.84615 421
2.5	34.46154	1.91176	31.0769	1.8529 4	31.384 6	2.26471	35.384 6	2.08824	35.53846 192
2.85294 1	36.15385	2.14706	33.0769	2.0882 4	33.076 9	2.58824	37.230 8	2.38235	37.38461 532
3.14705 9	37.53846	2.47059	35.0769	2.3235 3	35.230 8	2.82353	38.615 4	2.70588	39.07692 303

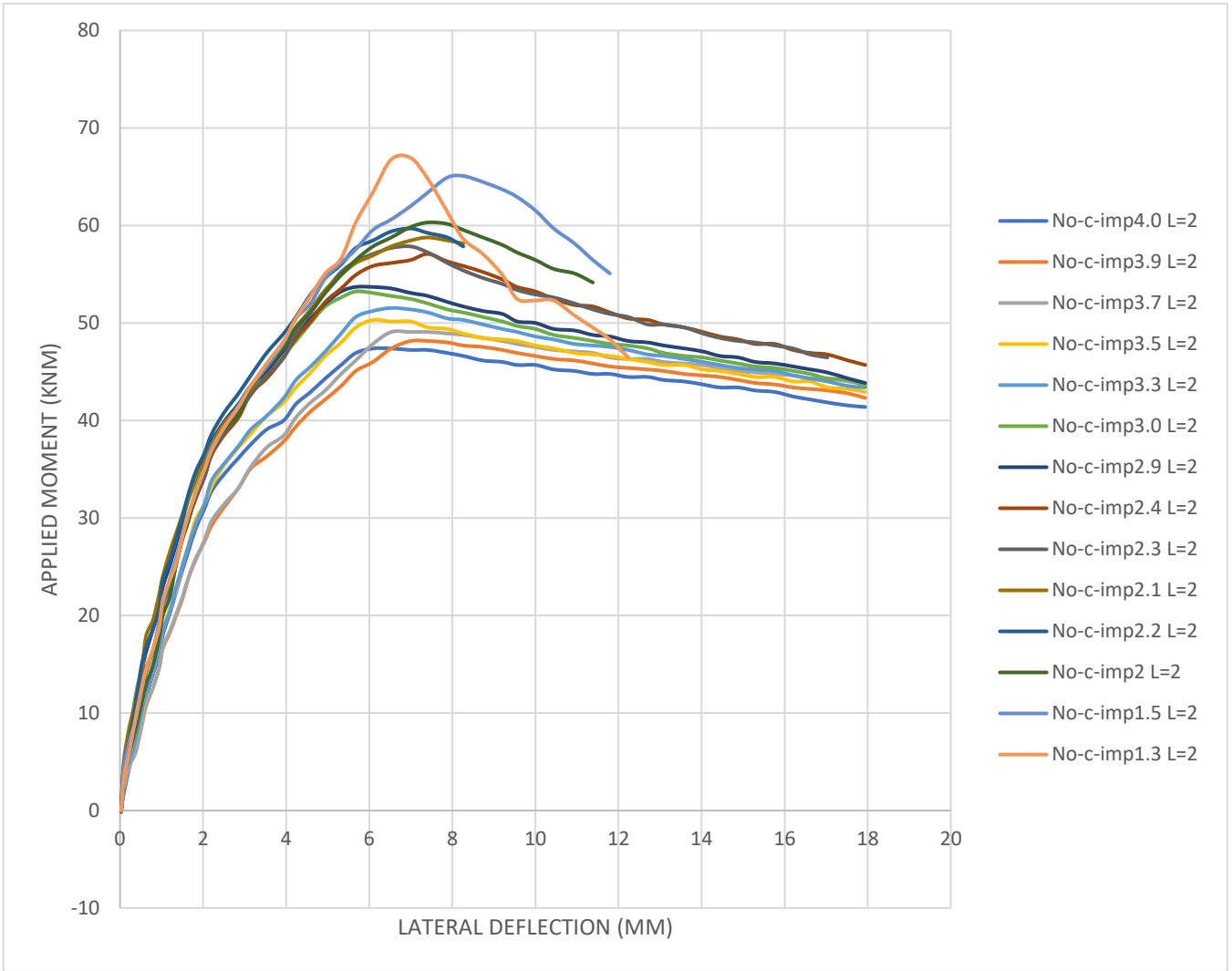


Fig. 4.4.4- No temperature L=2meters (Different Imperfection Scale Factor Values)

Table 11- No temperature, L=2m with Different Imperfection Scale Factor Values.

App. Moment	Case1-C-Imp1-L=1	App. Moment	Case2-C-Imp1-L=1	App. Moment	Case3-C-Imp1-Model1-L=1	App. Moment	App. Moment	No-C-Imp1-L=1
0.02537	0	0	-0.241758	-0.0254	0	-0.025368	0	-0.241758
0.12684	9.9121	0	5.802197	0.02537	9.428567	0.0253682	7.97802	11.362636
0.25368	18.615	0.05074	10.63736	0.0761	12.81319	0.0761045	18.3736	20.307688
0.30442	24.659	0.12684	20.06593	0.10147	16.68132	0.1522099	29.011	27.802195
0.482	33.604	0.22831	33.84616	0.20295	22.72527	0.2029462	36.7473	36.50549
0.68494	39.165	0.30442	38.1978	0.25368	31.91209	0.4312606	50.044	44.725274
1.16694	43.275	0.482	42.54945	0.43126	45.20879	1.293781	60.6813	51.252747
2.05483	45.692	0.86252	48.10989	0.71031	52.7033	2.3085105	64.0659	60.197803
3.34861	44.242	1.82651	52.46154	1.47136	56.81319	3.5769233	59.956	64.307693
4.92144	41.824	3.14566	51.73626	2.40998	57.53846	5.2004915	51.978	65.274723
6.77332	38.44	5.14976	46.41758	3.34861	56.32967	6.9508996	45.6923	61.648353

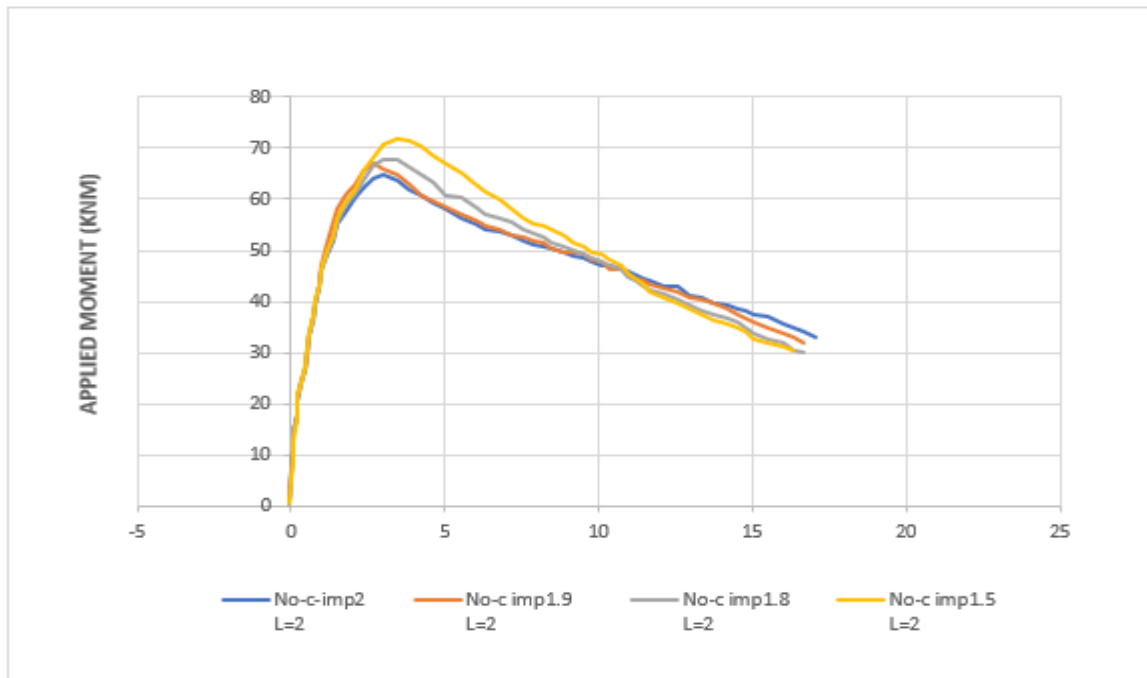


Fig. 4.4.5- No temperature, L=2m with Different Imperfection Scale Factor Values

Table 12- the values for App. Moment vs Lat. Deflection for L=1.5 m, for 5 cases

App. Moment	Case1-C-Imp1.5-L=1.5	App. Moment	Case3-C-Imp1.5-Model1-L=1.5	App. Moment	Case2-C-Imp1.5-L=1.5	App. Moment	Case3-C-Imp1.5-Model2-L=1.5	App. Moment	No-C-imp1.5-L=1.5
-0.00592	-0.35596	0.048309	2.906831	0	0	0	0	0	-0.2236
0.164126	5.547082	0.120773	8.273289	0.169082	8.049688	0.096618	7.826086	0.072464	8.944102
0.29166	10.85982	0.241546	13.19254	0.241546	15.87577	0.120773	11.18013	0.169082	16.54659
0.567984	18.73053	0.386473	19.90062	0.31401	18.3354	0.241546	17.6646	0.31401	25.26708
1.014355	26.60125	0.628019	27.95031	0.483092	26.8323	0.458937	28.17391	0.434782	32.42236
1.758305	35.06227	0.990338	39.57764	0.676328	34.21118	0.652174	35.55279	0.628019	39.80124
2.608534	42.14591	1.570049	50.08696	0.917874	41.36646	0.821256	42.26087	0.845411	47.18012
3.713831	45.09744	2.149759	53.6646	1.280193	48.29814	1.183575	54.3354	1.062802	54.55901
4.925407	44.31036	3.091787	54.1118	1.642512	54.3354	2.077294	67.30435	1.497584	61.26708
6.34954	42.73622	4.396135	53.6646	1.956522	57.24224	3.067633	68.86956	1.908213	67.75155
8.793948	39.7847	5.676329	52.09938	2.439614	59.25466	4.033817	65.73913	2.584541	70.65839
11.17459	36.83318	6.908213	49.41615	3.091787	59.25466	5.990338	58.58385	3.405797	69.76397
13.25765	35.06227	9.444445	45.1677	4.033817	57.91304	8.285025	52.77019	4.951692	62.8323
14.70304	33.88166	11.95652	41.81367	5.04831	56.34782	9.202898	50.53416	6.497584	57.68944

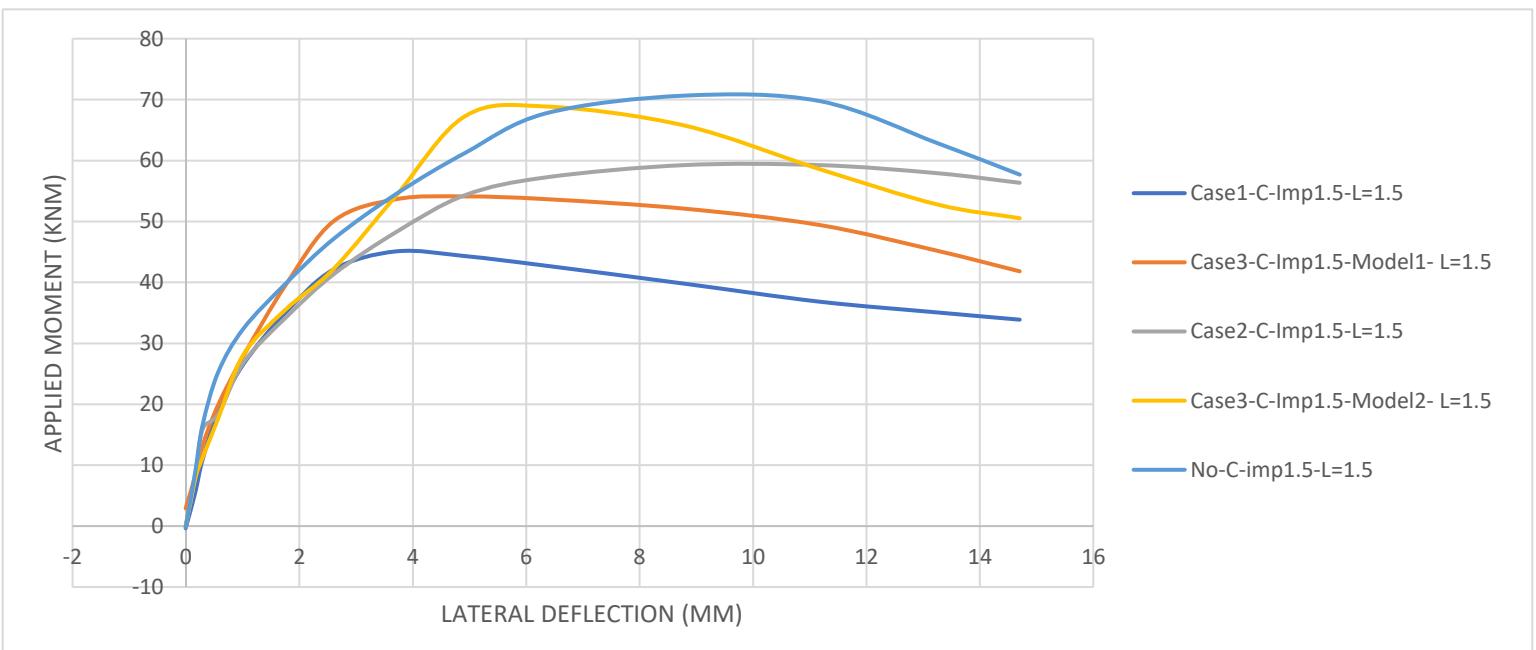


Fig. 4.4.6- App. Moment vs Lat. Deflection for L=1.5 m, for 5 cases

Table 13- the values for App. Moment vs Lat. Deflection for L=2 m, for 5 cases

App. Moment	Case1-C-Imp2-L=2	App. Moment	Case3-C-Imp2-Model1-L=2	App. Moment	Case2-C-Imp2-L=2	App. Moment	Case3-C-Imp2-Model2-L=2	App. Moment	No-C-Imp2-L=2
0.048006	-0.40737	-0.0037	-0.7534	0.02217	-0.0613	-0.0037	-0.0613	-0.0037	-0.0613
0.280564	4.437055	0.07385	2.36087	0.15137	5.30213	0.15137	6.1672	0.22889	9.10845
0.71984	10.66559	0.17721	5.64815	0.53896	15.337	0.38392	13.9529	0.38392	15.337
1.314154	16.5481	0.40976	11.5307	1.13328	26.41	0.74568	21.9116	0.66816	22.0846
2.270225	23.12267	0.66816	16.5481	1.80511	32.9845	1.0816	29.0052	1.23663	33.8496
3.536372	26.58297	1.02992	23.2957	3.04542	42.6734	1.52087	36.7909	1.77927	39.04
5.215955	30.90834	1.23663	25.7179	4.44076	45.7876	2.4511	45.4416	2.8387	49.767
6.869699	32.8115	2.03767	34.3686	5.96531	46.8257	4.00149	53.2273	4.3374	55.8225
8.911039	33.67658	3.0971	41.1162	9.0144	45.6146	5.08676	55.9955	5.44851	57.0336
11.36581	32.8115	4.51828	44.0575	11.9601	42.6734	7.48985	53.4003	7.30897	54.2654

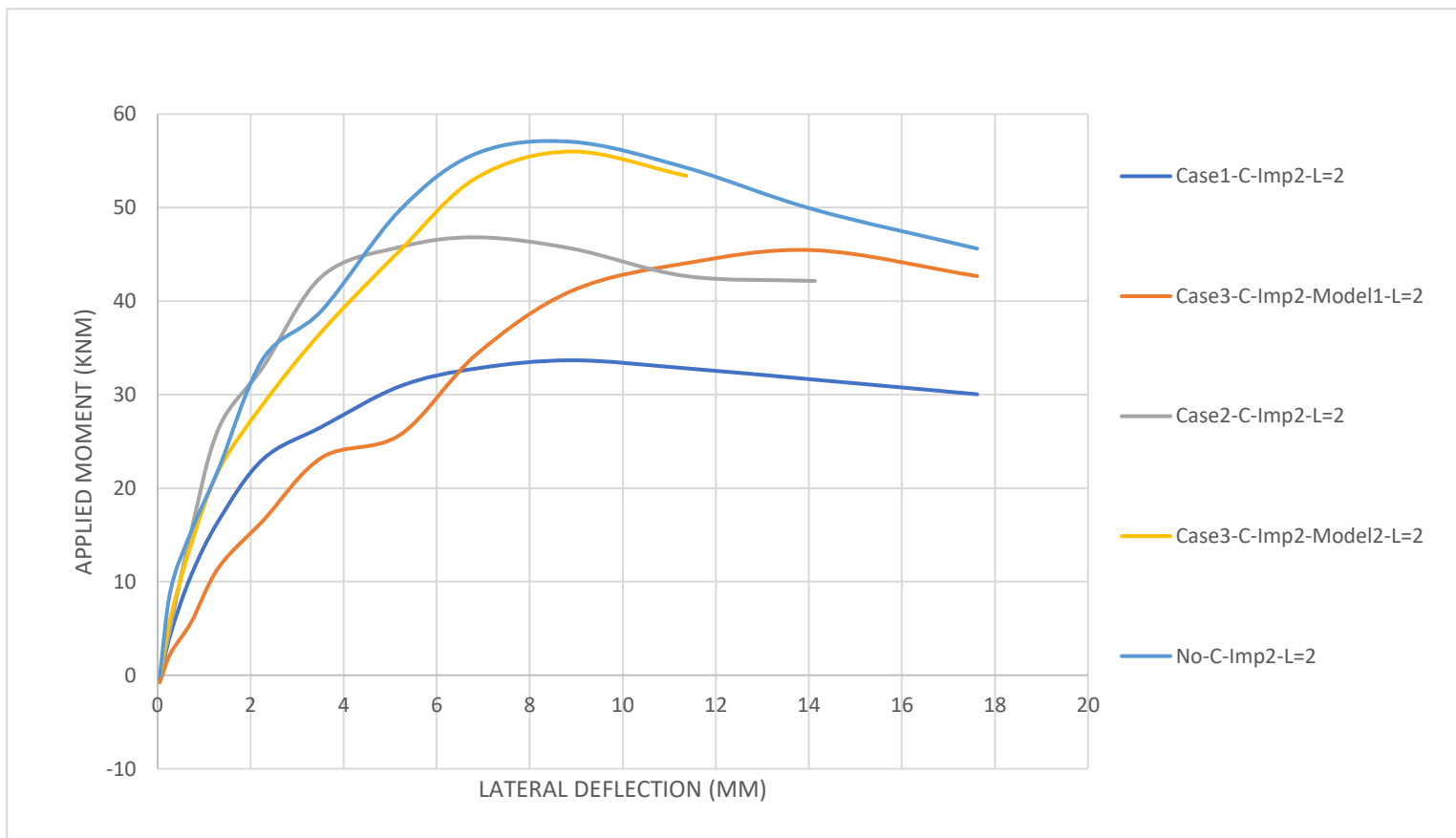


Fig. 4.4.6- App. Moment vs Lat. Deflection for L=2 m, for 5 cases

Table 14- the values for App. Moment vs Lat. Deflection for L=2.3m, for 5 cases

App. Moment	Case1-C-imp2.3-L=2.3	App. Moment	Case2-C-imp2.3-L=2.3	App. Moment	Case3-C-imp2.3-Model1-L=2.3	App. Moment	Case3-C-imp2.3-Model2-L=2.3	App. Moment	No-C-imp2.3-L=2.3
0.036023	- 223.656	0.036023	-222.94	-0.03602	-223.656	0	-213.637	-0.03608	-222.225
0.396254	- 192.885	0.072046	- 210.775	0.684438	-152.811	0.144299	-201.472	0.21645	-163.545
0.972622	- 165.692	0.252161	- 199.325	1.404899	-98.4245	0.324674	-169.985	0.829726	-102.718
1.729107	- 138.499	0.36023	- 180.719	2.557637	-49.7632	0.793651	-124.186	1.551226	-56.9193
3.134005	- 109.874	0.540345	- 166.407	3.818444	-22.5701	1.370851	-77.6719	2.741702	-5.39548
5.295389	- 87.6904	0.72046	- 149.233	6.592219	-6.82669	2.813852	-23.2857	4.58153	36.1098
8.573487	- 70.5158	1.080691	- 119.893	10.08645	1.760601	4.040404	14.64156	6.746032	54.71561
14.62536	- 65.5066	1.981267	- 79.8187	14.08501	-3.24865	6.060606	41.11905	9.632035	45.4127
18.08357	- 70.5158	3.025936	- 42.6071	20.10086	-21.1388	7.503607	45.4127	12.22944	33.24737
21.97406	- 76.2407	4.646974	- 14.6984	24.71182	-34.7354	9.776334	36.82541	14.82684	23.22884

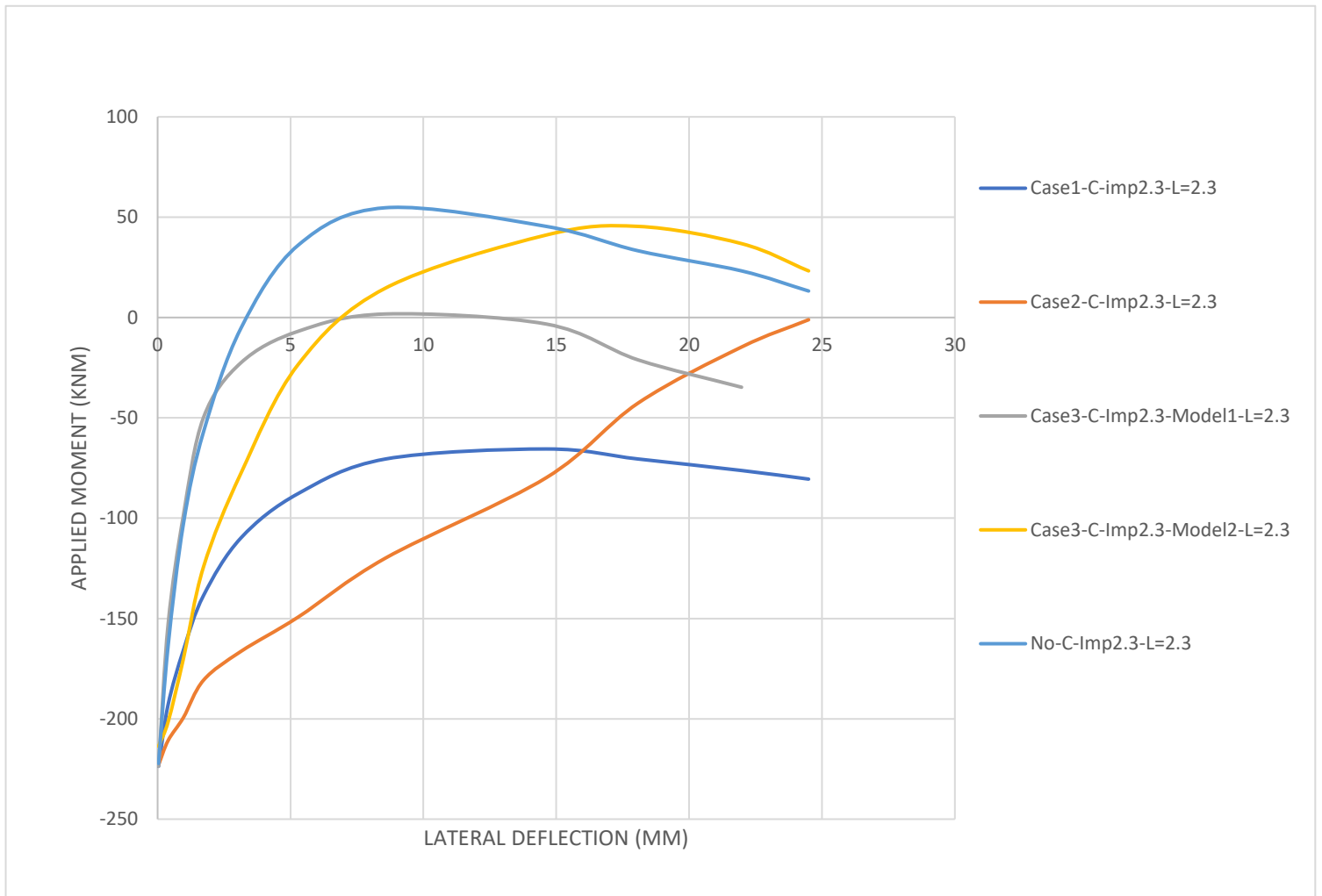


Fig. 4.4.7- App. Moment vs Lat. Deflection for $L=2.3m$, for 5 cases

Table 15- the values for App. Moment vs Lat. Deflection for L=2.5m, for 5 cases

App. Moment	Case1-C-Imp2.5-L=2.5	App. Moment	Case2-C-Imp2.5-L=2.5	App. Moment	Case3-C-Imp2.5-Model1-L=2.5	App. Moment	Case3-C-Imp2.5-Model2-L=2.5	App. Moment	No-C-Imp2.5-L=2.5
-0.02166	-0.16941	-0.02166	0.16941	-0.02166	0	-0.02166	-0.16941	-0.02166	0
0.170854	1.524691	0.235026	4.574068	0.235026	5.082297	0.074596	1.694101	0.010423	2.202329
0.459628	5.590531	0.716315	12.53634	0.812574	14.06103	0.267112	5.92935	0.267112	8.131679
1.358036	12.70575	1.293864	19.82097	1.293864	20.15979	0.491714	10.1646	0.587972	14.23044
2.577304	17.78805	2.320616	27.27501	1.871412	24.56445	0.716315	14.90808	0.908832	19.31274
4.406206	22.36212	3.507797	32.86554	2.641476	29.64676	1.037175	19.48215	1.293864	24.90327
5.946333	24.56445	4.342034	35.57611	3.507797	34.05141	1.80724	28.63029	1.839326	30.4938
8.288611	26.76678	5.176269	37.60902	4.342034	36.25374	2.93025	36.59256	2.320616	33.37377
11.11218	28.12206	6.84474	40.99722	4.791237	37.2702	4.277861	42.86073	3.25111	38.11725
13.90366	28.7997	8.673642	42.18309	5.561301	37.94784	6.106764	45.91011	4.117431	42.35251
16.66306	28.63029	10.43837	42.52192	6.45971	38.7949	8.352783	47.94303	5.112098	46.41835
20	28.29147	11.9785	42.01368	7.486461	39.64195	9.668308	48.9595	6.042592	48.62068

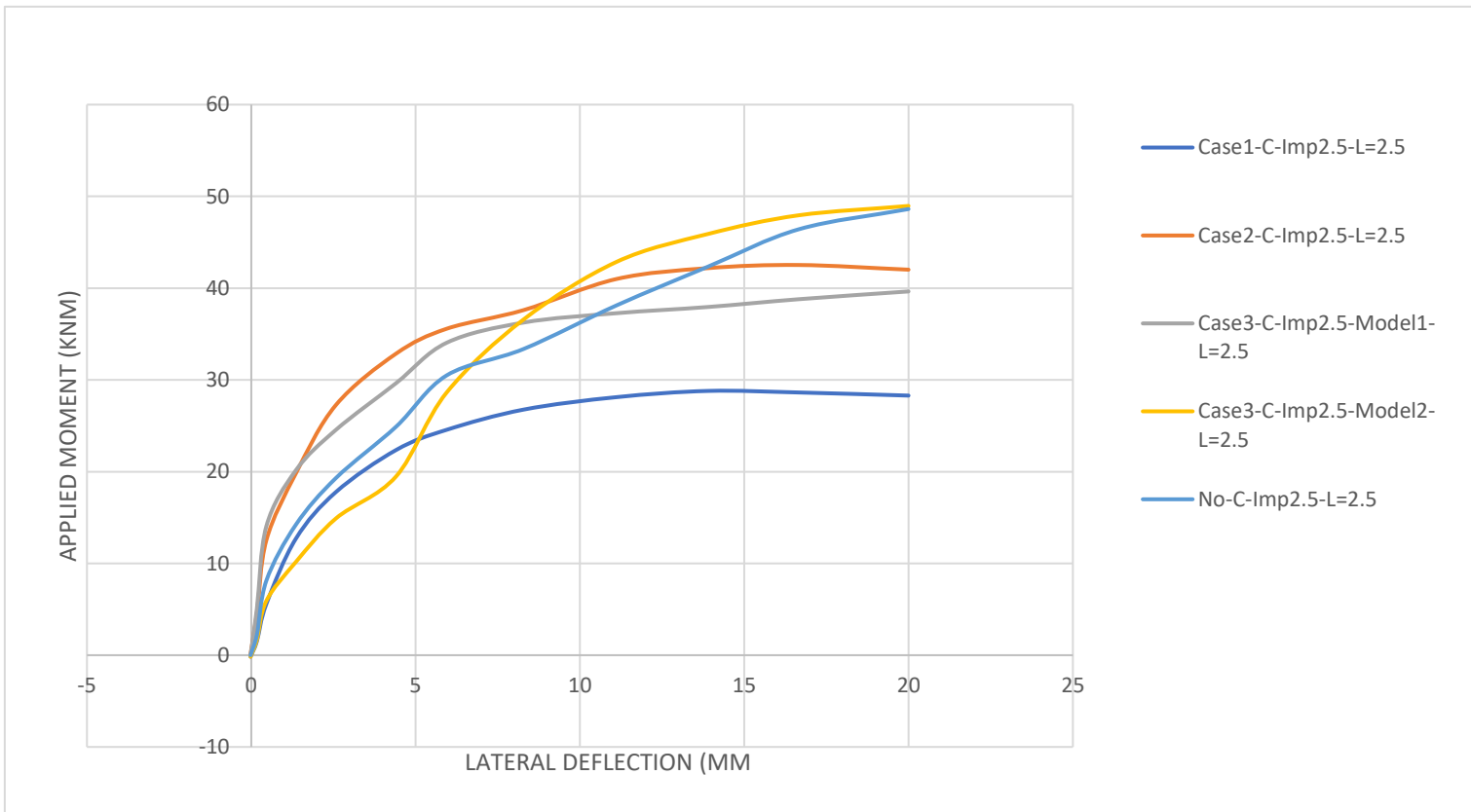


Fig. 4.4.8- App. Moment vs Lat. Deflection for L=2.5m, for 5 cases

Table 16- the values for App. Moment vs Lat. Deflection for L=3m, for 5 cases

App. Moment	Case1-C-Imp3-L=3	App. Moment	Case2-C-Imp3-L=3	App. Moment	Case3-C-Imp3-Model1-L=3	App. Moment	Case3-C-Imp3-Model2-L=3	App. Moment	No-C-Imp3-L=3
0.040519	-0.14618	0.040519	0	0.040519	0.146184	0.040519	-0.14618	0.040519	0
0.28363	2.485052	0.324148	4.239204	0.040519	1.607973	0.121556	3.215947	0.040519	3.50831
1.094003	7.308972	0.607779	7.162793	0.364667	5.408641	0.405187	7.016614	0.28363	7.308972
1.823339	10.52492	0.89141	9.940203	0.567261	7.893688	0.688816	10.6711	0.648298	11.25581
2.390599	12.42525	1.17504	13.44851	0.850892	10.23256	1.012966	14.61794	1.012966	15.6412
3.363046	14.47176	1.742302	16.37209	1.053484	12.57143	1.620745	19.73422	1.499189	20.31894
4.497569	16.37209	2.106968	19.00332	1.499189	15.93356	2.188007	23.38871	2.188007	24.41196
5.551053	17.39535	3.200972	23.82724	2.06645	19.1495	3.200972	28.21263	2.917341	28.65116
6.604537	19.00332	4.011345	26.16612	2.471636	21.04983	3.930307	31.42857	3.808751	32.59801
8.508914	20.31894	5.388979	28.94352	2.998378	23.24253	5.105348	34.64452	5.63209	37.42193
10.12966	21.19601	6.685575	31.42857	4.092382	26.45847	6.19935	36.83721	7.050242	39.61462
12.68233	22.21927	8.063209	33.03654	5.024311	29.52824	7.739058	38.88372	8.589951	41.22259
14.9919	22.80399	8.752025	33.47508	5.875202	31.13621	9.359804	40.63787	10.57537	43.2691

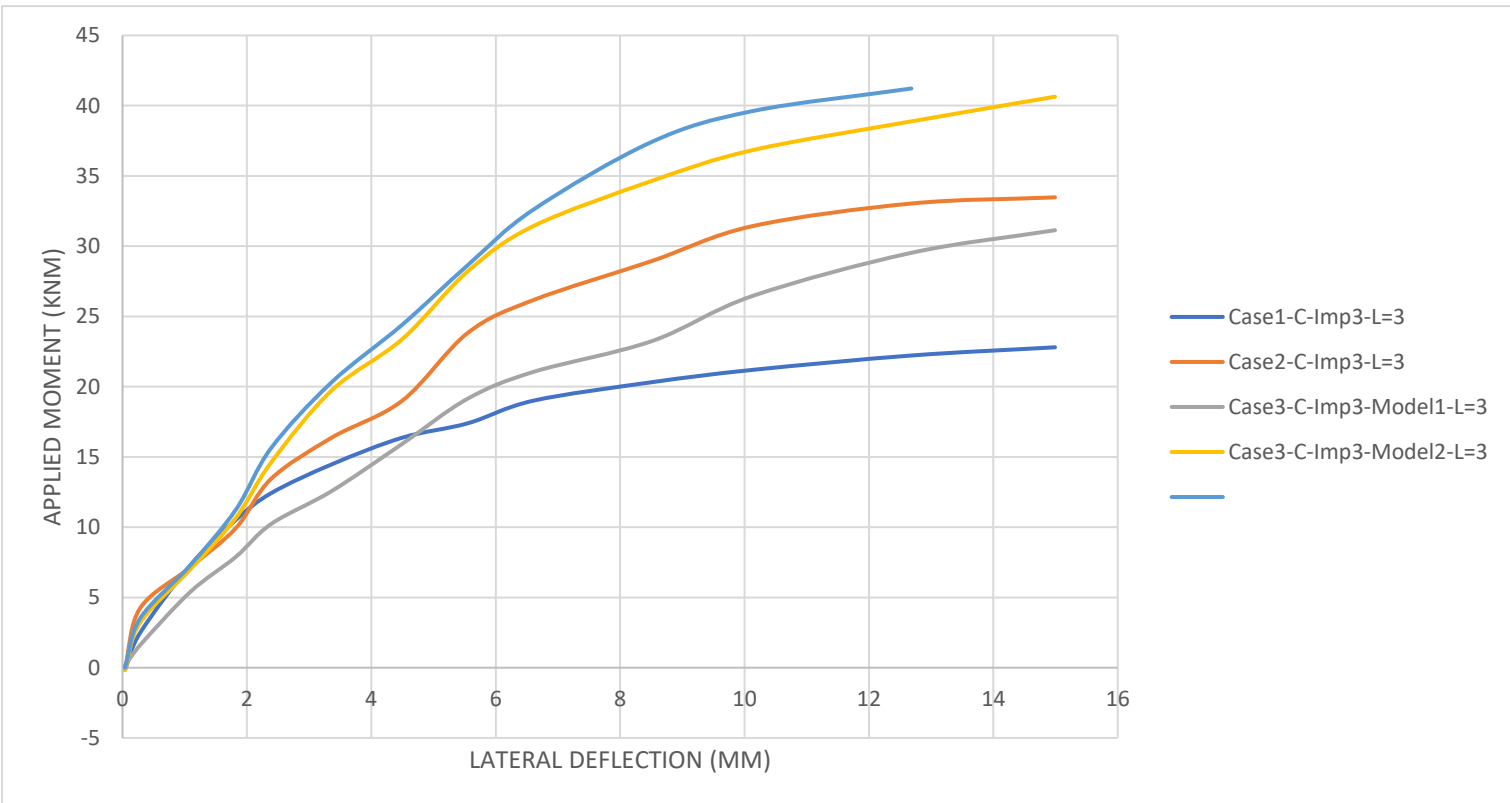


Fig. 4.4.9- App. Moment vs Lat. Deflection for L=3m, for 5 cases

Table 17- the values for App. Moment vs Lat. Deflection for L=3.4m, for 5 cases

Applied Moment	Case1-C-Imp3.4-L=3.4	Applied Moment	Case2-C-Imp3.4-L=3.4	Applied Moment	Case3-C-Imp3.4-Model1-L=3.4	Applied Moment	Case3-C-Imp3.4-Model2-L=3.4	Applied Moment	No-C-Imp3.4-L=3.4
0	-92.7754	0	-93.147	-0.04695	-93.147	0	-92.7754	0	-92.4038
0.516432	-81.6275	0.375587	-80.8843	0.093896	-87.9447	0.093896	-89.431	0.187793	-77.1683
1.455399	-69.3647	0.610328	-72.7091	0.375587	-77.9115	0.281689	-79.0263	0.657277	-62.676
2.957747	-54.8724	0.892019	-65.6488	0.798121	-66.0204	0.56338	-68.9931	1.032864	-51.528
4.929577	-45.2108	1.408451	-54.1292	1.455399	-50.0416	1.220657	-48.5552	1.549296	-37.4073
7.511736	-37.0357	2.159624	-40.3801	2.065728	-39.6369	2.206572	-29.2321	2.159624	-26.2593
9.342723	-33.3197	2.629108	-34.0629	3.004695	-27.7457	3.14554	-14.3682	2.816901	-15.1114
13.00469	-28.1173	3.755868	-21.0569	4.413145	-14.3682	4.929577	1.982163	4.741784	6.069746
15.25822	-26.2593	4.882628	-12.8818	6.713615	0.124171	7.323943	9.042537	7.089201	20.93368
19.01408	-24.0297	7.230047	-2.47702	9.061034	6.441344	10.70423	11.27213	10.14084	32.08164
23.70892	-22.5433	9.530516	5.698149	10.98592	10.90053	14.69484	12.75852	13.42723	38.77041
25.16432	-21.8001	11.40845	9.785732	13.61502	15.73131	19.53052	11.27213	14.50704	39.88521

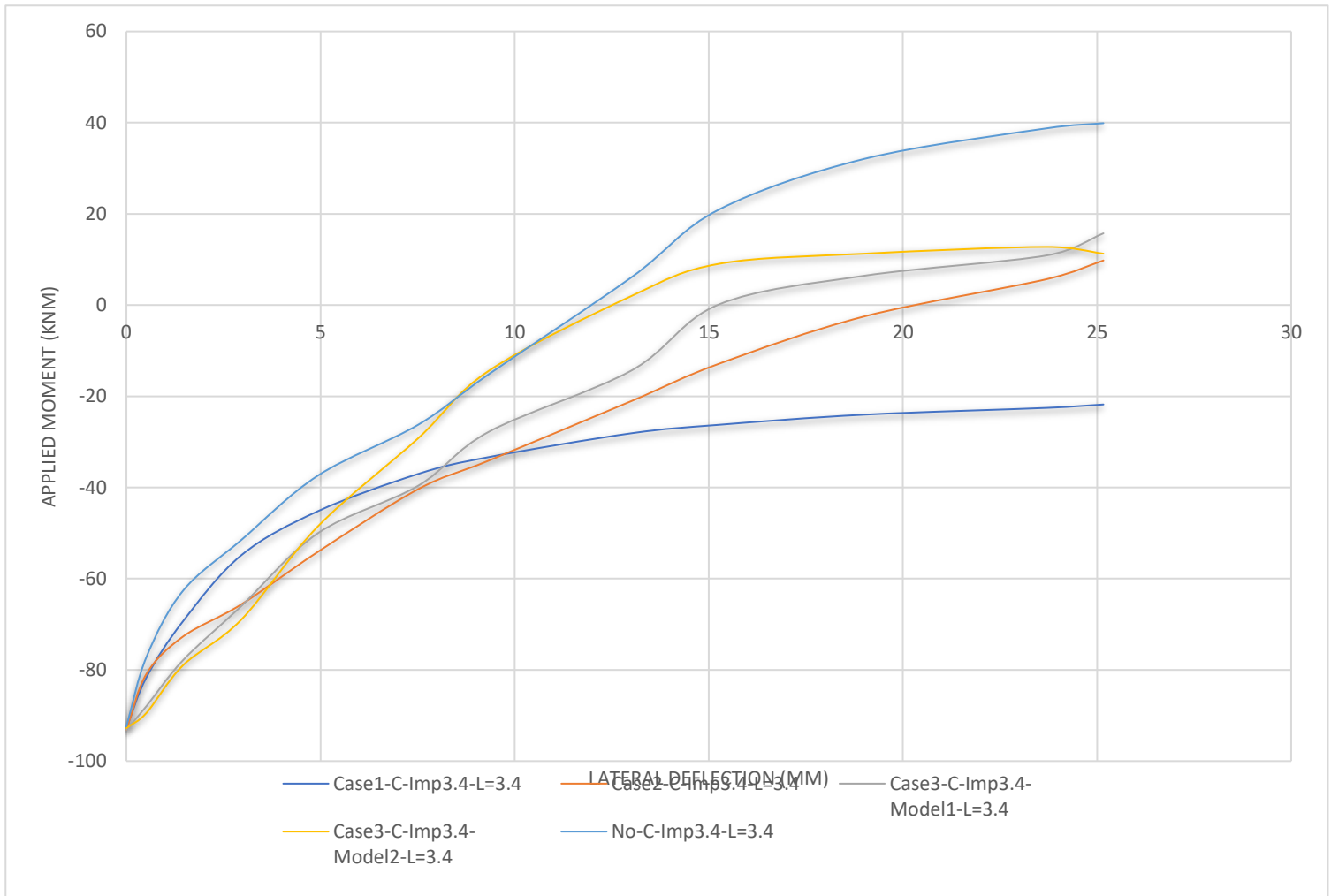


Fig. 4.4.10- App. Moment vs Lat. Deflection for L=3.4m, for 5 cases

Table 18- the values for App. Moment vs Lat. Deflection for L=4m, for 5 cases

App. Moment	Case1-C-Imp4-L=4	App. Moment	Case3-C-Imp4-Model1-L=4	App. Moment	Case2-C-Imp4-L=4	App. Moment	Case3-C-Imp4-Model2-L=4	App. Moment	No-C-Imp4-L=4
0	0.118421	0.16	0	0	0	0.480001	4.736844	0.16	-0.11842
0.640001	2.723684	0.640001	4.618419	0.08	1.184211	0.88	7.81579	0.400001	5.684209
2.160001	7.223682	1.200002	7.105261	0.480001	4.263157	1.6	12.19737	0.96	9.355263
4.559999	10.89474	1.520001	9.236842	0.96	7.105261	2.72	16.57895	1.6	13.26316
8.480001	13.85526	2.64	13.5	1.919999	12.19737	4.800001	22.85526	2.400001	16.81579
15.36	16.3421	4.800001	18.35526	3.280001	16.57895	7.92	26.64474	4.24	22.97368
19.68	17.05263	6.88	21.55263	4.559999	19.65789	11.84	28.06579	7.279999	28.65789
25.84	17.76316	9.120002	23.0921	5.840001	21.55263	15.76	28.65789	10.96	31.97368
31.12	18.11842	11.44	25.10526	8.480001	23.32895	21.12	29.13158	13.76	33.27631
38	18.35526	14.08	26.17105	13.04	25.46053			17.6	35.17105
46.08	18.35526	16.96	27.35526	16	25.93421			20.48	35.52632
49.44	18.47368	19.68	27.5921	20.16	26.17105			25.28	35.28947

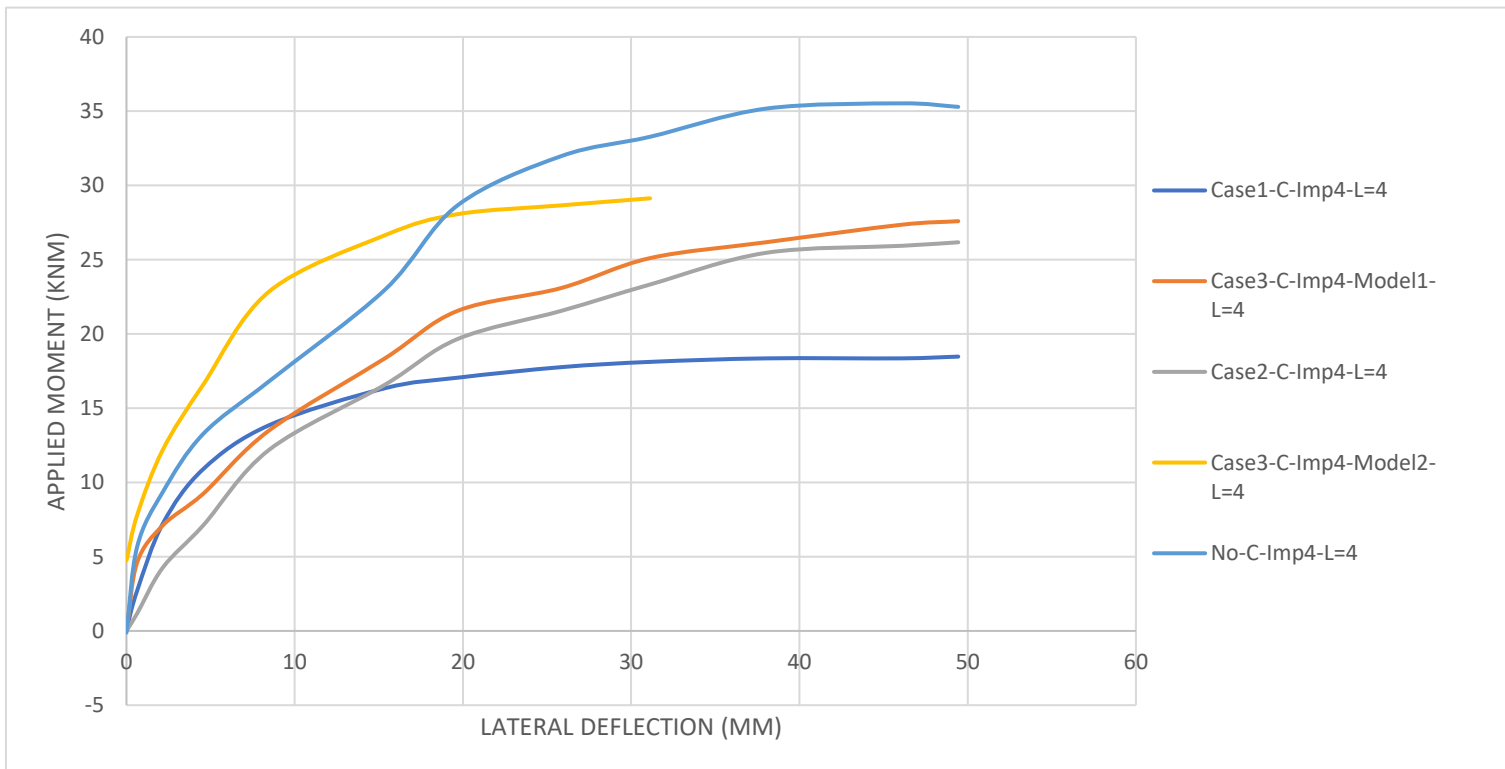


Fig. 4.4.11- App. Moment vs Lat. Deflection for L=4m, for 5 cases

Table 19- the values for App. Moment vs Lat. Deflection for L=5m, for 5 cases

App. Moment	Case1-C-Imp5-L=5	App. Moment	Case2-C-Imp5-L=5	App. Moment	Case3-C-Imp5-Model1-L=5	App. Moment	Case3-C-Imp5-Model2-L=5	App. Moment	Case3-C-Imp5-Model2-L=5
0	0	0.130935	0	-0.06547	0	0	0	-0.06547	-0.11429
1.243863	3.542858	0.720131	3.200002	0.130935	1.142857	0.261867	1.600003	0.523732	4.342859
3.797056	7.771432	1.112931	4.914286	0.458266	2.514286	0.458266	3.200002	1.178397	7.771432
6.350246	10.05714	1.505728	6.514289	0.851066	4.57143	0.916532	5.828573	1.833062	10.97143
9.034371	11.54286	2.880524	10.62857	1.636663	7.771432	1.571197	8.571429	2.749591	13.94286
11.78396	12.57143	4.320785	13.37143	2.42226	10.28572	2.356794	11.31429	3.797056	16.68572
13.87889	13.25714	6.743045	16.34286	3.666121	13.37143	3.469722	14.62857	5.040916	19.54286
		9.754502	19.2	5.433716	16.45714	5.106383	18.05715	6.350246	22.05714
		13.94435	21.48571	7.463176	19.08571	6.808512	21.02857	8.117841	24
		17.87234	22.85714	9.754502	21.02857	8.968904	23.2	9.754502	25.48572
		21.66939	23.88571	12.63503	22.62857	11.91489	25.14286	11.5221	27.08571
		24.09165	24.34286	15.64648	23.77143	18.13421	26.28571	17.08674	29.48571

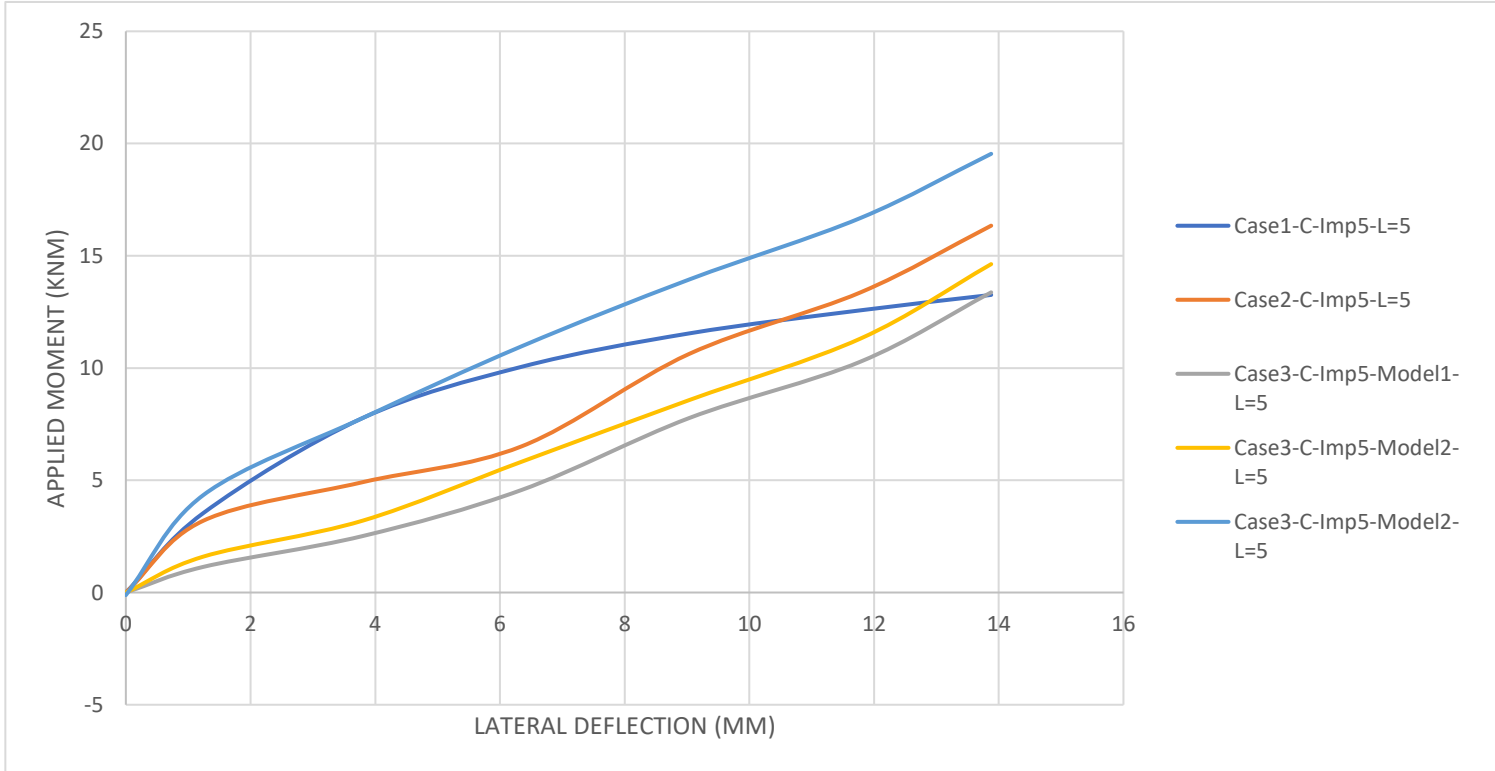


Fig. 4.4.12- App. Moment vs Lat. Deflection for L=5m, for 5 cases

Table 20- the values for App. Moment vs Lat. Deflection for L=7m, for 5 cases

App. Moment	Case1-C-Imp7-L=7	App. Moment	Case2-C-Imp7-L=7	App. Moment	Case3-C-Imp7-Model1-L=7	App. Moment	Case3-C-Imp7-Model2-L=7	App. Moment	No-C-Imp7-L=7
0.032374	-0.0519	0.032374	-0.0519	0	0	-0.03237	0	0	0.051903
0.776978	1.245674	0.323741	0.882354	0.161871	0.570934	0.226619	0.934257	0.097123	0.622837
1.910073	2.698962	0.776978	1.868512	0.388489	1.349482	0.582734	1.920416	0.453238	2.024222
3.366907	4.152249	1.035971	2.387543	0.744604	2.179931	1.003597	3.062285	0.971223	3.373703
4.953238	5.242214	1.586332	3.425606	1.327339	3.581315	1.586332	4.619377	1.424461	4.723183
7.607914	6.591697	2.233814	4.515571	1.910073	4.878894	2.330936	6.020762	1.877699	6.072665
		2.589928	5.034603	2.492806	5.968859	3.140288	7.577854	2.492806	7.31834
		3.269784	6.072665	2.848921	6.591697	3.982014	8.823529	3.043166	8.512111
		3.917266	6.903114	3.269784	7.31834	5.406475	10.48443	3.690648	9.809689
		4.726619	7.785468	3.917266	8.304499	6.766188	11.83391	4.33813	10.79585
		5.859713	8.875434	4.402879	8.771626	8.44964	13.13149	5.017986	11.93772
		6.733812	9.498271	4.88849	9.394463	9.744605	14.01384	5.76259	12.82007
		7.866908	10.32872	5.568346	10.12111	11.20144	14.79239	6.539568	13.65052

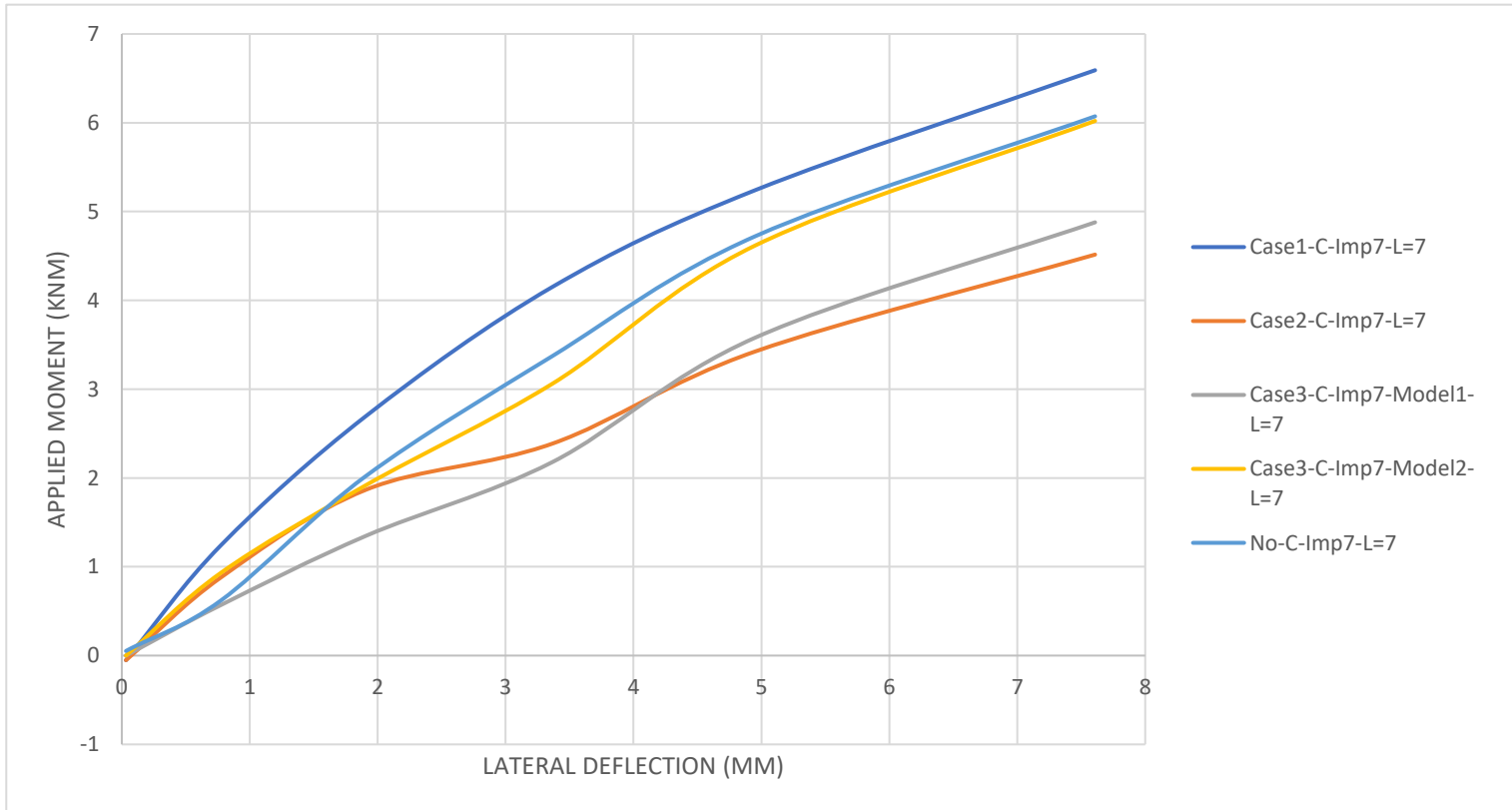


Fig. 4.4.13- App. Moment vs Lat. Deflection for L=7m, for 5 cases

Table 21- the values for App. Moment vs Lat. Deflection for L=10m, for 5 cases

App. Moment	Case1-C-10m-Imp10	App. Moment	Case2-C-Imp10-L=10	App. Moment	Case3-C-Imp10-Model2-L=10	App. Moment	No-C-10m-imp10	App. Moment	Case3-C-Imp10-Model1-L=10
-0.00019	-0.03297	-0.00019	-0.08962	-0.00019	0.023686	-0.00019	-0.03297	0.864758	1.752353
0.449584	0.306945	0.553378	0.590203	0.587976	0.986764	0.345791	0.590203	1.522116	2.939429
1.314528	1.270022	1.106942	1.100067	1.106942	1.666584	0.726367	1.213371	2.38706	4.239561
2.248668	1.779888	1.660506	1.723237	1.556713	2.289755	1.141539	1.893192	3.113613	5.313583
3.494189	2.51636	2.248668	2.176451	2.041082	2.912923	2.248668	3.53609	3.94396	6.331078
4.808904	3.252832	3.217406	2.912923	2.940624	3.989306	3.45959	5.405599	4.670512	7.348572
6.089022	3.649394	3.909361	3.422789	3.909361	5.065687	4.39373	6.651935	5.604652	8.196484
8.061093	4.272564	4.532122	3.932653	5.32787	6.595284	5.535456	8.294835	6.365803	8.874814
9.790982	4.725778	5.95063	4.839082	6.919367	8.011576	6.919367	9.711128	7.265345	9.553144
11.48627	5.065687	6.88477	5.235642	8.476267	9.144611	8.960636	10.95747	8.268681	10.288
14.46168	5.575553	8.199485	5.858812	10.13696	10.05104	11.0711	12.0905	9.272015	10.85328
17.16031	5.972116	9.37581	6.651935	12.35122	11.01412	13.49294	13.11023	10.24075	11.13591
20.23951	6.312025	11.24409	7.275105			15.7418	13.6201	11.27869	11.58813
22.59216	6.48198	12.90478	7.841622			17.99065	14.18661	12.31662	11.81424

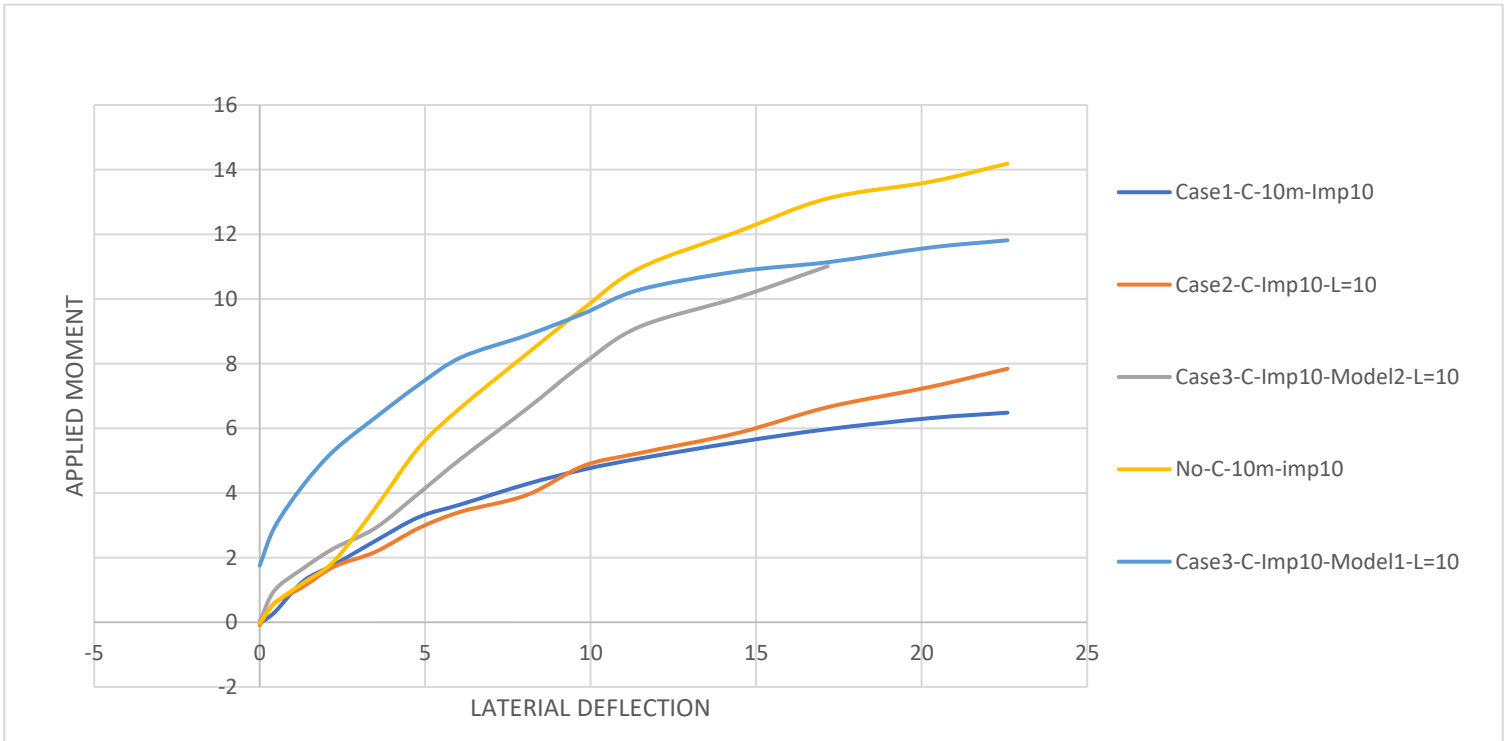


Fig. 4.4.14- App. Moment vs Lateral Deflection for L=10m, for 5 cases

Now we will see the increase in temperature of test specimen and then check how non-dimensional slenderness ratio and buckling moment capacity correlates.

Table 22- no change in temperature of the I-Beam

Non-dimensional slenderness λ_{LT}	Eurocode 3	Non-dimensional slenderness λ_{LT}	ANSYS- Corresponding to MbRd 2	Non-dimensional slenderness λ_{LT}	ANSYS- Corresponding to MbRd 3
0.195064	1.015429	0.688627	0.650286	0.693562	0.583429
0.328326	0.933143	0.915665	0.712	0.91073	0.660571
0.466524	0.871429	1.122961	0.588571	1.127897	0.521714
0.609657	0.809714	1.231545	0.532	1.236481	0.444571
0.787339	0.696571	1.305579	0.496	1.305579	0.372571
1.019313	0.552571	1.305579	0.496	1.468455	0.326286
1.246352	0.418857	1.468455	0.424	1.468455	0.326286
1.448712	0.331429	1.58691	0.372571	1.591846	0.290286
1.680687	0.244	1.774464	0.326286	1.769528	0.146286
1.991631	0.177143	2.06073	0.269714	2.06073	0.130857
2.243348	0.130857	2.648069	0.120571	2.648069	0.038286
2.504936	0.1				

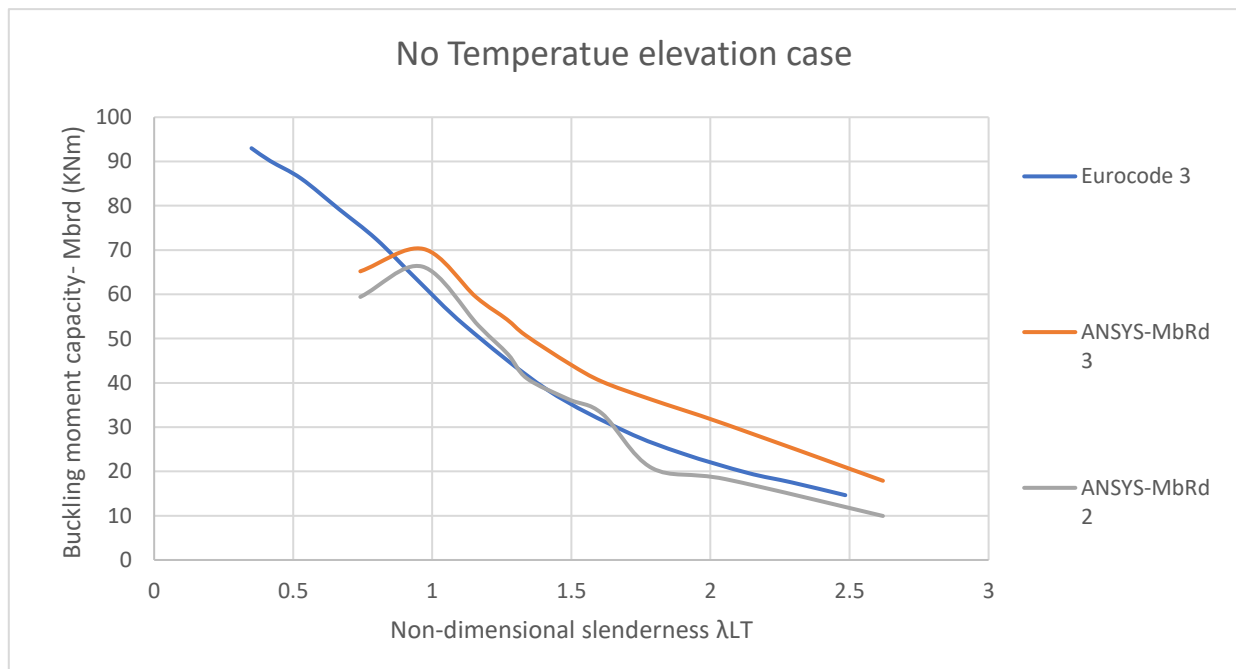


Fig. 4.4.15- no change in temperature of the I-Beam (Reduction factor vs Non-dimensional)

Table 23- At temperature of 500°C of the I-Beam

Non-dimensional slenderness λ_{LT}	Eurocode 3	Non-dimensional slenderness λ_{LT}	ANSYS- Corresponding to MbRd 2	Non-dimensional slenderness λ_{LT}	ANSYS- Corresponding to MbRd 3
0.35	93	0.741224	65.19445	0.741224	59.41667
0.417619	90.11111	0.968231	70.25	0.963401	66.27778
0.528707	86.13889	1.156598	59.41667	1.166258	52.91667
0.663946	79.27778	1.267687	54.36111	1.272517	46.41667
0.799184	72.41667	1.335306	50.75	1.340136	41.00001
0.944081	63.38889	1.494694	44.25	1.489864	36.30555
1.117959	52.91667	1.610612	40.27777	1.610612	33.05556
1.412585	38.47222	1.78449	36.30555	1.78932	20.77778
1.692721	29.08334	2.059796	30.52778	2.054966	18.25
1.900408	24.02777	2.620068	17.88889	2.620068	9.944448
2.132245	19.69444				
2.291632	17.52778				
2.48483	14.63889				

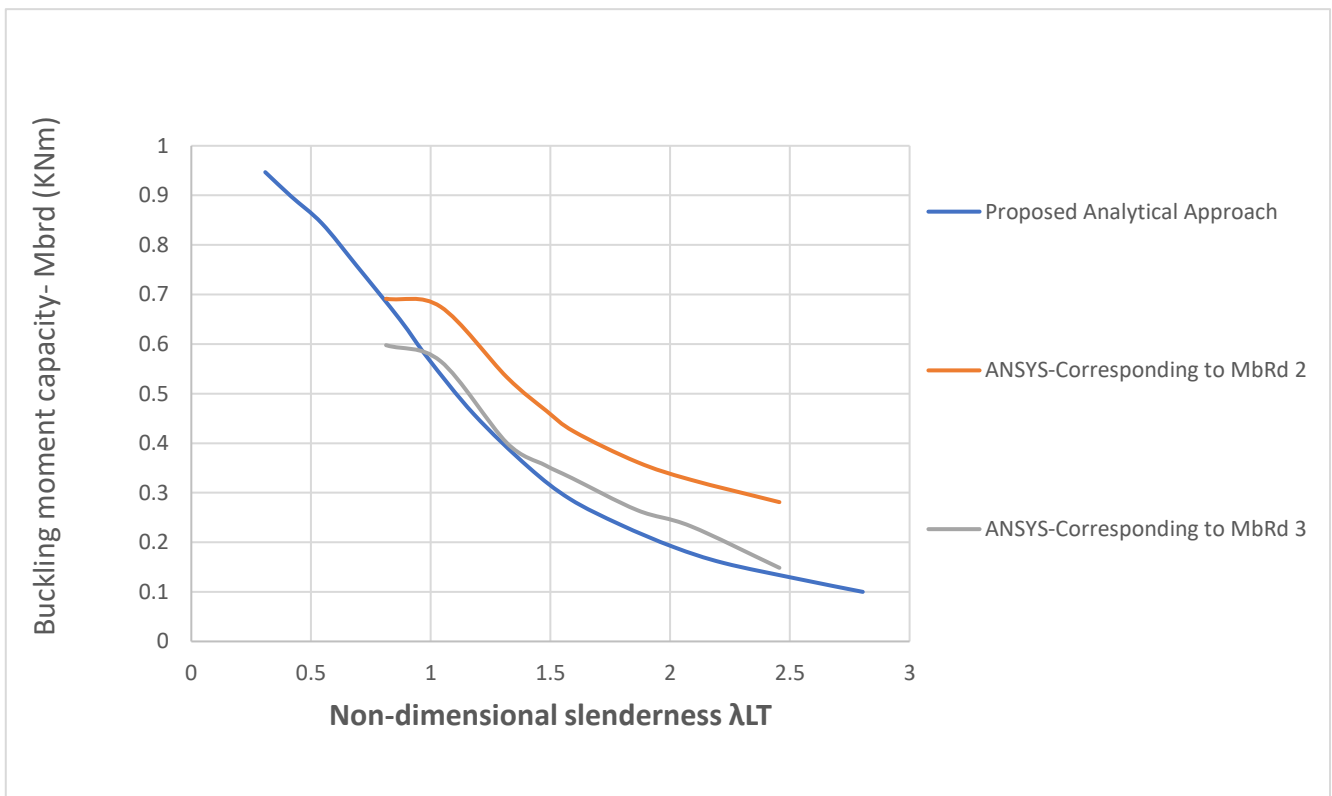


Fig. 4.4.16- Reduction factor vs non-dimensional – 500°C Temperature elevation

Table 24- At temperature of 800°C of the I-Beam

Non-dimensional slenderness λ_{LT}	Eurocode 3	Non-dimensional slenderness λ_{LT}	ANSYS- Corresponding to MbRd 2	Non-dimensional slenderness λ_{LT}	ANSYS- Corresponding to MbRd 3
0.308929	0.946768	0.813393	0.691445	0.813393	0.597719
0.416071	0.898289	1.041071	0.675285	1.041071	0.565399
0.545536	0.843346	1.317857	0.53308	1.317857	0.40057
0.688393	0.759316	1.483036	0.465209	1.478571	0.355323
0.871429	0.64943	1.599107	0.423194	1.590178	0.329468
0.9875	0.571863	1.8625	0.361787	1.8625	0.264829
1.179464	0.458745	2.085714	0.326236	2.085714	0.23251
1.407143	0.352091	2.45625	0.280989	2.45625	0.148479
1.58125	0.287453				
1.791071	0.235741				
2.014286	0.190494				
2.224107	0.158175				
2.536607	0.125856				
2.804464	0.1				

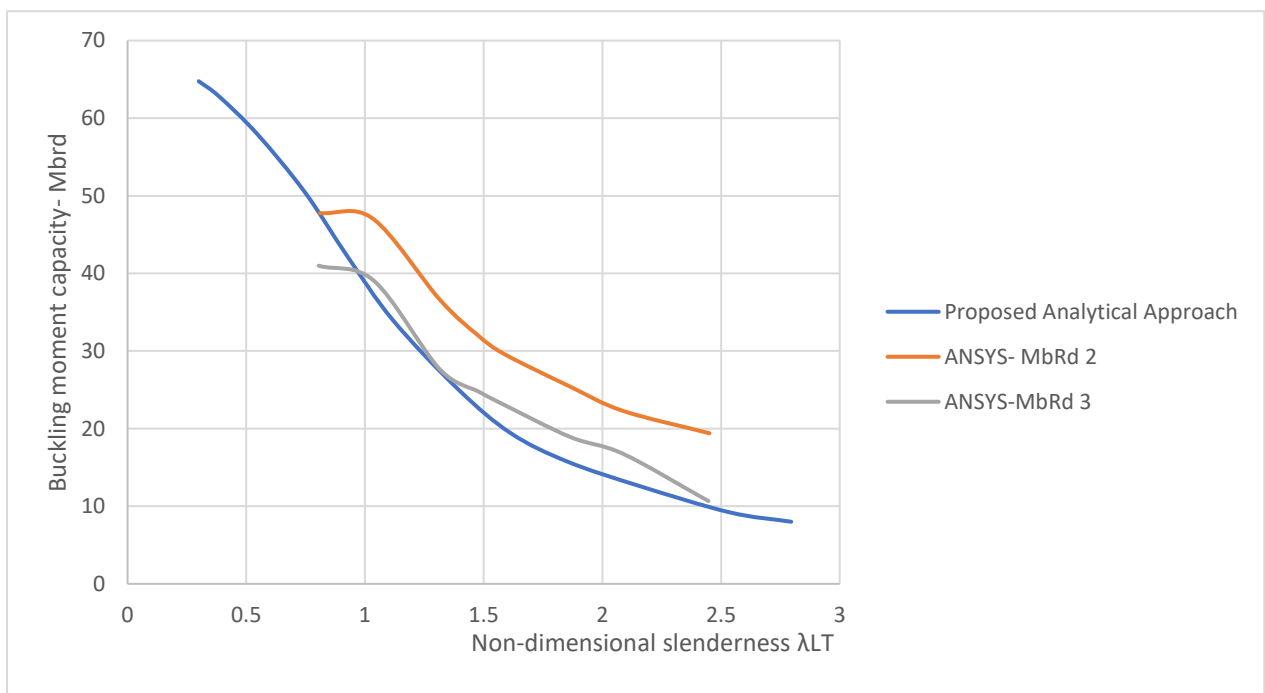


Fig. 4.4.17- Reduction factor vs non-dimensional – 800°C Temperature elevation

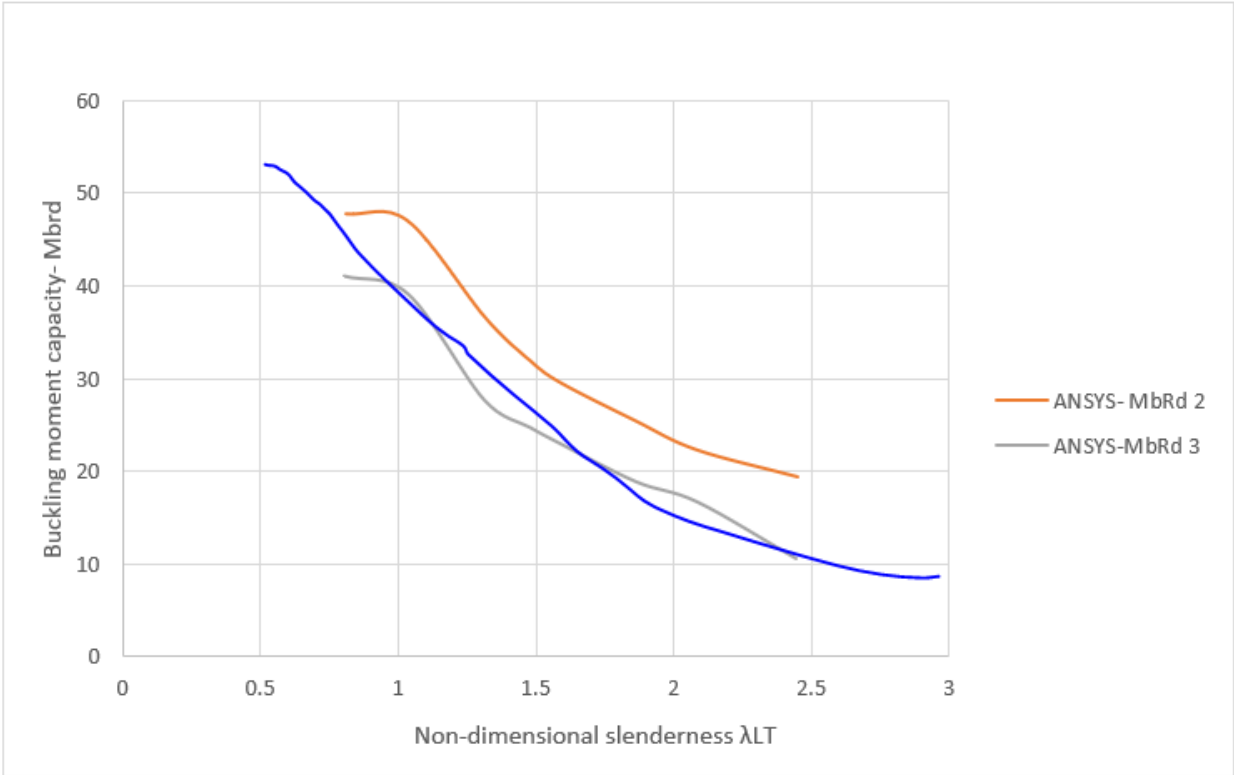


Fig. 4.4.18- Reduction factor vs non-dimensional – 1200°C Temperature elevation

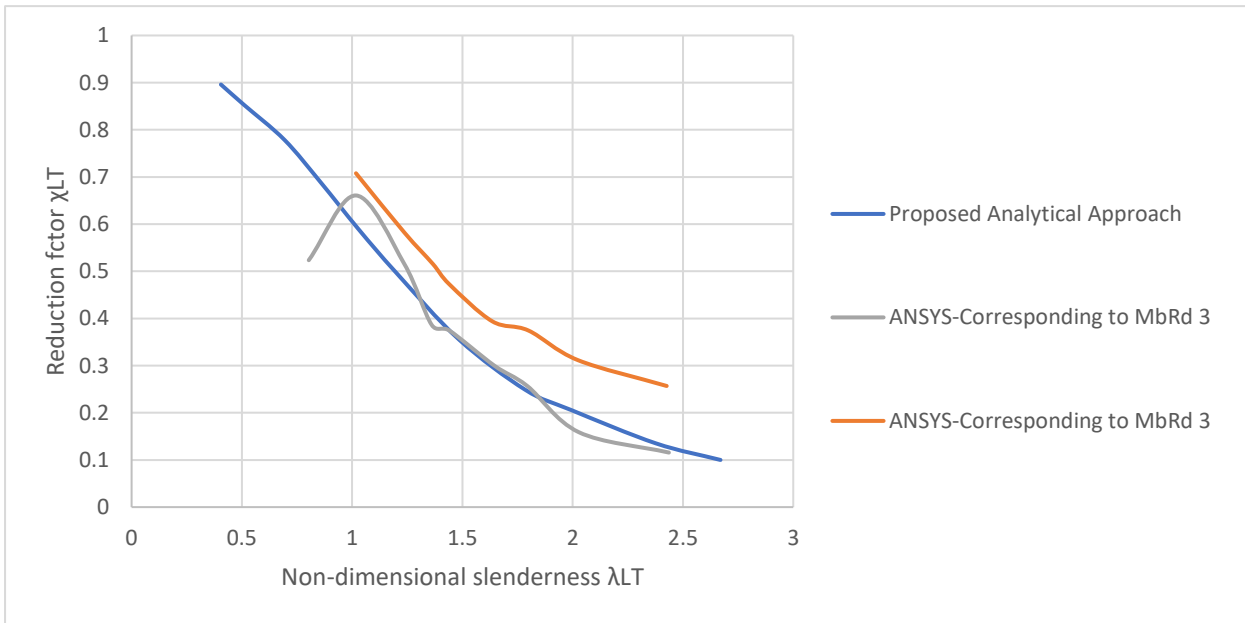


Fig. 4.4.19- Reduction factor vs non-dimensional – 1500°C Temperature elevation

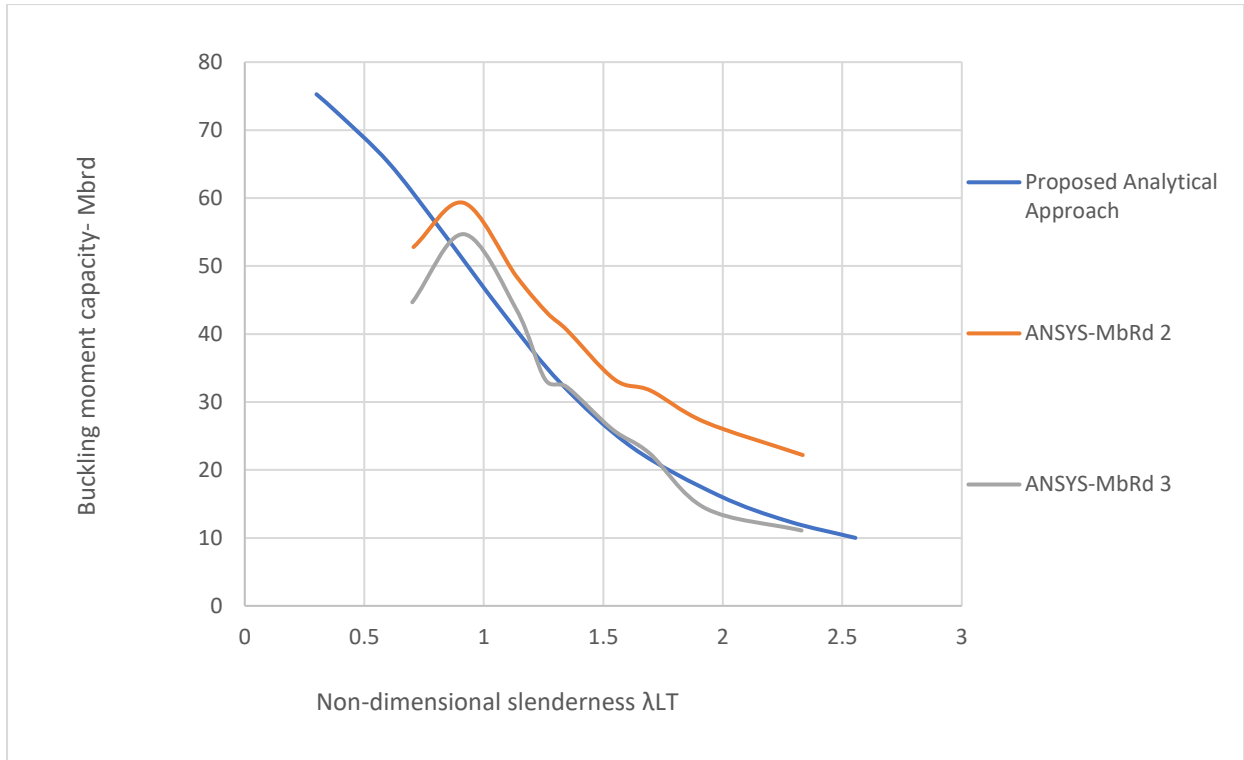


Fig. 4.4.20- Reduction factor vs non-dimensional – 2000°C Temperature elevation

Chapter 5

5-Discussion

5.1- Analysis

Material Properties

Table 25- the properties of I-Beam selected for FEM in ANSYS workbench.

Material	High strength low alloy steel, YS355
Modulus of elasticity	210000 Mpa
Shear modulus	80769 Mpa
Poisson's ratio	0.3
Tensile Yield Strength	390.2 Mpa
Tensile Ultimate Strength	486.3 Mpa

There are two types of loading acting, one is loads/stresses applied on the end of beam due to end moments and other is uniform line stress or pressure acting on a point or whole cross-section.

Critical Moment M_{cr}

Table 26- For calculation of M_{cr} from Eigenvalue

Type/Condition of Loading	$M_{cr} = \text{Eigenvalue (Deformation) from ANSYS * App. Moment}$
In the Case of Deformation	
loads/stresses applied on the end of beam due to end moments	$7.0688 * 10 = 70.688$
uniform line stress or pressure acting	$1.8607 * 10 = 18.8607$
In the Case of Buckling	
loads/stresses applied on the end of beam due to end moments	$4.5690 * 10 = 45.690$
uniform line stress or pressure acting	$1.8071 * 10 = 18.071$

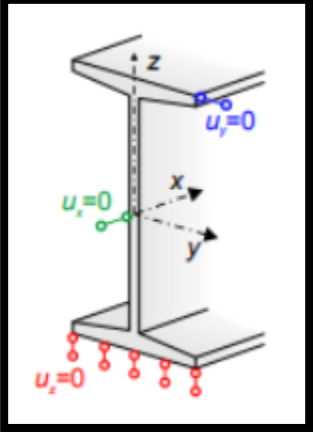
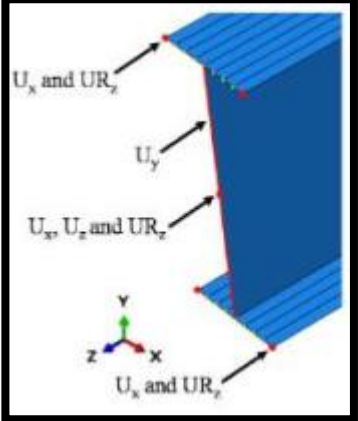
Boundary Conditions

The rotation is allowed in three dimensions.

1. Rotations at both ends of beam
2. Rotation along x-Corner
3. Rotation about Mid Node.

These three boundary conditions are explained in the figures tabulated below.

Table 27- the conditions for boundary values of FEM.

Boundary Condition	Source/Taken From	Pictorial View
First Boundary Condition	<i>“FE nonlinear analysis of LTB resistance”</i>	 <p data-bbox="1002 927 1385 1016"><i>Fig. 5.1.1- Assumptions of 1st Boundary Condition</i></p>
Second Boundary Condition	<i>“The influence of structural imperfections on the LTB strength of I-beams”</i>	 <p data-bbox="1002 1541 1385 1630"><i>Fig. 5.1.2- Assumptions of 2nd Boundary Condition</i></p>

Meshing

The experiments are performed with meshing. There are two conditions for meshing analysis, one is max. Stress/pressure against mesh density and other is max. Deflection or displacement against mesh density.

By conducting the linear and buckling analyses with different mesh densities, we can identify the appropriate mesh density for all of the FEM's situations. The software takes less time to do the analysis when the mesh density is reduced, however the results were not accurate. The software takes longer to run the analysis when the mesh density is increased, and the results are more accurate. The value of mesh for the models of FEM during analysis is taken as 5mm.

For Non-Linear Analysis

We are going to use the formula provided in the article for Finite Element Modeling of Non-linear LTB resistance.

The formula is

$$e_o = \frac{Length}{1000}$$

Where length must be in mm.

We had varied the length of specimen by splitting it from 1.0m to 10m.

Table 28- Table to determine the imperfection length

L (mm)	1000	1500	2000	2300	2500	3000	3400	4000	5000	7000	10000
$e_o = \frac{Length}{1000}$	1	1.5	2	2.3	2.5	3	3.4	4	5	7	10

Cross-Sectional Properties of I-Beam

Table 29- the cross-sectional properties of I-beam, an input in ANSYS workbench.

Hight (mm)	200
Top Flange Width (mm)	90
Bottom Flange Width (mm)	90
Web Thickness (mm)	7.5
Web hight (mm)	177.4
Top Flange thickness (mm)	11.3
Bottom Flange thickness (mm)	11.3
Hypotenuse (mm)	$\sqrt{5^2 + 5^2} = 5\sqrt{2}$
Wply (mm ³)	$250.92 * 10^3$
Izz (mm ⁴)	$1.38 * 10^6$
Iyy (mm ⁴)	$2.16 * 10^7$
It (mm ⁴)	$1.11 * 10^5$
Iw (mm ⁶)	$1.22 * 10^{10}$

Results Accuracy

Three types of analysis are performed on FEM model. These are;

1. **Static Linear Analysis**

Static analysis includes geometry, meshing, boundary, and load conditions.

2. **Linear Buckling Analysis**

Linear Buckling Analysis included geometry, meshing, boundary, and load conditions.

3. **Non-Linear Buckling Analysis**

It includes modeling, iterations, and convergence criteria.

Geometry

Geometry is the sectional properties of I-Beam like MOI about x-axis, y-axis, z-axis, areas, slenderness ratios etc. If we keep the geometry same and perform analysis, then there is no variation in results occurs and accuracy of results is disturbed. To change the geometrical properties of I-beam, help for better understanding of results and the better understanding of comparisons.

Meshing (Elements Size)

The experiments are performed with meshing. There are two conditions for meshing analysis, one is max. Stress/pressure against mesh density and other is max. Deflection or displacement against mesh density.

By conducting the linear and buckling analyses with different mesh densities, we can identify the right mesh density for all of the finite element model's situations. The software takes less time to do the analysis when the mesh density is reduced, but the results are less accurate. The software takes longer to run the analysis when the mesh density is increased, and the results are more accurate. The value of mesh for the models of FEM during analysis is taken as 5mm.

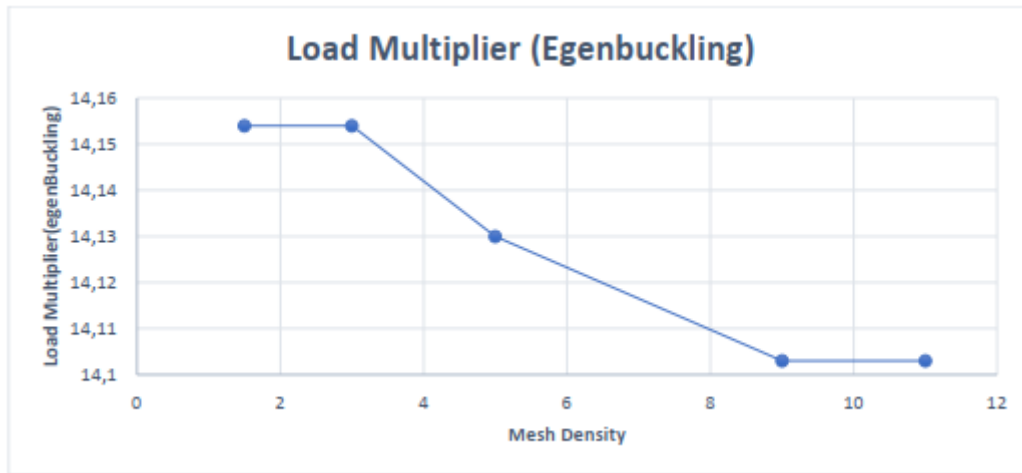


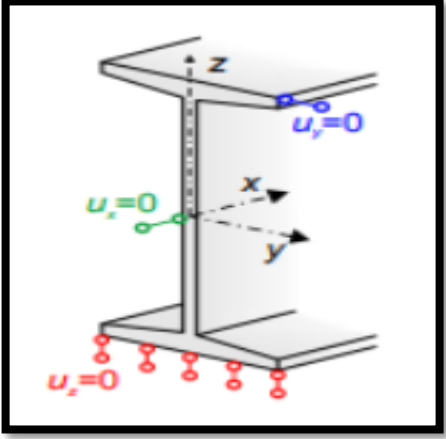
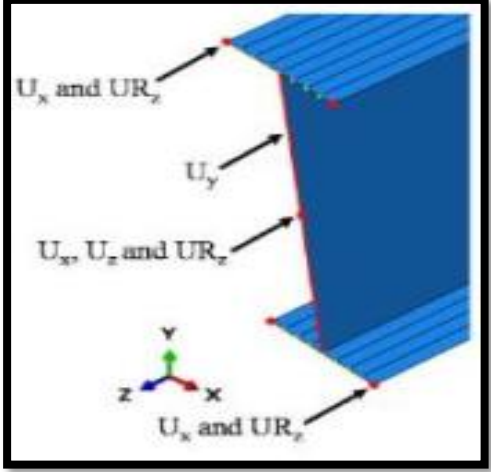
Fig. 5.1.3- Load Multiplier obtained from Eigenbuckling vs Meshing Size/Density

Criteria for Convergence

To operate the results obtained from FEM analysis, the criteria for convergence is introduced which results in the degradation of accuracy in the results obtained from FEM analysis. Different types of convergence options are available in ANSYS workbench, for instance, Convergences due to forces, displacements, applied moments, rotations and Newton-Raphson method. There are other options available as well instead of adjusting the convergence criteria. These options are; use of identical load conditions for both linear and non-linear static analysis, increase of size of steps and dividing them into more sub-steps in the buckling analysis, chose of exact load type for modeling, refine the mesh density etc.

Boundary Conditions

Table 30- This table illustrates the conditions for boundary values of FEM.

Boundary Condition	Local Deformation	Pictorial View
First Boundary Condition	While running a static linear analysis in ANSYS for all the models includes in this research, the first boundary condition introduces the unrealistic and unreasonable local deformation.	 <p data-bbox="863 1003 1385 1088">Fig. 5.1.4- Assumptions of 1st Boundary Condition</p>
Second Boundary Condition	While running a static linear analysis in ANSYS for all the models includes in this research, the first boundary condition introduces the non-unrealistic and non-unreasonable local deformation.	 <p data-bbox="863 1659 1385 1744">Fig. 5.1.5- Assumptions of 2nd Boundary Condition</p>

Iterations

To reduce the errors in FEM results, there need to divide the non-linear buckling analysis in variety of sub-steps to get the more accuracy. For this reason, the curves of different cases are plotted to get more results that need to easier them to compare and then for analysis. All the graphs plotted in the 4.1 Section are based on the Iteration or Sub-steps assumptions method. There are 12 number of lengths taken for applied moment against lateral deflection.

ARC-LENGTH Method

There are two methods used in order to determine the solution of nonlinear buckling analysis. One is displacement-controlled and other is Arc-length method. The predominant buckling analysis solution method is known as Force Controlled method and this method can work only for linear relationships between two variables. Force controlled method can't work for curved lines. As shown in the figure below, the moment applied gives two values of displacement at the start and end of curve.

When we observe that the plots obtained is in the form of curve, most efficient method for analysis used is displacement-controlled method. In this method, the selected displacement will gives the value of applied moment.

But in this research study, we used Arc-Length method for getting results of non-linear buckling and for performing the analysis. Following are commands used for this purpose.

- (i) Arc-length Key, (ii) MAXARC, for maximum multiplier (radius =25) and (iii) MINARC, for minimum multiplier (radius = 1/1000)

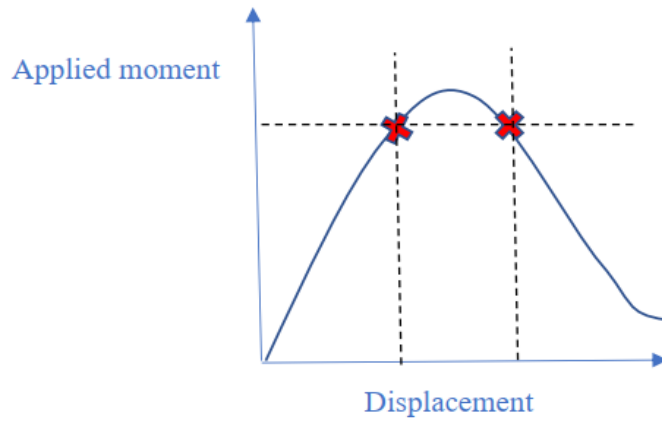


Fig. 5.1.6- App. Moment- Displacement Curve

Tangent Method

The method is well elaborated in the fig. given below. This method is used to find the accurate results for Lateral Torsional Buckling moment capacities of $M_{bRd 2}$ and $M_{bRd 3}$. The values are picked from this research that are calculated before in the plots of app. Moment against Lateral deflection graphs in 4.1 section of this research. The app. Moment is taken in (KNm) and displacement in (mm). A tangent is drawn on the curve to make the relation between variables.

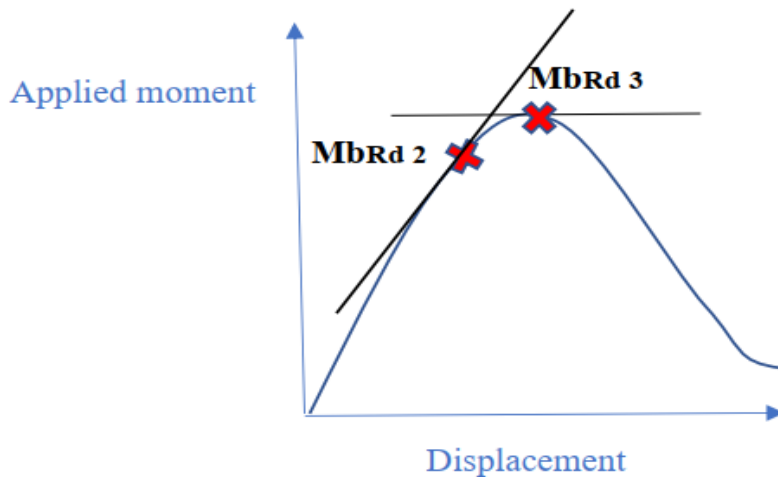


Fig. 5.1.7- Tangent method to find MbRd 2 and MbRd 3

From this graph, we came to know that, when the deviation starts in the line of graph, this point is for MbRd 2 and when the line reach maximum of its curve, then against the applied moment, this point is MbRd 3.

Load Condition

There are two types of loading applied on I-beam.

- (i) Uniform Line Pressure/stress
- (ii) End to end moments due to stress applied on both of beam.

Table 31- the calculation of elastic critical moment M_{cr}

Type/Condition of Loading	M _{cr} = Eigenvalue (Deformation) from ANSYS * App. Moment
In the Case of Deformation	
loads/stresses applied on the end of beam due to end moments	$7.0688 * 10 = 70.688$
uniform line stress or pressure acting	$1.8607 * 10 = 18.8607$
In the Case of Buckling	
loads/stresses applied on the end of beam due to end moments	$4.5690 * 10 = 45.690$
uniform line stress or pressure acting	$1.8071 * 10 = 18.071$

By analyzing the results tabulated above, the value of elastic critical moment (M_{cr}) changing its value by varying the condition of loading applied. This changing behavior can be noticed in both cases of deformation and buckling.

The question arises that due to changing the condition for loading in I-beam, the M_{cr} changes, why? The reason for this is that when line pressure is applied on I-beam, both web and flanges are stressed due to applied load and hence cause the reduction in the value of M_{cr} . We also know that uniform line pressure on any beam gives shear force and bending moment diagrams. Thus, we can conclude from the above discussion that, by increasing the load in the form of line pressure, M_{cr} will be reduced.

On the other hand, when end moment is applied on any end or both ends of beam, then only flange remains in the condition of stress, but web is not. Thus, the value of M_{cr} is higher in this case. As there is only moment applied on the beam and at the end, so there will be no shear force diagram but only bending moment diagram.

Identical/Same Load VS not same Load Condition

Same Load is defined as; the load type used for linear and non-linear analysis for buckling such as line or point pressure.

Not Same Load is defined as; when load conditions for linear or non-linear analysis of buckling are not the same. For example, for linear buckling analysis, line pressure and for non-linear buckling analysis as end moment at the end of I-beam.

For no temperature case, when the length of beam is selected as 1.5m and imperfection factor is taken as 2, the table and graph plotted in the above 4.2 section of same research, difference is taken as follows.

$$\left(\frac{34.67 - 34.32}{34.67} \right) * 100$$
$$= 1.009\%$$

In no temperature increase case, when the value of beam selected is 1.5m and imperfection factor is taken as 1.5, the table and graph plotted in the above 4.2 section of same research, difference is taken as follows.

$$\left(\frac{38.79 - 38.85}{38.79}\right) * 100$$
$$= 0.158\%$$

Results from Finite Element Modeling from different Scale Factors against Eurocodes

When graphs are plotted at different temperatures between imperfection factors and MbRd with Eurocodes, then there are six cases at different temperatures. These are;

- (i) No temperature
- (ii) 500°C
- (iii) 800°C
- (iv) 1200°C
- (v) 1500°C
- (vi) 2000°C

The question is, why the graphs are plotted at these temperatures. The reason is that there is no deformation occurred in steel beam sections when there is no rise in temperature. When temperature reaches in between 450°C to 600°C, research shows that steel start deforming because buckling phenomenon begins. At 800°C, there is observed that cracks occurred in steel beam section. At 1200°C, permanent deformation start which may cause the collapse of structure. Finally, when the beam reaches at its maximum temperature of 2000°C, the whole steel melts and there is no chance to save the structure.

We are discussing about how FEM results differs when there is drawn a relation between scale factor and Euro Code MbRd. The first mission is to compare the results obtained from

FEM and buckling moment capacity taken from the Euro code. It is noticed that buckling moment capacity is changed by varying the imperfection scale factor. And code doesn't consider the scale factor during the procedure.

The case when there is no increase in temperature and length of beam is 1.5m, the imperfection scale factor is changing. It is observed that LTB moment capacity of beam is decreased by increasing the “imperfection scale factor”. It is noticed that buckling moment capacity is changed by varying the imperfection scale factor. And code doesn't consider the scale factor during the procedure.

When taking the length of beam as 2m, and changing the imperfection scale factor, it is noticed that “lateral torsional buckling moment capacity” of the beam is reducing the enhancing the value of imperfection scale factor.

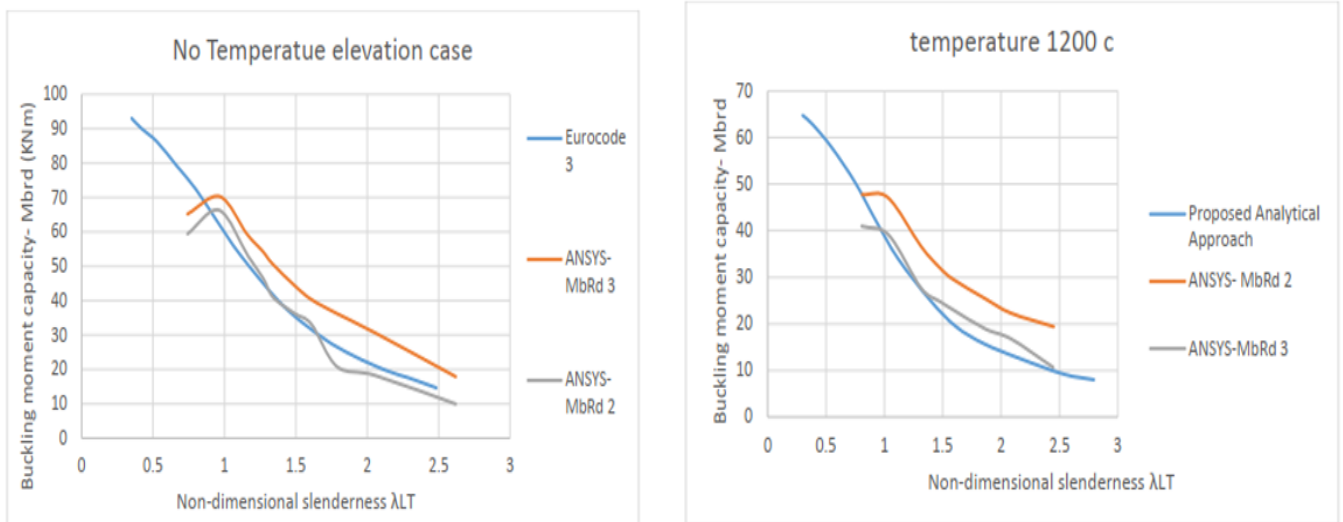


Fig. 5.1.7- the increase in non-dimensional slenderness ratio, decreases the MbRd.

5.1.1- Static Linear Analysis

Linear static analysis is checked by the maximum stress applied and resulting maximum displacement due to applied stress.

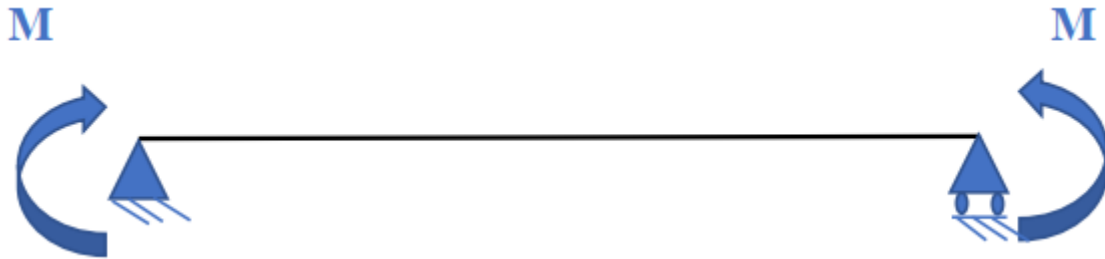


Fig. 5.1.8- A simply supported Beam with App. moments on both ends.

$$\sigma_{\max} = \frac{M_y}{I_{yy}}$$

This formula is used to calculate the maximum stress of any beam. M_y is the moment applied and I_{yy} is moment of inertia along y-axis.

When there is no increase in temperature, the maximum displacement and maximum stress equations are used to see the accuracy of results obtained from FEM analysis. In appendix, the steps, and tables for calculating and checking of these results in the tables are given.

The results obtained from ANSYS workbench (FEM results) and results from the equations has slight difference. The maximum displacement obtained is very low because there are only moments applied at both ends of beam. The maximum stress from both cases is also very low.

5.1.2- Linear Buckling Analysis

Equations and formulas written in chapter 2 are used to calculate the value of LTB when there is no rise in temperature. When the temperature is elevated, then reduction factor is applied to find the Lateral Torsional Buckling of beam.

Mcr-A is the elastic critical moment resulted from Ansys and Mcr-C is the elastic critical moment from the code. Tables documented in appendix are demonstrating the difference between Mcr-A and Mcr-C by taking into consideration of all beams for different lengths except 0.5m. The question is why 0.5m is not considered, the reason is that LTB behavior is not occurred for the beams of short lengths. The difference is calculated in percentage,

$$\left(\frac{102.65 - 87.32}{102.65}\right) * 100$$
$$= 14.93\%$$

The difference in the case of no elevated temperature is given as;

$$\left(\frac{102.65 - 97.53}{102.65}\right) * 100$$
$$= 4.98\%$$

5.1.3- Non-Linear Buckling Analysis

Equations and formulas written in chapter 2 are used to calculate the value of LTB when there is no rise in temperature. When the temperature is elevated, then reduction factor is applied to find the Lateral Torsional Buckling of beam.

The graphs and tables presented in 4.1 section represents the difference between the value of MbRd 2 and MbRd 3 with the MbRd determined from the code for all lengths except 0.5m. The question is why 0.5m is not considered, the reason is that LTB behavior is not occurred for the beams of short lengths. MbRd 2 and MbRd 3 are determined from the FEM results and MbRd-Code is determined from the formulas. The difference is explained in the graph inserted below.

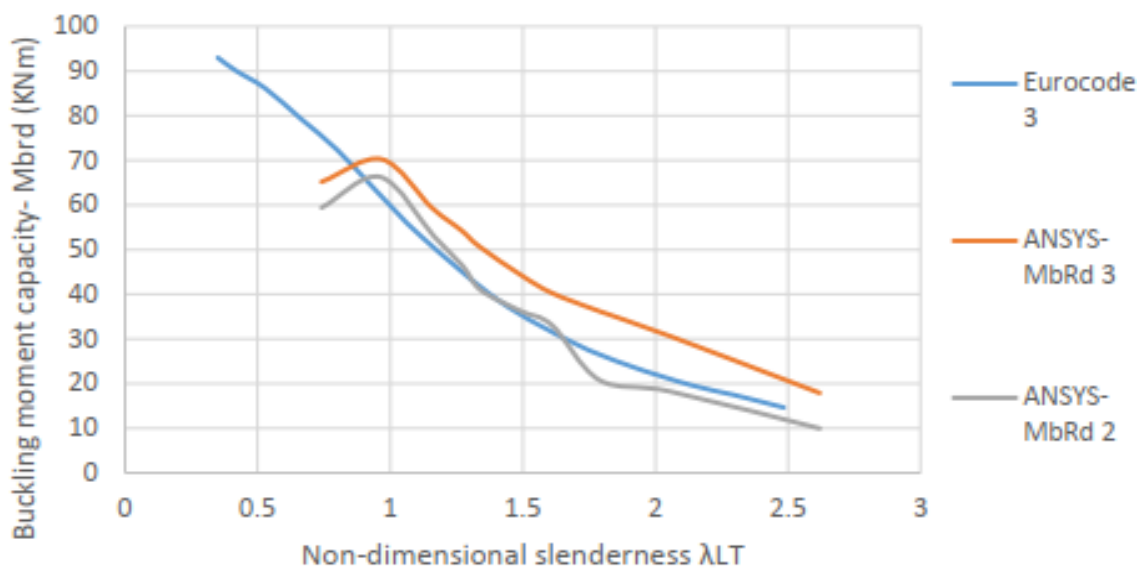


Fig. 5.1.9- Graph between FEM calculated MbRd and determined from the code.

5.1.4- Non-Linear Buckling Analysis

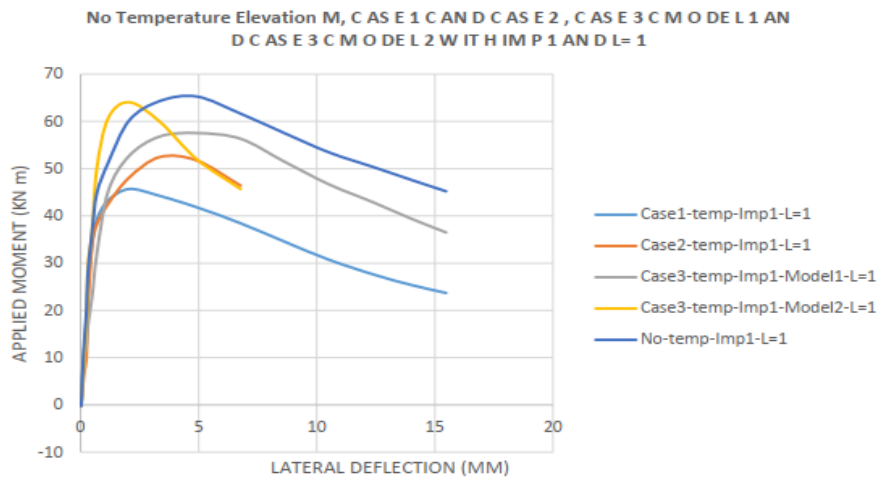


Fig. 5.1.10- App. Moment vs Deflection for 5 cases.

Table 32- The curves order obtained from the fig.

Order of Case	Name of Case	Length of Beam (mm)	Imperfection Scale Factor = $\frac{L}{1000}$
1	No temp. case	1000	1
4	Case Temp. 01	1000	1
2	Case temp. 02	1000	1
3	Case Temp. Model 01	1000	1
5	Case temp. Model 02	1000	1

From the figure, it is clear that the curve of no elevated temperature has more LTB moment capacity as compared to curve of case temp. 01.

5.1.5- LTB Moment Resistance

The final results are plotted between lateral torsional buckling moment and the non-dimensional slenderness ratio. The picture inserted below shows the complete variation of results occurring in the case when temperature of I-beam is increased up to the limit of its cracking and then make the relationship between these variables.

It is clear from the fig. inserted below that with the increase in value of slenderness ratio of cross-section reduces the value of lateral buckling moment capacity of the beam.

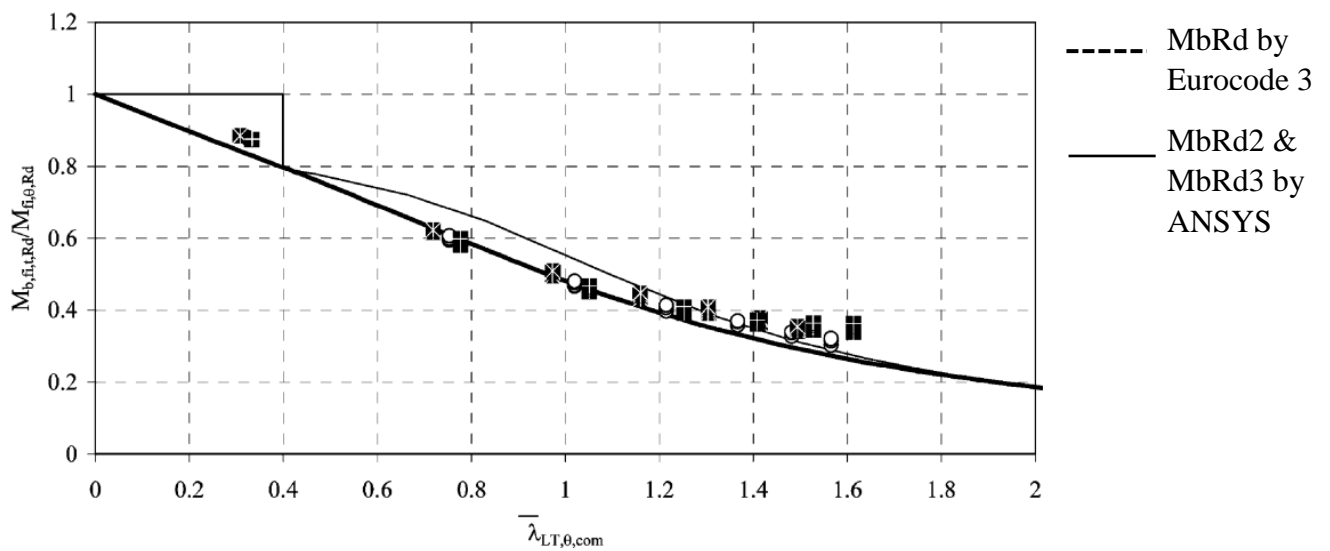


Fig. 5.1.11- non-dimensional slenderness ratio with LTB moment capacity.

Chapter 6

6- Conclusion

A parametric of LTB moment capacity was conducted on I-beam in this thesis. The considered parameters are length that was varied from 0.5m to 10m and temperature which was from the range of room temperature i.e. 25°C to 2000°C. The LTB moment capacity was obtained from non-linear buckling analysis for the case being considered using FEM employed ANSYS software.

During this study, the following points are identified and listed below as concluding remarks.

- (i) At an elevated temperature, there is reduction in strength of steel and stiffness of material with which beam is made, i.e., stainless steel. As stainless steel is alloy of different material, so it provides better retention as compared to carbon steel.
- (ii) Stainless steel beams are capable of bearing more temperature because they have high value of coefficient of thermal expansion as compared to carbon steel.
- (iii) LTB moment capacities are obtained from two references, one is from FEM analysis and other from the Euro-code 3. The observed moment capacities are M_{bRd2} and M_{bRd3} with the Euro-code moment capacity are plotted with “non-dimensional slenderness ratio against the reduction factor”. The line resulted is an inverted straight line showing the inverse relation between two variables.
- (iv) In the case when length of beam is taken 10.0m, in the cases of elevated temperatures of model 1 and model 2, the behavior expected is not resulted because there is small ratio in depth and length of beam and this ratio effect the graph curve.
- (v) All M_{bRd2} and M_{bRd3} moment capacities obtained from the FEM and Euro code 3 are compared expect those taken at the length of 0.5m. The reason for not

considering is that small length beams are not prone to the phenomenon of LTB in beams. The short beams or columns are expected to have local buckling than LTB.

6.1- Recommendation for future studies

It is recommended for future studies to make an experimental comparison although the temperature used in these cases are not practically possible but using these results and by performing experiments, a relation or trend can be produced.

It is also recommended to repeat the parametric study by changing the dimensions of the cross-section of the I-beam and take it to class 4 cross sections. As the behavior of these cross sections under these conditions would be different so under all these cases in software simulations and physical experiments, same trend should be produced and a comparison can be made to identify the deviation of results.

7- References

- [1] K. T. N. a. L. Gardner, "Buckling of stainless steel columns and beams in fire," p. 46.
- [2] A. Santiago, "NUMERICAL STUDY OF A STEEL SUB-FRAME IN FIRE," p. 39.
- [3] L. C. Z. Selvarajah Ramesh, "Experimental investigation of structural steel beams subjected to localized," *Engineering Structures*, 2020.
- [4] J. T. Allan Jowsey, "Heat Transfer to the Structure during the Fire," 2007.
- [5] M. Kucukler, "Lateral instability of steel beams in fire: Behaviour, numerical modelling and design," *Journal of Constructional Steel Research*, July 2020.
- [6] S. A. T. A. Pournaghshband, "Elevated temperature performance of restrained stainless steel beams," pp. 278-290., 2019.
- [7] G.-q. L. Chao Zhang, "FIRE DYNAMIC SIMULATION ON THERMAL ACTIONS," *Advanced Steel Construction*, vol. 8, pp. 124-136, 2012.
- [8] A. Jian Jiang, "Modeling of steel frame structures in fire using OpenSees," *Computers & Structures*, vol. 18, pp. 90-99, March 2013.
- [9] I. P.-Z. A. H. Myriam Rocío Pallares Muñoz, "New modeling strategies for analyzing lateral-torsional buckling in class-4 steel structural members at elevated temperatures using beam-type elements," *Structures*, pp. 3508-3532, December 2021.
- [10] P. P.-M. F. P.M.M. Vila Real, "A new proposal of a simple model for the LTB of unrestrained steel I-beams in case of fire," *Journal of Constructional Steel Research*, pp. 179-199, 2003.

-
- [11] D. R. A. Í. J. P. A. Rafael C.Barros, "Advanced inelastic analysis of steel structures at elevated temperatures by SCM/RPHM coupling," *Journal of Constructional Steel Research*, vol. 145, pp. 368-385, June 2018.
- [12] Ö. F. T. S. Klopovic, "A comprehensive study of externally venting flames," *Fire Safety Journal*, pp. 135-172, March 2001.
- [13] A. S. Saurabh Suman, "A new proposal for design of laterally unsupported monosymmetric steel I-section beams at elevated temperature," *Structures*, pp. 1277-1294, April 2022.
- [14] H. G. Shengbin Gao, "NUMERICAL SIMULATION OF HOLLOW AND," *Advanced Steel Construction*, vol. 3, pp. 668-678, 2007.
- [15] M. F. H. A. E. H. M. H. E.-B. A.A. Elkawas, "Behaviour of Corrugated Web Girders Subjected to Lateral-Torsional Buckling: Experimental Tests and Numerical Modelling," *Structures* , pp. 152-168, October 2021.
- [16] Z. X. L. G. Merih Kucukler, "Behaviour and design of stainless steel I-section columns in fire," *Journal of Constructional Steel Research* , February 2020.
- [17] S. A. N. S. Jie Wang, "Material properties and compressive local buckling response of high strength steel square and rectangular hollow sections," *Engineering Structures*, January 2017.
- [18] D. N. M.P. Byfield, "Material and geometric properties of structural steel for use in design," *Structural Engineer*, pp. 363-367, November 1997.

-
- [19] S. A. Asif Mohammed, "Numerical modelling and fire design of stainless steel hollow section columns," *Thin-Walled Structures*, November 2019.
- [20] I. K. Alexandre Danilov, "The Concept of Bearing Capacity Distribution in the Supports of Arches," in *Proceedings of FORM 2021*, 2021, p. 281–288.
- [21] C. S. M. B. S. Chiorean, "Ultimate strength analysis of steel-concrete cross-sections at elevated temperatures," *International Colloquium on Stability and Ductility of Steel Structures*, 2019.
- [22] R. S. R. R. P. P. D. L. Í. Barros, "Numerical advanced analysis of steel-concrete composite beams and columns under fire," *International Colloquium on Stability and Ductility of Steel Structures*, 2019.

Appendix

Appendix A

Formulas used for theoretical calculations

$$M_{b,fi,t,Rd} = \frac{\chi_{LT,fi}}{1.2} w_{pl,y} k_{y,\theta,com} f_y \frac{1}{\gamma_{M,fi}}$$

$$\chi_{LT,fi} = \frac{1}{\phi_{LT,\theta,com} + \sqrt{[\phi_{LT,\theta,com}]^2 - [\lambda_{LT,\theta,com}]^2}}$$

$$\phi_{LT,\theta,com} = \frac{1}{2} [1 + \alpha(\bar{\lambda}_{LT,\theta,com} - 0.2) + (\bar{\lambda}_{LT,\theta,com})^2]$$

$$\bar{\lambda}_{LT,\theta,com} = \bar{\lambda}_{LT,fi} = \bar{\lambda}_{LT} \sqrt{\frac{k_{y,\theta,com}}{k_{E,\theta,com}}}$$

where

$$\lambda_1 = \pi \sqrt{\frac{E}{f_y}}$$

$$\lambda_{LT} = \pi \sqrt{\frac{E w_{pl,y}}{M_{cr}}}$$

$$\bar{\lambda}_{LT} = \sqrt{\frac{w_{pl,y} f_y}{M_{cr}}}$$

$$\bar{\lambda}_{LT} = \frac{\lambda_{LT}}{\lambda_1}$$

$$M_{b,fi,t,Rd} = \chi_{LT,fi} w_{pl,y} k_{y,\theta,com} f_y \frac{1}{\gamma_{M,fi}}$$

$$\frac{M_{b,fi,t,Rd}}{M_{fi,\theta,Rd}} = \chi_{LT,fi}$$

$$\frac{M_{b,fi,t,Rd}}{M_{fi,\theta,Rd}} = \chi_{LT,fi}$$

$$M_{\bar{n},\theta,Rd} = k_{y,\theta} \frac{\gamma_{M0}}{\gamma_{M,\bar{n}}} M_{Rd}$$

$$\varepsilon = \sqrt{\frac{235}{f_y}} \quad (0.65)$$

$$M_{Rd} = \frac{w_{pl,y} f_y}{\gamma_{M0}}$$

Critical Moment determined from Euro Code 3 by using,

$$(EI_y u''')'' + (M_x \phi)'' = 0 \quad (EI_w \phi'')'' - (GI_t \phi')' + (M_x u'') = 0$$

$$M_{cr} = \alpha_M M_{cr}^{pb} = \alpha_M \frac{\pi^2 EI_y}{(kL)^2} \sqrt{\left(\frac{k}{k_w}\right)^2 \frac{I_w}{I_y} + \frac{(kL)^2 GI_t}{\pi^2 EI_y}}$$

Nomenclature

a	Maximum amplitude of the beam lateral imperfection
E	Young's modulus of elasticity
G	Shear modulus of elasticity
I_x, I_y	Second moments of area about the x, y axes
I_t	Torsion section constant
I_w	Warping section constant
f_y	Yield strength
k	Effective length factor
k_w	Warping effective length factor
$k_{y,\theta,\text{com}}$	Reduction factor for the yield strength at the maximum temperature in the compression flange $\theta_{a,\text{com}}$, reached at time t
$k_{E,\theta,\text{com}}$	Reduction factor for the slope of the linear elastic range at the maximum steel temperature in the compression flange $\theta_{a,\text{com}}$ reached at time t
L	Length of the beams
$M_{b,fi,t,Rd}$	Buckling resistance moment in the fire design situation
M_{cr}	Elastic critical moment for lateral-torsional buckling
$M_{fi,\theta,Rd}$	Design moment resistance of a Class 1 or 2 cross-section with a uniform temperature θ_a
M_{SAFIR}	Buckling resistance moment in the fire design situation given by SAFIR
M_{Rd}	Plastic moment resistance of the gross cross-section, $M_{pl,Rd}$ for normal temperature
M_x	Bending moment about x axis
t	Time
u	Lateral displacement
v	Vertical displacement
$w_{pl,y}$	Plastic section modulus
x, y	Principal centroidal axes
z	Longitudinal axis through centroid

γ_{M0}	Partial safety factor (usually $\gamma_{M,1} = 1.0$)
$\gamma_{M,fi}$	Partial safety factor for the fire situation (usually $\gamma_{M,fi} = 1.0$)
θ	Rotation
ϕ	Twist rotation
λ_{LT}	Slenderness
λ_{LT}	Non-dimensional slenderness at room temperature
$\lambda_{LT,\theta,com}$	Non-dimensional slenderness for the maximum temperature in the compression flange $\theta_{a,com}$
$\lambda_{LT,fi}$	Non-dimensional slenderness in the fire design situation
$\chi_{LT,fi}$	Reduction factor for lateral-torsional buckling in the fire design situation

Appendix B
Dimensions used for case of no fire

Hight (mm)	200
Top Flange Width (mm)	90
Bottom Flange Width (mm)	90
Web Thickness (mm)	7.5
Web hight (mm)	177.4
Top Flange thickness (mm)	11.3
Bottom Flange thickness (mm)	11.3
Hypotenuse (mm)	$\sqrt{5^2 + 5^2} = 5\sqrt{2}$
Wply (mm^3)	$250.92 * 10^3$
Izz (mm^4)	$1.38 * 10^6$
Iyy (mm^4)	$2.16 * 10^7$
It (mm^4)	$1.11 * 10^5$
Iw (mm^6)	$1.22 * 10^{10}$

Dimensions used for elevated temperature case model 1

Hight (mm)	196.908
Top Flange Width (mm)	86.908
Bottom Flange Width (mm)	86.908
Web Thickness (mm)	4.408
Web hight (mm)	180.492
Top Flange thickness (mm)	8.208
Bottom Flange thickness (mm)	8.208
Hypotenuse (mm)	$\sqrt{5^2 + 5^2} = 5\sqrt{2}$
Wply (mm^3)	170.49 x10³
Izz (mm^4)	9.06 x10⁵
Iyy (mm^4)	1.49 x10⁷
It (mm^4)	3.72 x10⁴
Iw (mm^6)	7.99 x10⁹

Dimensions used for Case of elevated temperature for model 2

Hight (mm)	198.454
Top Flange Width (mm)	90
Bottom Flange Width (mm)	86.908
Top Web Thickness (mm)	7.5
Bottom Web Width(mm)	4.408
Web hight (mm)	178.946
Top Flange thickness (mm)	11.3
Bottom Flange thickness (mm)	8.208
Hypotenuse I-NC (mm)	$\sqrt{5^2 + 5^2} = 5\sqrt{2}$
Hypotenuse I-C (mm)	$\sqrt{2.81^2 + 2.81^2} = 3.974$
Wply (mm^3)	199.931×10^3
Izz (mm^4)	1.139×10^6
Iyy (mm^4)	1.766×10^7
It (mm^4)	7.383×10^4
Iw (mm^6)	9.643×10^9

Appendix C

Linear Buckling Analysis and results tabulated

For static linear analysis case

L (m)	0.55	1	1.5	2	2.3	2.5	3	3.4	4	5	7	10
MSM (N/mm²)	46.3	46.3	46.3	46.3	46.3	46.3	46.3	46.3	46.3	46.3	46.3	46.3
MSWA (N/mm²)	44.2	45.1	45.3	45.4	45.4	45.4	45.4	45.4	45.5	45.5	45.4	45.5
MDM (mm)	0.083	0.28	0.62	1.1	1.46	1.72	2.48	3.18	4.41	6.9	13.5	27.5
MDWA (mm)	0.163	0.31	0.59	0.98	1.28	1.49	2.12	2.695	3.69	5.72	11.12	22.64

Linear Buckling Analysis For no temperature elevation case

L (m)	0.55	1	1.5	2	2.3	2.5	3	3.4	4	5	7	10
MS	-	6	4	5	5	5	5	5	5	5	5	2
EB	-	19.041	11.15	7.62	6.37	5.74	4.57	3.91	3.19	2.38	1.46	0.76
AM (KNm)	10	10	10	10	10	10	10	10	10	10	10	10
Mcr-A (KNm)	-	190.41	111.5	76.2	63.7	57.4	45.7	39.1	31.9	23.8	14.6	7.6
Mcr-C (KNm)	936.2	313.3	160.5	104.7	86.3	77.3	61.3	52.6	43.5	33.9	23.6	16.3

Non-Linear Buckling Analysis For no temperature elevation case

L (m)	0.55	1	1.5	2	2.3	2.5	3	3.4	4	5	7	10
Mbrd-C (KNm)	93.5	83.9	72	60.5	54.5	50.9	43.5	38.9	33.5	27.2	19.8	14.2
Mbrd2 (KNm)	-	60	67.3	53.4	47	41	36	33	20	18	9	-
Mbrd3 (KNm)	-	65.3	70.7	59.5	54	50.6	44.3	40	36	30	17	-

Static Linear Analysis Case for model 1

L (m)	0.55	1	1.5	2	2.3	2.5	3	3.4	4	5	7	10
MSM (N/mm ²)	66.2	66.2	66.2	66.2	66.2	66.2	66.2	66.2	66.2	66.2	66.2	66.2
MSWA (N/mm ²)	62.3	63.8	64.1	64.2	64.2	64.3	64.3	64.24	64.24	64.21	64.1	64.1
MDM (mm)	0.12	0.40	0.90	1.60	2.12	2.50	3.60	4.63	6.41	10.01	19.6	40
MDWA (mm)	0.26	0.47	0.88	1.45	1.87	2.18	3.07	3.90	5.35	8.3	16.0	32.6

Linear Buckling Analysis Results from FEM Case for model 1

L (m)	0.55	1	1.5	2	2.3	2.5	3	3.4	4	5	7	10
MS	-	6	2	3	3	4	3	3	5	5	5	2
EB	-	9.063	5.524	3.475	2.750	2.387	1.738	1.385	1.009	0.606	0.169	- 0.154
AM (KNm)	-	10	10	10	10	10	10	10	10	10	10	10
Mcr-A (KNm)	-	90.63	55.24	34.75	27.50	23.87	17.38	13.85	10.09	6.06	1.69	-1.54
Mcr-C (KNm)	598.9	191.7	93	57.9	46.7	41.2	31.8	26.8	21.8	16.6	11.3	7.7

Non-Linear Buckling Analysis Results from FEM Case for model 1

L (m)	0.55	1	1.5	2	2.3	2.5	3	3.4	4	5	7	10
Mbrd-C (KNm)	63.3	56.1	46.3	36.7	32	29.4	24.1	21	17.6	13.9	9.8	6.9
Mbrd2 (KNm)	-	40	38	27	24	22.133	18	16	10	7	3.5	6.6
Mbrd3 (KNm)	-	46.1	45.4	35.6	31	28.7	24	21.5	18.8	13	7	6.6

Static Linear Analysis Case for model 02

L (m)	0.55	1	1.5	2	2.3	2.5	3	3.4	4	5	7	10
MSMC (N/mm ²)	48.5	48.5	48.5	48.5	48.5	48.5	48.5	48.5	48.5	48.5	48.5	48.5
MSWAC (N/mm ²)	45.1	43.2	43.2	43.2	43.2	43.2	43.2	43.2	43.2	43.2	43.2	43.2
MSMT (N/mm ²)	63.9	63.9	63.9	63.9	63.9	63.9	63.9	63.9	63.9	63.9	63.9	63.9
MSWAT (N/mm ²)	62.8	62.5	62.5	62.5	62.5	62.5	62.5	62.5	62.5	62.5	62.5	62.5
MDM (mm)	0.10	0.34	0.757	1.35	1.77	2.1	3.02	3.89	5.38	8.41	16.5	33.6
MDWA (mm)	0.21	0.396	0.739	1.22	1.58	1.84	2.6	3.31	4.54	7.02	13.6	27.7

Linear Buckling Analysis Results from FEM Case for model 2

L (m)	0.55	1	1.5	2	2.3	2.5	3	3.4	4	5	7	10
MS	-	5	5	7	4	7	6	6	6	6	5	5
AM (KNm)	10	10	10	10	10	10	10	10	10	10	10	10
EB	-	15.7	9.36	6.16	5.02	4.44	3.39	2.81	2.18	1.495	0.742	0.211
Mcr-A (KNm)	-	157.12	93.6	61.6	50.2	44.4	33.9	28.1	21.8	14.95	7.42	2.11
Mcr-C (KNm)	749.8	248	124.8	80.4	66	59	46.3	39.6	32.6	25.3	17.5	12

Non-Linear Buckling Analysis Results from FEM Case for model 2

L (m)	0.55	1	1.5	2	2.3	2.5	3	3.4	4	5	7	10
Mbrd-C (KNm)	74.5	66.8	56.95	47.3	42.3	39.4	33.4	29.7	25.4	20.5	14.8	10.6
Mbrd2 (KNm)	-	45.2	55.5	44.4	34	33	27	24	16	12.5	6.5	-
Mbrd3 (KNm)	-	53.1	59.5	49.1	44	41.2	34.4	32.4	28	23	13.5	-

In these tables

L is the length of beam

MbRd is the buckling moment obtained from code.

MbRd 2 and MbRd 3 are the buckling moments resulted from FEM Simulations

AM is moment applied in ANSYS

EB is the Eigen Buckling obtained from ANSYS.

MS is shape of the mode chosen.

Appendix D

I-Beam Models

Beam model used in ANSYS workbench for different lengths is

